The Thermo-Catalytic Cracking of Hydrocarbons: Hybrid Catalyst Configuration and the Phenomena of Hydrogen Spill-over

HaiTao Yan

A Thesis

in

The Department

of

Chemistry and Biochemistry

Presented in Partial Fulfillment of the Requirements
for the Degree of Master of Science (Chemistry) at
Concordia University
Montreal, Quebec, Canada

August 2009

Your file Votre référence
ISBN: 978-0-494-63116-4
Our file Notre référence
ISBN: 978-0-494-63116-4

CONCORDIA UNIVERSITY

School of Graduate Studies

This is certify that the thesis prepared

By: **HaiTao Yan**

Entitled: **The Thermo-Catalytic Cracking of Hydrocarbons: Hybrid Catalyst Configuration and the Phenomena of Hydrogen Spill-over**

and submitted in partial fulfillment of the requirements for the degree of

Master of Science (Chemistry)

Complies with the regulations of this University and meets the accepted standards with respect to originality and quality.

Signed by final examining committee:

_____ Chair

_____ Examiner

_____ Examiner

_____ Examiner

_____ Supervisor

Approved by _____

Chair of Department or Graduate Program Director

_____ 20__ _____

Dean of Faculty

ABSTRACT

The Thermo-Catalytic Cracking of Hydrocarbons: Hybrid Catalyst Configuration and the Phenomena of Hydrogen Spill-over

HaiTao Yan

Light olefins and diolefins such as ethylene, propylene, butenes and 1,3-butadiene are considered as the backbone of the petrochemical industry. They are precursors of numerous plastic materials, synthetic fibers, and rubbers. In recent years, the thermo catalytic cracking (TCC) process has been developed in our lab with the objective to selectively produce light olefins, particularly ethylene and propylene, from liquid hydrocarbon feedstocks such as petroleum naphtha and gas oils. With the continuous decline of conventional oil reserves, heavy petroleum feedstocks become essential alternatives for commercial petroleum products. However, the preliminary catalytic results in the TCC of heavy feedstock have indicated insufficient on-stream long-term stability and a high selectivity to polyaromatic hydrocarbons, which are usually considered as precursors for coke.

In this dissertation, hybrid catalysts have been developed and studied with the goal of resolving the problems of stability of catalyst activity and selectivity. Several active metal species (such as Ni, Re, Ru) have been loaded on the co-catalyst component surface. These metal species are able to produce very active hydrogen species, in virtue of its steam-reforming activity, and to spill them over to the acidic sites of the main catalyst component. These hydrogen species, once transferred (or "spilt over") onto the

surface of the main cracking catalyst component, might interact with the reaction intermediate being adsorbed on the acidic sites. This resulted in a decreased formation of coke precursors, and consequently, catalyst deactivation was significantly retarded. The results obtained from cracking tests on both petroleum feedstocks and model molecules indicated that the spilt-over hydrogen species had significant effects on heavy hydrocarbon feedstocks, such as vacuum gas oil, and they could affect the reaction intermediates only when the latter were formed on the external surface of microporous ZSM-5 zeolite particles. Moreover, data of the most recent work show that it is necessary to choose the ZSM-5 zeolite (that is the cracking component of the hybrid catalyst) that has a high density of acid sites; however, its acid strength should be relatively mild in order to achieve a high total conversion and a high propylene/ethylene product ratio. These mild acid sites also lead to lower coke deposition and a lighter nature of coke thus improving the cleaning action of the hydrogen spilt-over species.

PROFESSIONAL ACKNOWLEDGMENTS

First and foremost, I would like to express my extreme gratitude to my supervisor Prof. Raymond Le Van Mao for giving me the opportunity to work in his lab over the past 3 years. I would like to thank you for introducing me to the world of catalysis, petroleum chemistry and zeolites. I also want to thank you for your guidance, encouragement, kindness, and patience during my time at Concordia University. Without your valuable insight and input, as well as your entensive expertise, this work would not have been possible or might not have ever come to fruition.

I cannot fail to mention my thesis committee members, Prof. Louis A. Cuccia and Prof. Xavier Ottenwaelder. I would like to express my thanks and appreciation for their helpful suggestions, encouragement and support throughout the course of this degree.

I would like to sincerely thank the current and past Industrial Catalysis Group: Dr. Ngoc Thanh Vu, Lin Lu, and Dr. Nabil Al-Yassir. Thank you for your support, helpful advices.

I would like to express my sincere appreciation to the Science Technical Center: Mr. Richard Allix, Mr. Aldo Dissegna, Mr. Gheorghe Dan Duru, Mr. Chris Kowalewski, and Mr. Robert Pisarsky. I always had a tremendous respect for your endless support, and my words cannot entirely express my sincere gratitude.

PERSONAL ACKNOWLEDGMENTS

Needless to say, this entire M.Sc. dissertation would be at most a dream if there were not my mother Hua Mei. I do not know how to start this, but I do know that no matter how much I say, or how long it will take me to finish it, my words will not be enough or definitely will run out before I adequately express my deep gratitude and appreciation to my mother. You have supported me in many, many ways and this M.Sc. is as much as yours as it is mine. Your countless emotional and moral support, endless love, and unconditional sacrifice are the reasons why I make it to this point in my life. Your encouragement meant the whole to me. You have waited so long for this moment to come true; I am glad that your waiting has finally been rewarded.

"No matter who wrote it, there's nothing we can't make intelligible."

{Pinball, 1973/Murakami Haruki}

"The introduction to *Bonus Light*, that exegesis of pinball, has this to say:

There is precious little you can gain from a pinball machine. Only some lights that convert to a score count. On the other hand, there is a great deal to lose. All the coppers you'd ever need to erect statues of every president in history (provided, of course, you thought well enough to erect a statue of Richard M. Nixon), not to mention a lot of valuable and nonreturnable time.

While you're playing yourself out in lonesome dissipation in front of a pinball machine, someone else might be reading through Proust. Still another might be engaged in heavy petting with a girlfriend at a drive-in theater showing of *Paths of Courage*. The one could well become a writer, witness to the age; the others, a happily married couple.

Pinball machines, however, won't lead you anywhere. Just the replay light. Replay, replay, replay .... So persistently you'd swear a game of pinball aspired to perpetuity.

We ourselves will never know much of perpetuity. But we can get a faint inkling of what it's like.

The object of pinball lies not in self-expression, but in self-revolt. Not in the expansion of the ego, but in its compression. Not in extractive analysis, but in inclusive subsumption.

So if it's self-expression or ego expansion or analysis you're after, you'll only be subjected to the merciless retaliation of the tilt lamps.

Have a good game"

{Pinball, 1973/Murakami Haruki}

Not for anyone, just for myself.

TABLE OF CONTENTS

LIST OF FIGURES

LIST OF SCHEMES

LIST OF TABLES

CONTRIBUTIONS OF AUTHORS

The following summarizes the contributions of each the authors cited in this dissertation.

CHAPTER II: "Effect of the spilt-over hydrogen species on the product yields of the hybrid catalysts used in the Thermo-Catalytic Cracking (TCC) process for the production of light olefins"

R. Le Van Mao: project supervisor and manuscript preparation

N. T. Vu: experimental work

N. Al-Yassir: experimental work

H. T. Yan: experimental work

CHAPTER III: "The Thermo-catalytic Cracking of hydrocarbons: Effect of polymethylbenzenes added to the *n*-hexane feed on the reactivity of ZSM-5 zeolite containing hybrid catalyst"

H. T. Yan: experimental work and manuscript preparation

R. Le Van Mao: project supervisor and manuscript preparation

CHAPTER IV: "Hybrid catalysts used in the Thermo-Catalytic Cracking process (TCC): influence of the pore characteristics and the acidity properties of the ZSM-5 zeolite-based component on the overall catalytic performance"

H. T. Yan: experimental work and manuscript preparation

R. Le Van Mao: project supervisor and manuscript preparation

CHAPTER I

GENERAL INTRODUCTION

1.1. PREAMBLE

Light olefins and diolefins such as ethylene, propylene, butenes and butadienes are the key building blocks for the production of important petrochemicals. They are the precursors of numerous plastic materials, synthetic fibers and rubbers, so that they are considered as the backbone of the petrochemical industry. These basic chemicals are currently manufactured mainly by Steam Cracking (SC) and recently Fluid Catalytic Cracking (FCC) using ZSM-5 zeolite containing catalysts. Other technologies such as Deep Catalytic Cracking, Catalytic Dehydrogenation, Methanol to Olefins and Olefin Metathesis have also been studied and developed; however, these processes only cover a small part of the light olefins demand. As the rapid growth of the world demand (particularly for propylene that is produced as a co-product by conventional light olefins technologies) and the increasingly stringent environmental regulations requiring lower greenhouse gases emissions, it is imperative to develop a new process with improved production of light olefins.

The Thermo Catalytic Cracking (TCC) process has been developed and extensively studied since 1998, that can be regarded as a promising alternative process for light olefins production. The preliminary results show that the TCC offers several advantages when compared to the conventional SC: it gives higher combined yields of ethylene and propylene from the low-commercially valued heavy products, it results in lower emission of greenhouse gases, and it consumes less energy. The TCC process combines the effects of thermal and catalytic cracking reactions. Most catalysts used are in the hybrid configuration, which contain two components: a main component having cracking properties owing to acidic surface sites and a co-catalyst that is capable of

affecting the product selectivity of the former components. These two components are firmly bound to each other within an inert binder, so that a "pore continuum" is developed whose effect is to ease the transfer of the reaction intermediates within the catalyst network.

Various aspects of the catalytic configuration and the reaction parameters need to be balanced in order to further improve the TCC. For example, the hydrogen spillover (HSO) effect can be introduced to improve the catalyst stability and reactivity. A deeper understanding of the synergy between the different components of the hybrid catalyst structure and the influence of its physical and chemical factors can help improve the TCC efficiency significantly.

1.2. Light Olefins

1.2.1. Light Olefins as Precursors in Petrochemical Industry

In organic chemistry, an olefin is defined as an unsaturated chemical compound containing at least one carbon-to-carbon double bond. [1] The simplest acyclic alkenes, with only one double bond and no other functional groups, form a homologous series of hydrocarbons with the general formula C_nH_{2n}. [2] In comparison with paraffinic hydrocarbons, olefins are characterized by their higher reactivities. They can easily react with inexpensive reagents such as water, oxygen, hydrochloric acid, and chlorine to form valuable chemicals. In addition, polymers such as polyethylene and polypropylene can be produced by polymerization. [3] Since light olefins are the precursors of numerous plastic materials, synthetic fibers, and rubbers, they have been recognized as key building blocks of the petrochemical industry. The market demand for ethylene and propylene in the year 2005 was 107 and 67.1 million metric tons (Mt), respectively. Global ethylene demand

growth is about 4.5-5% per year; global propylene demand growth typically averages over around 5% per year. [4] The demand for ethylene and propylene is projected to increase to about 140 and 90 million Mt by 2010, respectively. [5] The significance of light olefins industry stems from the great demands for polyolefins particularly polyethylene and polypropylene. [6] Fig.1.1 and Fig.1.2 show the main end uses of ethylene [7] and propylene (1970 and 2004) [8]. The share of polyolefins of the total polymer market increased approximately from 30% to 60% since 1970, and this demand will continue to grow, because of the constant growing demands from developing countries like China and India, where only few materials can match their versatility and economy. [9 and references therein]

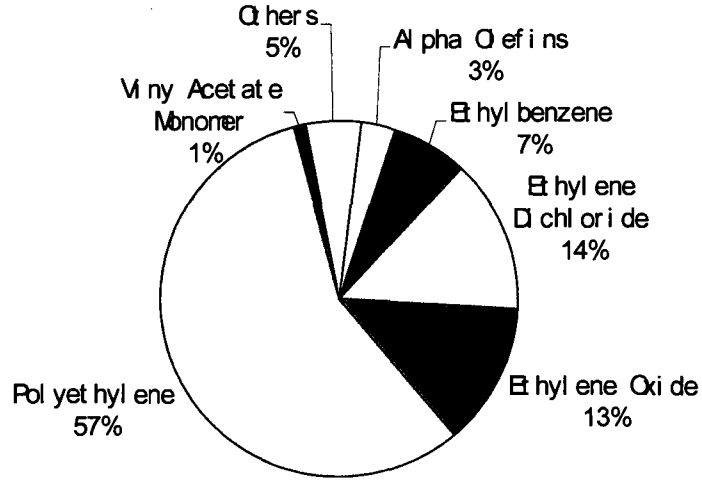

Fig.1.1: World ethylene end use, 2000 [7]

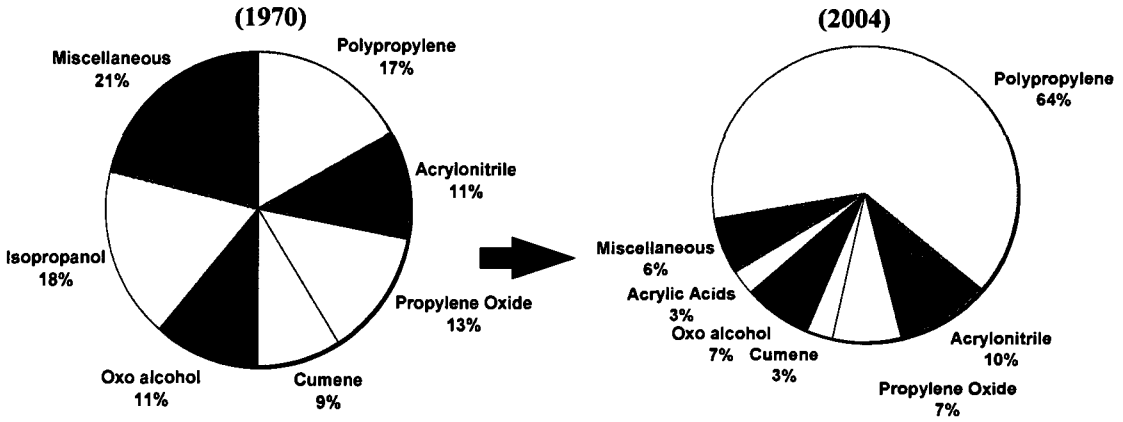

Fig.1.2: World propylene end use [8]

1.2.2. Ethylene

Ethylene is sometimes considered as the "king of petrochemicals". [10] This is because more commercial chemicals are produced from ethylene than from any other intermediate due to its several favorable properties as well as technical and economical factors. Ethylene has a simple structure with high reactivity. It is a relatively inexpensive compound, which can be easily produced from any hydrocarbon source through refinery process like steam cracking and in high yields. In addition, there are less by-products generated from ethylene reactions with other compounds than from other olefins. As shown in Fig.1.1, valuable chemicals can be produced from ethylene by reacting with many inexpensive reagents such as water, chlorine, hydrogen chloride, and oxygen. Ethylene can be polymerized by free radicals or by coordination catalysts into polyethylene, which is the largest-volume thermoplastic polymer. Also, the copolymerization of ethylene with other olefins can produce copolymers with improved properties. [10]

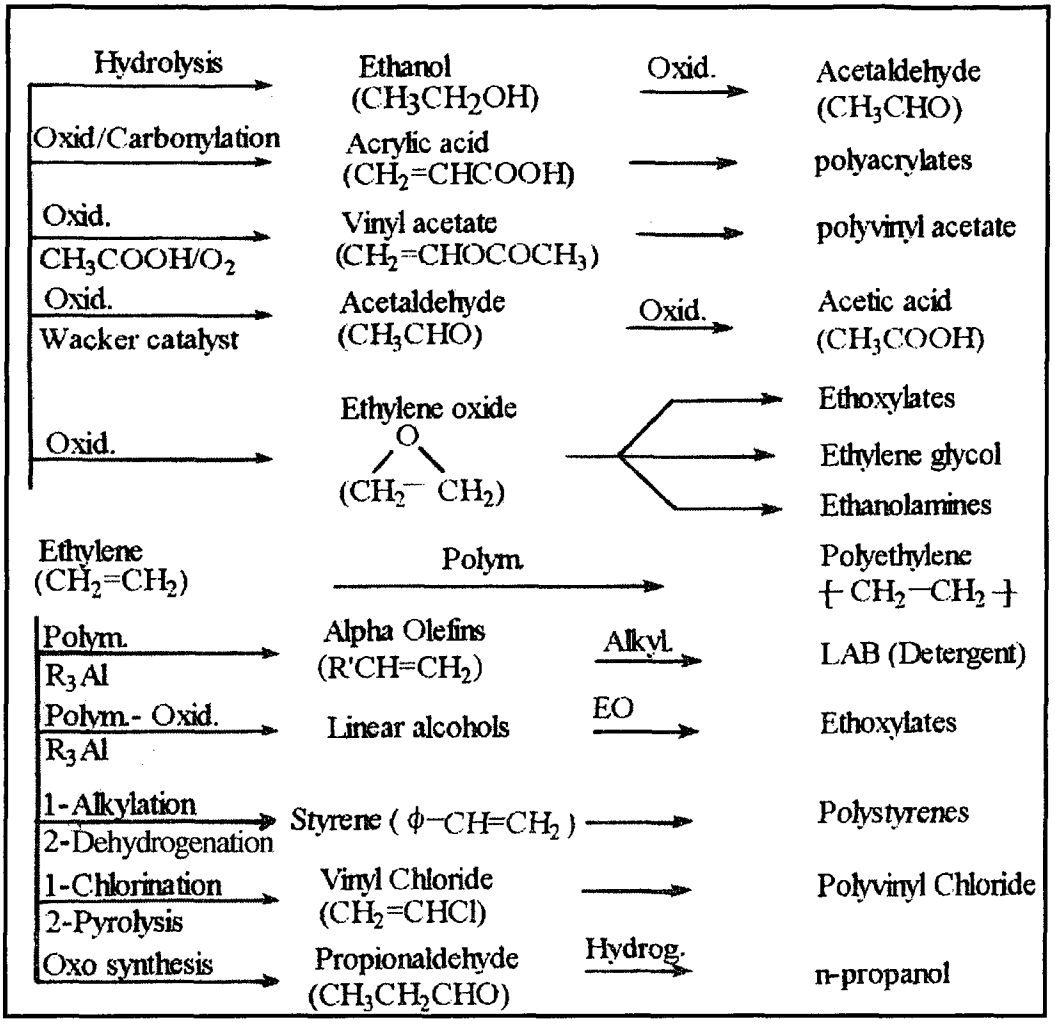

Scheme 1.1: Major chemicals based on ethylene [10]

1.2.3. Propylene

Propylene, which is second to ethylene as the largest-volume hydrocarbon intermediate for the production of chemicals, has been regarded as "the crown prince of petrochemicals." [10] Like ethylene, propylene is a reactive compound that can react with many common reagents such as water, chlorine, and oxygen. However, propylene has different reactivities toward these reagents as its structure is different from that of ethylene. For instance, instead of yielding propylene oxide as in the case of ethylene, the

oxidation of propylene using oxygen produces acrolein. This is due to the ease of oxidation of allylic hydrogens in propylene. [10] Fig.1.2 shows the important chemicals based on propylene.

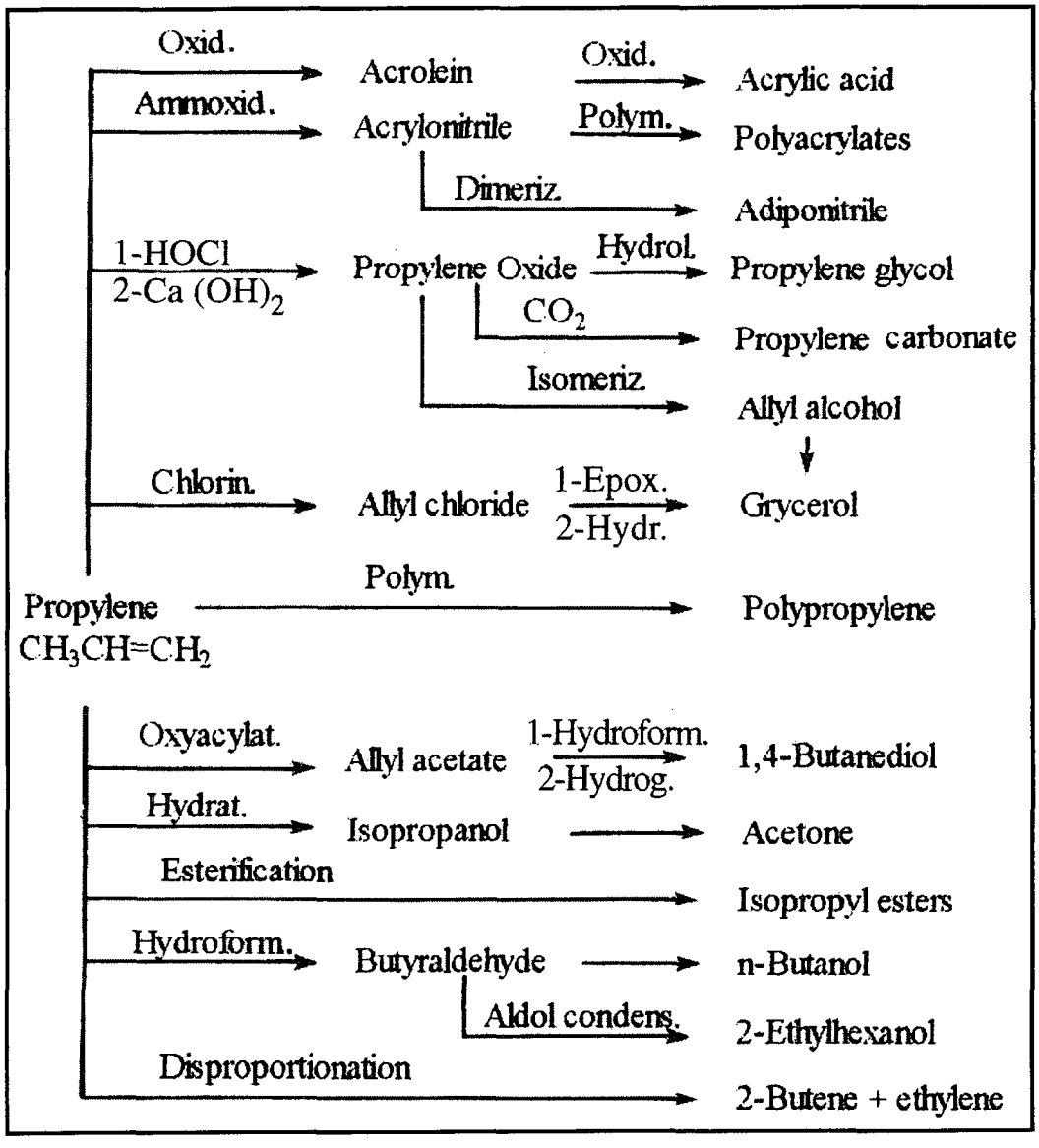

Scheme 1.2: Important chemicals based on propylene [10]

1.3 Light Olefins Production

1.3.1. Main Industrial Technologies for Light Olefins Production

At first, light olefins were produced industrially by several chemical processes. For instance, the dehydration of ethyl alcohol or partial hydrogenation of acetylene was used to produce ethylene. [11] However, producers turned to petroleum feedstocks as a vital source for light olefins as the demand for light olefins increased rapidly. Currently, steam cracking (SC) and fluid catalytic cracking (FCC) are among the most important processes that produce light olefins from natural gas and petroleum fractions (i.e. gaseous hydrocarbons, naphtha, gas oil). These processes are fully developed and commercialized. Other on-purpose processes, such as propane dehydrogenation, olefins metathesis, and methanol-to-olefins process, are also widely studied and developed. However, they cover only a small part of the olefins demand. Thus, this thesis will limit its discussion to the most prevalent processes: steam cracking and catalytic cracking.

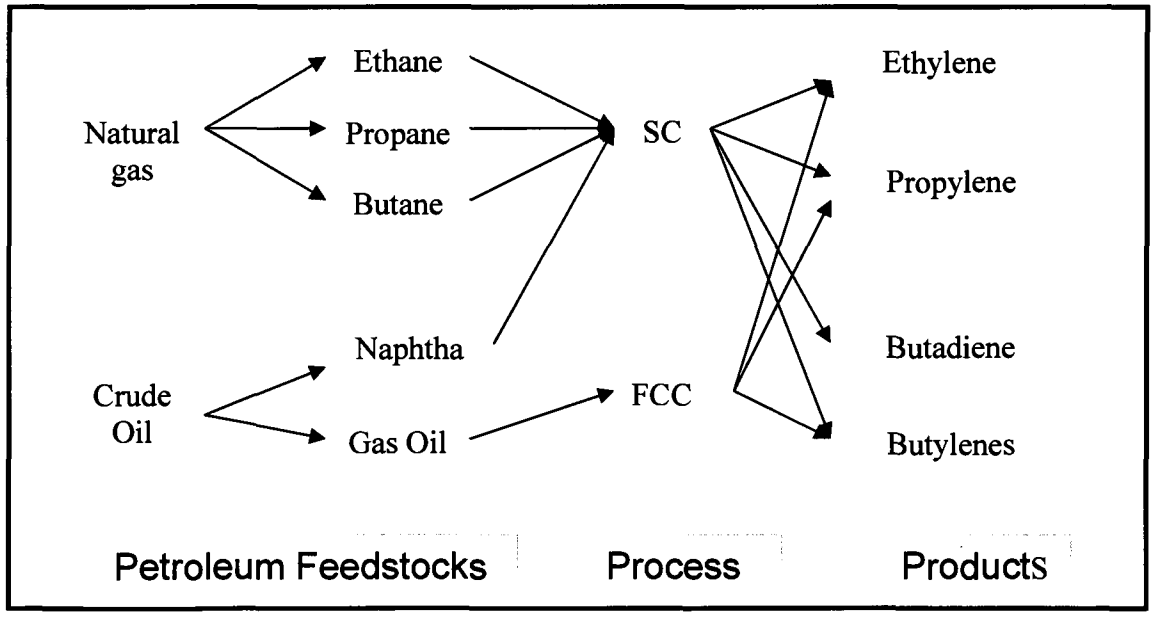

Scheme 1.3: The main important current sources of light olefins [6]

1.3.2. Thermal (steam) Cracking (SC)

Currently, the main source of light olefins specifically, ethylene and propylene, is steam cracking, which involves the pyrolysis of a paraffin feedstock which can have a wide range in number of carbon atoms and can even include mixtures of hydrocarbons. SC has a worldwide production of more than 150 million metric tons of ethylene and propylene annually. [12] This process is known as a non-catalytic, radicals-promoted, thermal cracking process, which is performed in the presence of steam at high temperature. Steam acts as a diluent to lower the hydrocarbon partial pressure and suppresses to a significant degree the formation of coke deposits throughout the reactor ($C+ 2H_2O \rightarrow CO_2 + 2H_2$). [11] The SC reaction is highly endothermic, and the typical temperatures for this process range from 700 to 900℃, and higher, according to the type of feedstock used. The residence time ranges from a few seconds to a fraction of a second. [11] The product spectrum for steam cracking is rather large. Light olefins are primarily produced, but a cut of C4 fraction containing paraffins, olefins, and butadienes is also formed. A third cut, that of C5 and higher hydrocarbons, contains pentanes/pentenes and BTX (i.e. benzene, toluene, and xylenes). [11] The light fraction is in the gaseous state, so that to isolate them, the product stream is passed through a series of units which in turn removes a single compound from the stream. Thus, there is a demethanizer, a deethanizer and so on until only the liquid fraction remains. The products in the liquid fraction are separated by distillation. Coke and heavy oils are also formed in lesser quantities but have the unfortunate quality of forming deposits throughout the system, which must be removed. Cyclic alkanes can be formed and subsequent dehydrogenations also produce aromatics. Diolefins are also produced and are very

reactive. They can combine with olefins to produce larger molecules by Diels-Alder cycloaddition reaction. Condensation of aromatics leads to coke particles. Scheme 1.4 offers some examples of the reaction mechanism of steam-cracking using ethane as example. [13]

Initiation:

(a) $CH_3CH_3 \rightarrow CH_3\cdot + CH_3\cdot$

Propagation:

(b) $CH_3CH_3 + CH_3\cdot \rightarrow CH_4 + CH_3CH_2\cdot$

(c) $CH_3CH_2\cdot \rightarrow CH_2{=}CH_2 + H\cdot$

(d) $H\cdot + CH_3CH_3 \rightarrow H_2 + CH_3CH_2\cdot$

Termination:

(e) $2CH_3CH_2\cdot \rightarrow CH_3CH_2CH_2CH_3$

(f) $CH_3CH_2\cdot + H\cdot \rightarrow CH_3CH_3$

Disproportionation:

(g) $CH_2{=}CH_2 + CH_3CH_2\cdot \rightarrow CH_3CH_2CH_2CH_2\cdot$

$2CH_3CH_2CH_2CH_2\cdot \rightarrow CH_3CH_2CH{=}CH_2 + CH_3CH_2CH_2CH_3$

(h) $CH_2{=}CH_2 + CH_3\cdot \rightarrow CH_3CH_2CH_2\cdot$

$2CH_3CH_2CH_2\cdot \rightarrow CH_3CH{=}CH_2 + CH_3CH_2CH_3$

Scheme 1.4: Steam cracking. Reaction mechanism [13]

The reaction mechanism, which proceeds through the formation of free non-selective radicals, is a chain reaction that entails initiation, propagation, and termination. The initial step involves the cleavage of a C-C bond or a C-H bond leading to the formation of

free radicals. Propagation of the chain mechanism occurs by several different radical reactions which in turn produce radicals as products. These radicals can, at anytime, react with each other to produce a non-radical species. These latter reactions, where radicals are consumed, are called termination steps because the products have no further reactivity with respect to chain initiation.

1.3.3. Catalytic Cracking

Catalytic cracking is defined as a cracking process that operates at quite moderate temperature in the presence of an acidic catalyst. It is a remarkably versatile and flexible process with principal aim to crack lower-value stocks and produce higher-value lighter liquids and distillates. Also, light hydrocarbon gases, which are important feedstocks for the petrochemical industry, can be produced by this process. [3] The products of catalytic cracking are basically the same as those of thermal cracking besides the use of a catalyst to improve process efficiency. [14] A wide range of solid acidic catalysts are employed but zeolites are the most performing ones. The Y zeolite is the main zeolitic component of the FCC process, which can be incorporated in industrial catalysts in various form: REHY (rare earth-exchanged HY), REY (rare earth-exchanged Y), HUSY (H form of ultra stable Y zeolite), and REHUSY (rare earth-exchanged H form USY). [15] Fluid Catalytic Cracking (FCC), hydrocracking, and Deep Catalytic Cracking (DCC) are the most common examples of catalytic cracking process. Fluid Catalytic Cracking (FCC) is the most widely used process which can be regarded as the main process for large-scale gasoline production with high octane number. [16] The main catalyst used in FCC process is Y zeolite. Currently, ZSM-5 Zeolite is used to increase the yield of light olefins which are produced as secondary products. [17, 18] The reaction is endothermic.

The reaction temperature ranges from 450 to 560℃. In the FCC process, a fluidized bed is used in order to provide an instantaneous regeneration of zeolite as deactivation of catalysts by the coke (i.e. non-volatile carbonaceous deposits) formation on the surface of the catalysts during the hydrocarbon reactions is a serious problem. Fig.1.3 illustrates a fluid catalytic cracking reactor. [14]

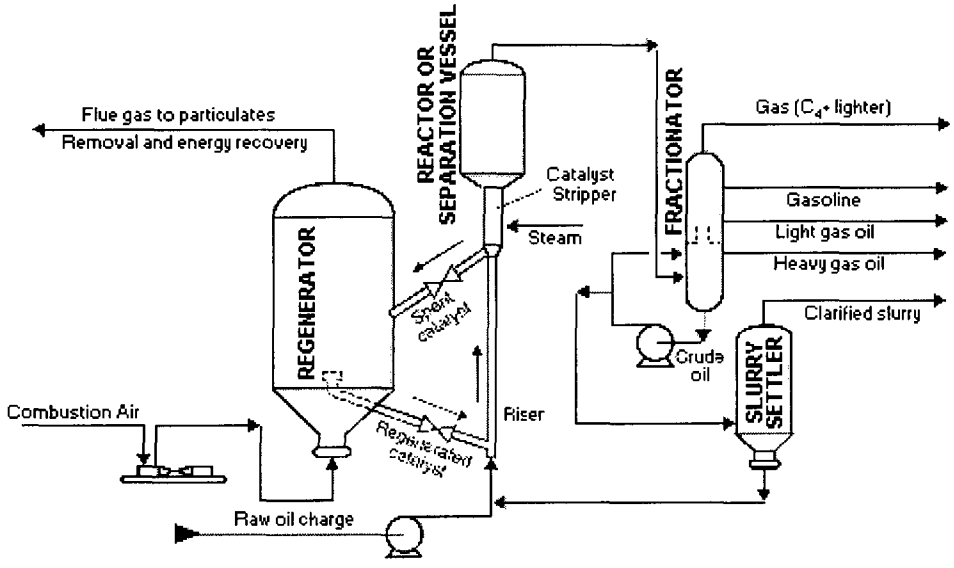

Fig.1.3: Detailed schematic of a fluid catalytic cracking reactor

Catalytic cracking is a heterogeneously acid catalyzed reaction. In order for catalytic cracking reactions to take place, the reactants should be able to reach the active sites on the surface of the catalysts. There are several steps involved in the introduction of reactant and its final formation as product. As shown in scheme 1.5, these reaction steps are including: 1) external diffusion of reactants from the bulk phase to catalyst surface, 2) internal diffusion into pores, 3) adsorption of the reactants onto active sites, 4) transformation into products via chemical reactions on the active sites, 5) desorption of the products from active sites, 6) internal counter-diffusion, and 7) external counter-

diffusion of the products from the catalyst surface into the buld phase. [15, 19-23] Step 4 is the key step of cracking of hydrocarbons which occurs via carbocation intermediate on the acidic catalysts that contain Brönsted and Lewis acid sites as active sites. Carbocations are longer lived and accordingly more selective than free radicals. The sequential catalytic reaction proceeds through three steps, the initiation (formation of carbocation), "propagation", and termination (desorption of product and restoration of active sites).

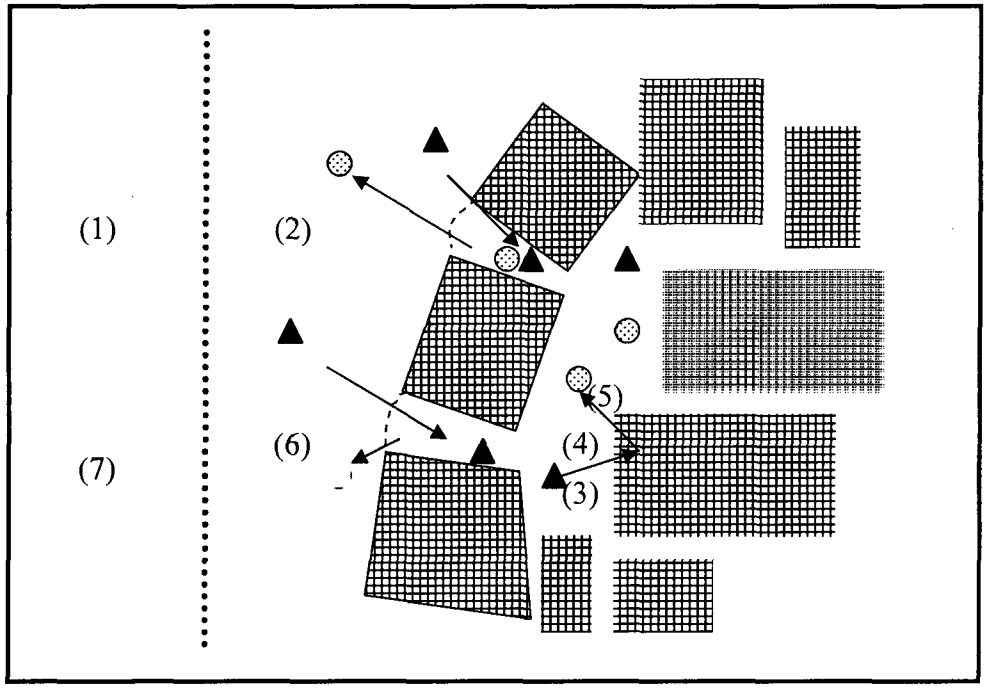

Scheme 1.5: Individual steps of catalytic cracking reactions

The initiation step involves the formation of carbocations through the interaction of adsorbed hydrocarbon with the active sites. Suggested forms of carbocations include carbenium and carbonium. Several reaction pathways have been proposed and are widely accepted in the literature.

1) Tung et al. [24] and others [25, 26] have suggested that the abstraction of a hydride by a Lewis site can lead to the formation of a carbenium ion.

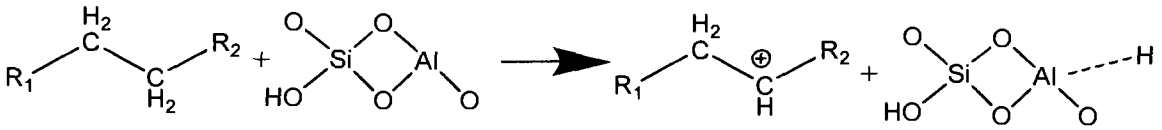

"paraffins" "Lewis Acid Sites" "carbenium"

2) On the other hand, carbonium ions can be formed via abstraction of a hydride ion by a strong Brönsted site as suggested by Greensfelder et al. [27] and others [28-31].

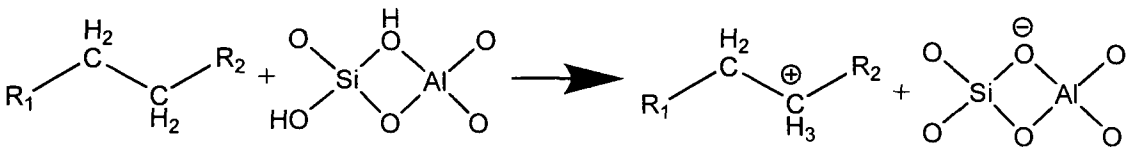

"paraffins" "Bronsted Acid Sites" "carbonium"

3) In addition, the formation of an initial carbenium ion via the protonation of olefinic species has been proposed. The olefinic species are present in the feed as either impurities or the products from thermal cracking. [32, 33]

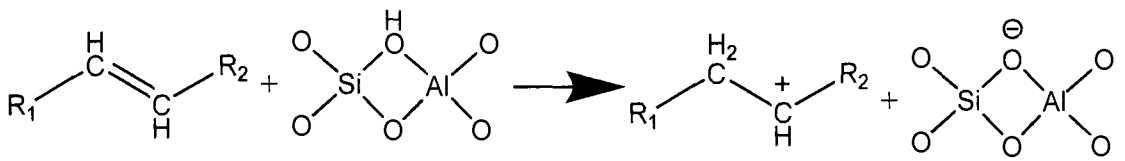

"olefins" "Bronsted Acid Sites" "carbenium"

4) Besides the carbenium pathway, it was also proposed that the paraffin cracking could start the carbonium ion transition state, which was proposed by Haag and Dessau. [34] They suggested that a C-C bond could be protonated by Brönsted acid sites forming pentacoordinated carbonium ions, which can in turn split to produce smaller paraffin and a carbenium ion. The carbonium ions may also convert into carbenium ions by the loss of hydrogen molecules.

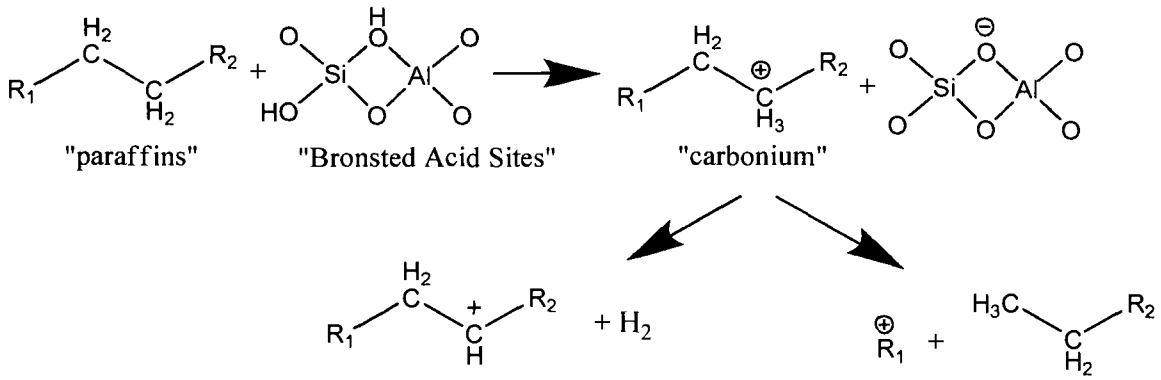

After the initiation step, there are several possibilities for the formed carbenium ions described as follows.

1) The carbenium ion formed on the acid sites (Brönsted and/or Lewis) may desorb as an olefin and restore the active sites. [19] If the carbonium comes from a pentacoordinated carbonium ion, then this is the Haag-Dessau cracking mechanium, also known as monomolecular cracking mechanism. This reaction is favoured at high temperature, at low conversion and under low hydrocarbon partial pressure, and also by zeolites with high constraint indexes, for example ZSM-5 zeolite. [21, 35 and references therein]

2) Also, the carbenium ion undergoes a β-scission cracking, leading to the formation of a smaller olefin and a smaller carbenium ion. [35] The C-C β-scission may occur on either side of the carbenium ion.

$$\mathbf{R\text{-}CH_2\text{-}CH^+\text{-}CH_2\text{-}CH_2\text{-}R' \rightarrow R\text{-}CH_2\text{-}CH_2{=}CH_2 + CH_2^+\text{-}R'}$$

$$\mathbf{(or\ R^+ + CH_2{=}CH\text{-}CH_2\text{-}CH_2\text{-}R')}$$

3) In addition, the adsorbed carbenium ion may go through several types of reactions such as hydrogen transfer (HT), isomerisation, aromatization, cyclization, polymerization, etc. [32 and references therein]

a) The adsorbed carbenium can interact with a neutral paraffin molecule via hydride transfer. This bimolecular reaction will lead to the formation of a new carbenium ion, which in turn undergoes a β-scission cracking. In contrast to the monomolecular cracking reaction, bimolecular reaction is favoured at low temperature, under high hydrocarbon partial pressure, and by zeolite with low constraint indexes and high acid sites density, for example Zeolite Y.

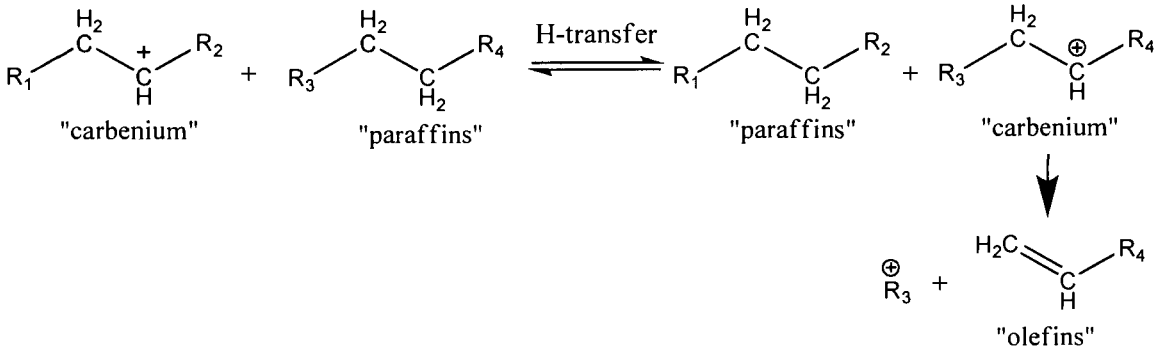

b) Isomerization of the adsorbed carbenium ion via hydride shift or methyl shift may lead to the formation of more stable carbenium ions.

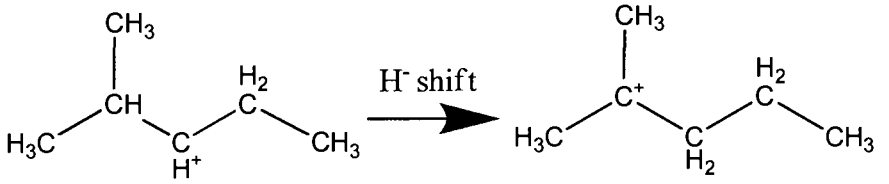

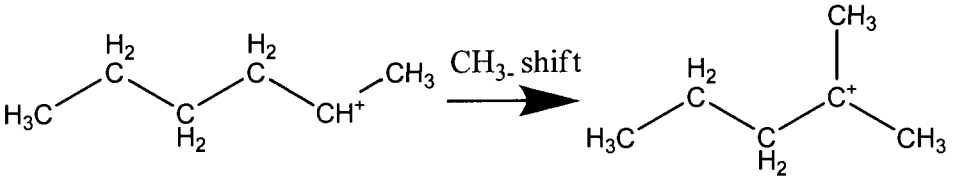

c) Aromatization reaction of the adsorbed carbenium ion may occur via the dehydrocyclization of paraffin, as long as the formed olefinic species has a configuration that is conductive to cyclization. [3]

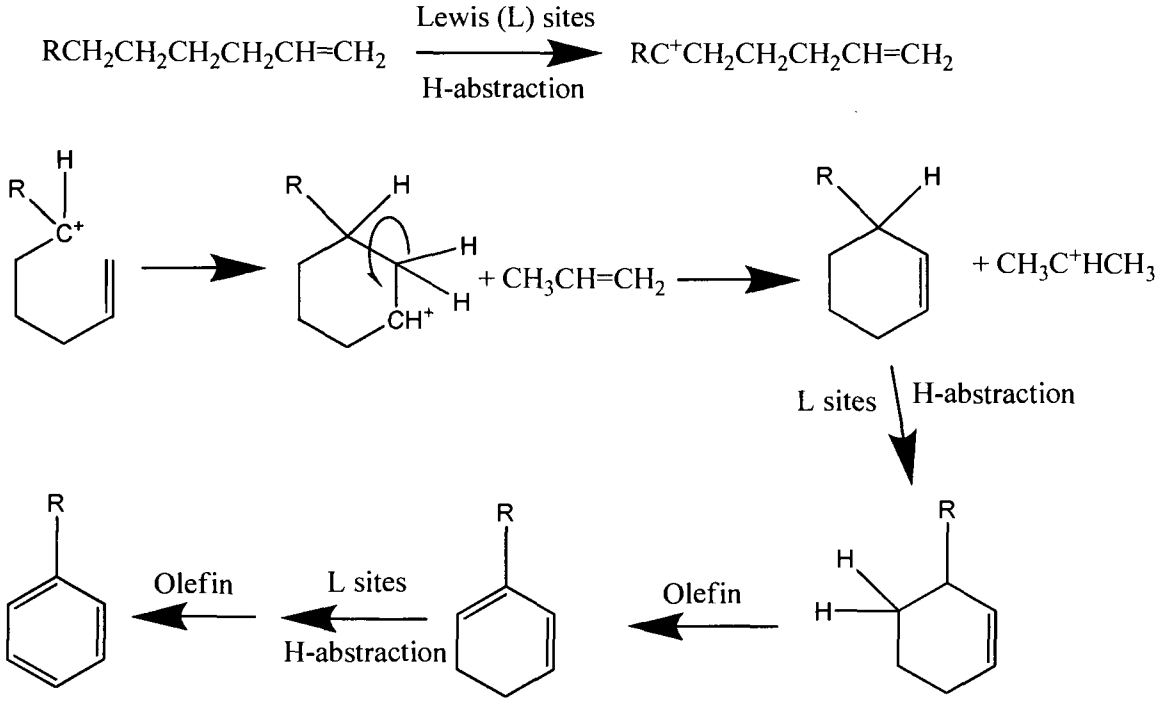

Aromatization can also occur via hydrogen transfer reaction. [35, 36]

$3C_nH_{2n}$ (olefin) + C_mH_{2m} (naphthalene) → C_nH_{2n+2} (paraffin) + C_mH_{2m-6} (aromatics)

1.3.4. Challenges in the Light Olefins Industry

First, the rapid growth in the world demand for propylene is one of the main significant obstacles facing the current light olefin industry, which is due to the continuous demand growth for polypropylene (Fig.1.4). Polypropylene is important for the business of injection molding and fiber segments. [4, 8, 37]

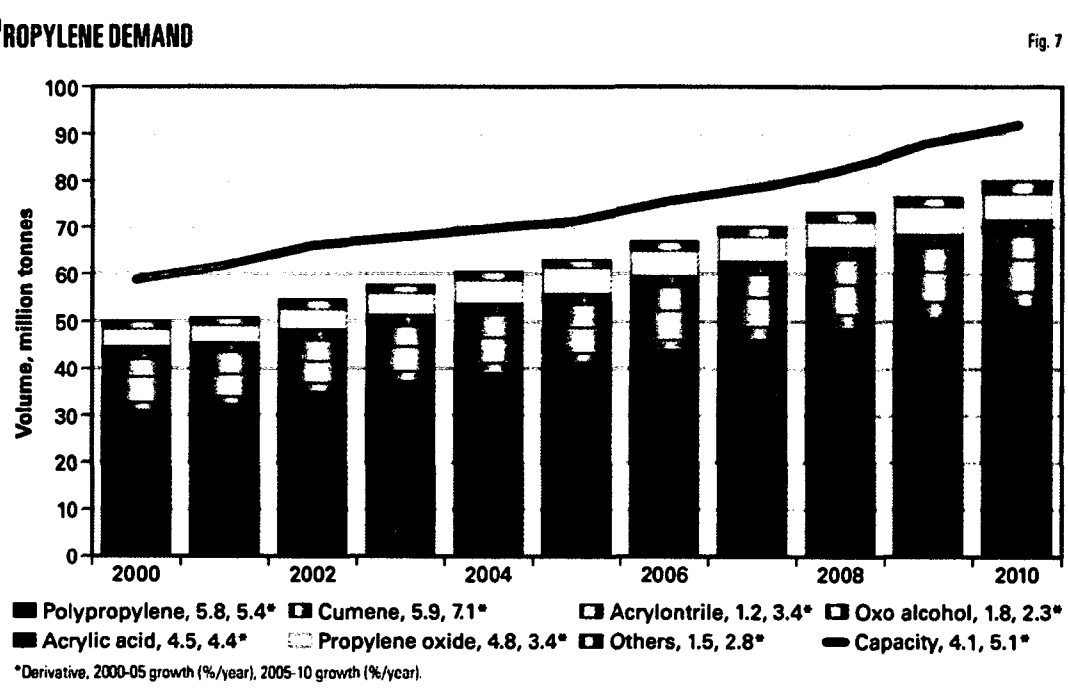

Fig.1.4: Propylene Demand 2000-2010 [4]

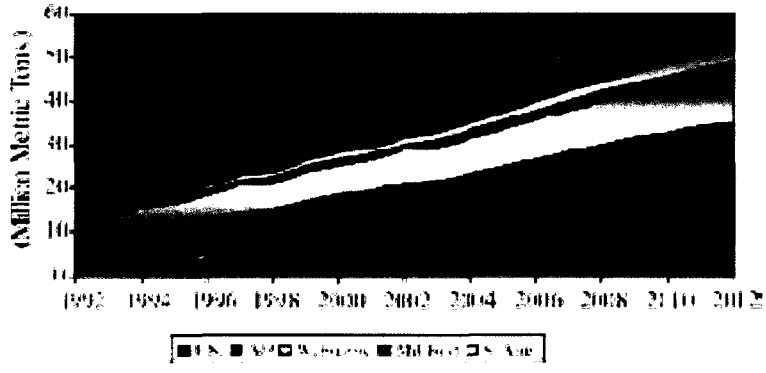

Fig.1.5: Regional Polypropylene Demand [8]

As shown in Fig. 1.5 [8], Asia is going to be the dominant region with respect to the high world propylene demand in the near future. However, with the current technology, propylene is only produced as a by-product or at best a co-product. About 70% of worldwide production for propylene comes from steam cracking as a co-product to ethylene, 28% from fluid catalytic cracking as a co-product to gasoline and the remaining

2% from on-purpose processes such as catalytic propane dehydrogenation, metathesis and other. [37] As a result of continuous rapid growth in the demand for propylene, a great deal of pressure will be added on conventional olefin technologies. [6]

In addition to the rapid growth in the demand for propylene, the energy consumption is another significant roadblock in the light olefins industry. The current steam cracking process consumes as much as 40% of the energy used by the entire petrochemical industry due to the high operation temperature. [38]

Also, global environmental issues have stimulated the development that minimizes greenhouse gases (GHG) emissions. [38] Greenhouses gases such as CH_4 and CO_2 are produced during the run-regeneration cycle. For example, total greenhouse gas emissions in Canada in 2006 were 721 mega tonnes of carbon dioxide equivalent (Mt of CO_2 eq). [39] The emission from fossil fuel industries was 43.1 mega tonnes. Thus, more strict environmental regulations require low greenhouse gases emission also put a strain on the conventional olefins technologies. [6]

1.4 Newly Developed Thermo Catalytic Cracking (TCC) Process

1.4.1. Overview of the TCC process

The thermo catalytic cracking (TCC) has been developed and extensively studied since 1998 with the objective to selectively produce light olefins, particularly ethylene and propylene in quite equal proportions, from liquid hydrocarbon feedstocks (i.e. petroleum naphthas and gas oils). [40-45] This process has been recognized as a promising alternative route for light olefins. [6] The TCC process combines the (mild) thermal cracking with the effect of a moderately acidic catalyst. By doing this, high yields of ethylene and propylene (and other light olefins) can be produced while

operating at a temperature much lower than those used for the steam cracking process. Also, this process shows a significantly lower emission of greenhouse gases, compared to the conventional steam cracking. [43]

There are two versions of the TCC process: one-zone and multi-zone reactors. on a one-zone reactor, the catalysts need to work under steam atmosphere and at quite high temperature. As show in scheme 1.6, the multi-zone reactor configuration comprises a precatalytic zone (quartz beads) and a catalyst bed (catalyst extrudates). [6]

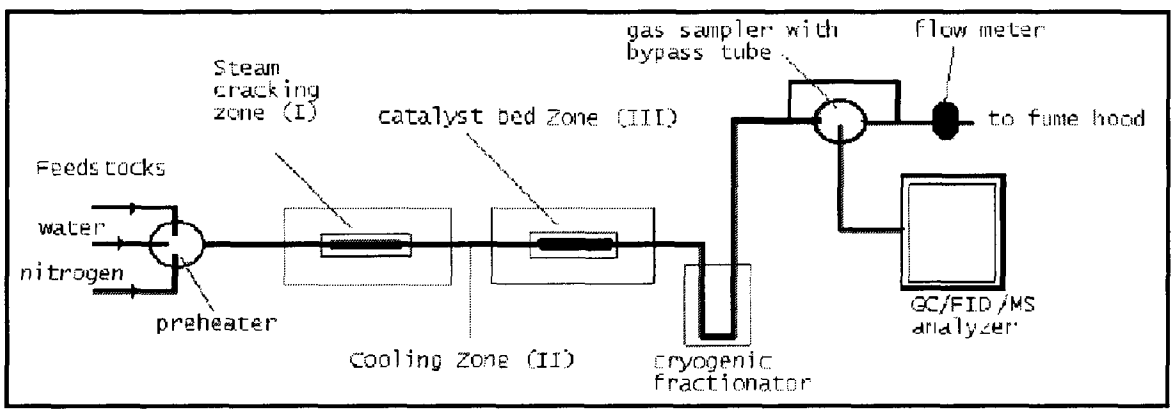

Scheme 1.6: Schematic representation of TCC multi-zone reactor configuration [6]

1.4.2. The Hybrid Catalyst Used in the TCC process

Most catalysts used in the TCC process are in hybrid configuration. They are constituted of two porous components. The main component has active sites having cracking properties (acid sites). The co-catalyst has an active surface that can affect the product selectivity of the former (cracking) sites. For the most recent version of the TCC catalysts, the role of the main component is to crack large hydrocarbon molecules over the active sites provided by the (Mo-P) species while the resulting smaller molecules are subsequently cracked over the acid sites from the surface of a zeolite (i.e ZSM-5). [42] The co-catalyst contains active metal species (Ni, Re, Ru) that are dispersed on a

thermally and hydrothermally stable support. [42, 43, 46] Finally, these two components are bound to each other by bentonite clay, which is an inert inorganic binder. The "ideally sparse particles configuration" in the hybrid catalyst ensures an easy two-way diffusion of reaction intermediates within the catalyst network, in virtue of the "pore continuum" effect (Fig.1.6). [47-49]

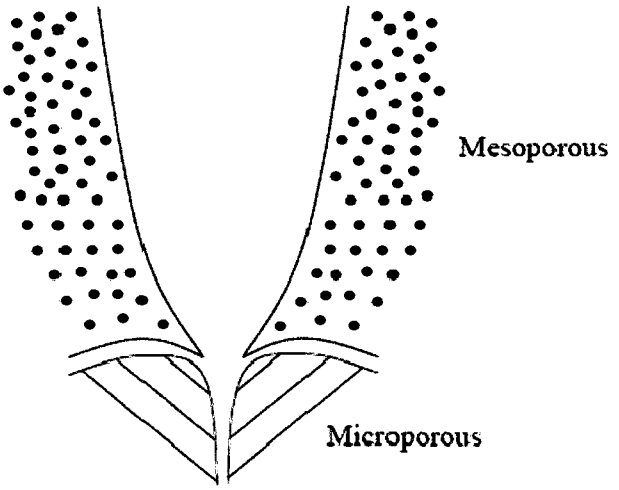

Fig.1.6: Concept of pore continuum in hybrid catalysts

1.4.3. The Hydrogen Spillover Phenomenon

Particularly in the present study, the role that the co-catalyst is expected to play is to promote the hydrocarbon steam-reforming. Then, some hydrogen species can be produced and then spilt over onto the surface of the main acidic component. These hydrogen spilt-over (HSO) species may interact with the intermediates of the cracking reaction on the surface of the main component. Thus, the formation of coke precursors can be retarded, so that the run length can be improved(Fig.1.7).

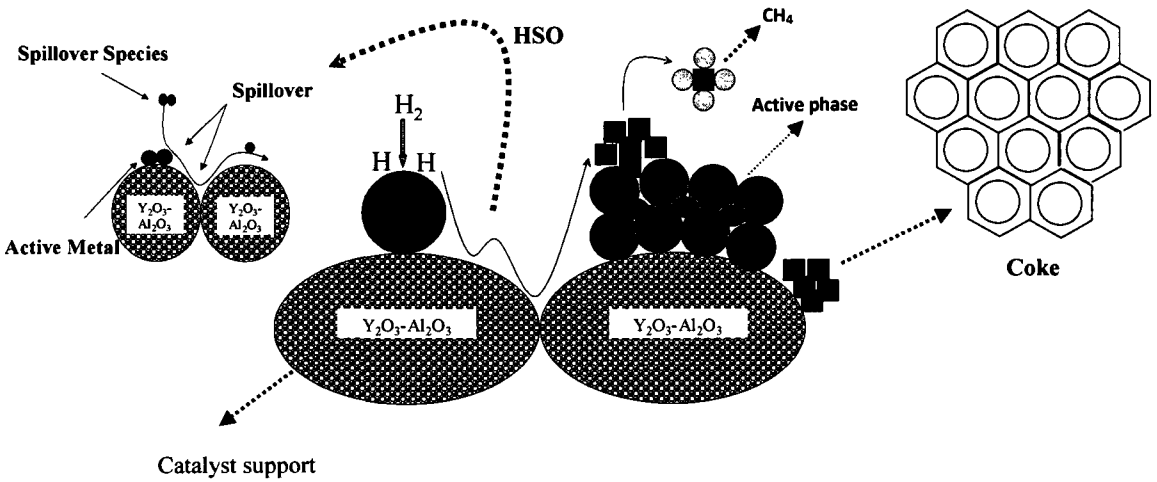

Fig.1.7: Concept of hydrogen spillover phenomenon [55]

At this moment, the actual nature of spilt over hydrogen species is not known with absolute certainty. Possible forms include H atoms, radicals, H^+ and H^- ions, ion pairs, H^{3+} species or protons and electrons. [50, 51] Several explanations have been proposed and some were widely accepted in the literature. For example, Nakamura et al. suggested that H^+ regenerates Brönsted acid sites while H^- stabilizes the carbenium ion intermediate by its hydrogenation. [52] Hattori et al. suggested that Brönsted acid sites, which are generated from spilt-over hydrogen, can act as the active sites for the catalytic reaction. [53] Hosoi et al. found the hydrogen could remove coke by hydrogenation it. [54 and reference therein] Ueda et al. observed that migration of pyridine from the Lewis acid site to the Brönsted acid site was drastically promoted by the hydrogen spillover effect. It is suggested the desorption of basic molecules on Lewis acid sites is promoted by spilt over hydrogen, which means that hydrogen spillover has some effect on the inhibition of poisoning acid sites in catalytic reactions. These explanations show that spilt over hydrogen may affect the acidic sites of solid catalysts significantly.

1.5. Principles of Catalyst Characterization

1.5.1. Brunauer Emmet and Teller (BET) Technique

BET technique can be used to determine certain textural properties of porous solids, for example the specific surface area, the pore volume, the average pore diameter, the pore shape, the pore size distribution, and the shape of the nanometric cavities and pore openings. [56]

The specific area is defined as the measurement of the accessible surface area per unit mass of solid (adsorbent); this surface S is the sum of the internal pore surface area and of the external boundary surface area,

$$S = A_m \frac{Na * V_m}{\bar{V}_m}$$

where S is the specific surface area, Na is the Avogadro constant, $\bar{V}_m$ is the molar volume of the adsorbate, A_m is the part of surface occupied by one molecule of adsorbate in a close layer (for example, for nitrogen, A_m is equal to $16.2*10^{-20}$ m^2), V_m is the monolayer capacity of the unit mass of adsorbent (the volume of adsorbate just sufficient to cover the surface developed by the unit mass of adsorbent) and can be determined by BET method.

In 1938, Brunauer, Emmett and Teller (BET) proposed a model for physical adsorption of gas molecules on a solid surface and V_m can be estimated by the BET equation,

$$\frac{x}{V_a(1-x)} = \frac{1}{V_m C} + \frac{C-1}{V_m C} x$$

where V_a is the adsorbed volume of the adsorbate per unit mass of adsorbent, V_m is the monolayer capacity of the unit mass of solid, x is the relative pressure p/p_0, C is a

constant that is dependent on the adsorbent-adsorbate interaction. [56] It behaves as a straight-line in the form of y = ax + b for x varying from 0.05 to 0.35. Subsequently, V_m and C can be derived from the slope and intercept of the line on the graph. To apply the equation, they assumed the following facts: (1) a multilayer adsorption even at very low pressure; (2) the adsorption occurring on well defined sites and all the sites have the same energy, each of them can only accommodate one adsorbate molecule; (3) adsorption-desorption equilibrium is supposed to be effective between molecules reaching and leaving the solid surface.

The specific pore volume is defined as the accessible pore void space in the particles per unit mass of solid.

The cumulative specific surface or pore volume (S_{cum} and V_{cum}) are the sum on k of

$$S_{cum} = \sum S_k \qquad V_{cum} = \sum V_k$$

where S_k and V_k are respectively the specific surface area and the volume of the pores of radius r_k for the k_{th} interval: $S_k = 2V_k/r_k$.

The pore size distribution is the distribution of the pore volume versus the pore size.

The average pore size is obtained by the equation: $r_{average} = 2V_p/S$, where V_p is the pore volume, and S is the total surface area. The pores are classified into macropores (with size larger than 50nm), or mesopores (with size in the range from 2nm to 50 nm) or micropores (with size smaller than 2nm).

For the BET method, the most popular adsorbates are nitrogen and argon. Usually, nitrogen is preferred due to its availability and low cost. In this work, all the

measurements of solids and catalysts were carried out on the basis of nitrogen adsorption isotherms. The textural studies were carried out with a Micromeretics ASAP 2000 Model system. The specific surface area was measured by BET method (i.e. BET plot at relative pressure between 0.05 and 0.35). Microporous volume and surface area were measured by t-plot method, which is a linear curve of the adsorbed volume against t (the statistical thickness t of the adsorbed layer) in the range of 0.35 and 0.5 nm. Its slope is directly proportional to the surface area and its positive intercept by extrapolating the line to t = 0 corresponds to the adsorbed volume of micro pores. The reference isotherm used to determine the dependence of t vs. p/p_0 is derived from the Harkins-Jura equation:
$t = (13.99 / (0.034 - \log (p/p_0))^{1/2}$. Mesoporous volume and mesopore size distribution were determined by the method of Barrer, Joyner and Halenda (BJH). In mesopores regions, the adsorption capillary condensation takes place when p/p_0 is greater than 0.4 based on Kelvin equation. The physical volume of pores and the average pore size can be calculated from the adsorbed volume and the assumed pore geometry. The pore size distribution was investigated by plotting the differential pore volume F = dV/dlogD as a function of the pore diameter D (desorption phase, V and D in cm^3 and nm, respectively). Macropore volume was the difference between the total volume of uptake and the sum of microporous and mesoporous volume. [57]

1.5.2. Thermogravimetric and Differential Thermal Analyses (DTA/TGA)

In the present work DTA/TGA techniques were carried out on a PL Thermal Sciences, STA-1500 Model apparatus to investigate the amount and the nature of coke deposited on surface of the catalysts used in the on-stream tests for the cracking of hydrocarbons.

TGA is a technique in which the variation of the mass of a substance is measured as the temperature of the substance is varied. Changes in the mass are caused by decomposition or oxidation in the air of the substance. DTA is a technique which detects the temperature changes between the sample and an inert reference material during a programmed change of temperature, involving an exchange of energy ($\Delta H \neq 0$), for example a chemical reaction or a first order phase transition. The peaks on the DTA curve show either exothermic or endothermic process which takes place in the sample during the temperature programmed heating. Combined with the TGA curve, whether a chemical reaction or a first order phase transition occurs can be determined. [58]

1.5.3. Temperature Programmed Desorption of Ammonia (TPD-NH_3) and Adsorption/Desorption of Pyridine

1.5.3.1 Ammonia TPD

Temperature programmed desorption of ammonia is a method which can be used to measure the density of acid sites and to determine their distribution in terms of acid strength. [59] A new method for the study of surface acidity of zeolites by TPD-NH_3 was developed in our Industrial Catalysis Laboratory, Department of Chemistry and Biochemistry, Concordia University, several years ago. It uses a pH-meter equipped with an ion selective electrode, instead of the classical analytical method making use of a gas chromatograph equipped with a thermal conductivity detector. Desorbed ammonia is captured by an acetic acid solution. An ion selective electrode (ISE) is used to continuously record the concentration of ammonium ions formed by the neutralization reaction. The acidity density can be calculated, and an "acid site strength profile" can be obtained by plotting the relative rate of desorbed NH_3 versus the temperature.

1.5.3.2 Adsorption/Desorption of Pyridine

FT-IR using pyridine as probes can be used to determine the acidity type, i.e. Brönsted or Lewis acid site. In this work, the nature of the surface acid sites was studied by chemical adsorption of pyridine onto clean self-bonded sample wafers after an outgassing under vacuum at 200°C for 3 h. The adsorption of pyridine was done at 100°C for 2 h. Finally, the physisorbed pyridine was removed under vacuum at various temperatures (100, 300, or 500 etc.) for 1 h. The spectra were recorded in the 400 – 4000 cm^{-1} region (with resolution of 4 cm^{-1}) using transmission mode on a Nicolet Magna IR Spectrometer 500 Model. The main peaks of interest for the sorbed pyridine are the ones at 1450 cm^{-1} and 1550 cm^{-1} that are usually assigned to the Lewis and Brönsted acid sites, respectively. [60]

1.6. OUTLINE

This section outlines the format of this Manuscript-based thesis.

Chapter I

This chapter provides a general introduction to light olefins and related reaction mechanisms in petroleum conversion (both catalytic and non-catalytic), as well as any necessary background information that are required to read this thesis. In particular, I will present an overview of the industrial significance of light olefins and the current technologies for their production. In addition, I will discuss about the roadblocks in the conventional light olefins production technologies. Then, the newly developed Thermo Catalytic Cracking (TCC) process will be described in detail.

Chapter II

This chapter shows the effect of the spilt-over hydrogen species on the product yields of the hybrid catalysts used in the thermo catalytic cracking (TCC) process for the production of light olefins. The supported Ni co-catalyst surface of the thermocatalytic cracking (TCC) hybrid catalyst produces very active hydrogen species. Such species, once transferred (spilt-over) onto the surface of the main catalyst component (cracking sites), interact with the adsorbed reaction intermediates, resulting in a decreased formation of coke precursors (polynuclear aromatics) and in the dearomatization/ring-opening of some heavy compounds of the feed. Simultaneously, there is a significant increase in the product yields of light olefins, particularly ethylene and propylene. Analysis of reaction products after 10 h of continuous reaction shows the very significant effects of these co-catalysts on heavy feedstocks such as vacuum gas oils, although the amounts of these (spilt-over) hydrogen species are very small, in comparison with the molecular hydrogen produced by the cracking reactions.

Chapter III

In our previous work (Le Van Mao, R.; Vu, N. T.; Al-Yassir, N.; Yan, H. T.; *Ind. Eng. Chem. Res.* (**2008**) 47:2963, (Chapter II), we have found that the hydrogen spill-over effect may play a key role in improving the catalytic activity of the hybrid catalysts of the TCC process. This effect advantageously contributes to (1) increasing the yields of light olefins, (2) producing less heavy compounds, and (3) lengthening the run length when a fixed bed (and tubular) reactor is used. In addition, the hydrogen spill-over effect was found to be more pronounced when a heavy feedstock (i.e. gas oil), which usually contains large amount of polynuclear aromatics, was used. Thus, our attention was diverted into the effect of existing aromatics on the reactivity of hybrid catalysts.

Polymethylbenzene (1,2,4-trimethylbenzene or pentamethylbenzene) was chosen as model molecule and added into n-hexane feedstock, and the cracking reaction of the mixture was performed. The obtained results showed that at large concentrations of 1,2,4-trimethylbenzene, the hydrogen spillover species showed some significant retarding effect on the coke formation while with a n-hexane feed containing pentamethylbenzene, this effect was much less visible because the adsorbed PMB was structurally much closer to coke-precursor ion than the 1,2,4-trimethylbenzene, or because the less methylated benzene could undergo conversion in accordance with a newly hypothesized mechanism. Finally, the (HSO) species could affect the reaction intermediates only when the latter were formed on the external surface of the zeolite. This means that there was a limitation in the motion of the hydrogen spilt-over species.

Chapter IV

It has been found that hydrogen spillover effect has significant retarding effect of coke formation, and the hydrogen spilt-over species may only be transferred onto the external surface of the main component of the hybrid catalyst (i.e. it has a limited effective distance). In this chapter, we provided more evidence in support of the previous proposal (Yan, H. T.; Le Van Mao, R.; *Catal. Lett.* (**2009**) 130:558, (Chapter III)). In addition, the influence of the pore characteristics and the acidity properties of the ZSM-5 zeolite-based component on the overall catalytic performance has been investigated. Data of the present work shows that, in order to obtain higher yields in light olefins, the ZSM-5 zeolite - the cracking component of the hybrid catalyst, must have a relative low SiO_2/Al_2O_3 ratio, so that its density of acid sites is high (resulting in high total conversion) with a relatively mild acid strength (favouring a high propylene/ethylene

ratio). On the other hand, such milder acid sites also lead to a lower amount of deposited coke, the latter exhibiting actually a lighter chemical nature. This may ease the cleaning action of the hydrogen spilt-over species, resulting finally in a greater on-stream stability of the hybrid catalyst. The present data, related to the intrinsic properties of the zeolite component, are useful for the development of the hybrid catalysts being used in the Thermo-Catalytic Cracking process (TCC, fixed-bed technology).

Chapter V

This chapter gives brief conclusions of the work presented in this thesis as well as some suggestions for future work.

Chapter II

Effect of the Spilt-over Hydrogen Species on the Product Yields of the Hybrid Catalysts Used in the Thermocatalytic Cracking (TCC) Process for the Production of Light Olefins

Published as:

R. Le Van Mao, N. T. Vu, N. Al-Yassir, and H. T. Yan

Ind. Eng. Chem. Res. (**2008**) 47:2963

2.1. INTRODUCTION

Ethylene and propylene are the most important "first generation" intermediates of the petrochemical industry, whose end-products include main plastics and synthetic fibres. [61] The current technology of production of these olefins is steam cracking, using various hydrocarbon feedstocks (ethane, propane, naphthas, and gas oils). Market demands for ethylene and propylene recently have experienced significant and constant increases, showing, in particular, a higher growth rate for propylene. [62] However, because the product selectivity of the steam cracking for propylene is quite low, the supply of this light olefin can be compensated through the use of other processes, such as propane dehydrogenation, olefin metathesis, and, primarily, fluidized catalytic cracking (FCC). The latter technology, whose main mandate is to produce gasoline, must incorporate some ZSM-5-type zeolite as a catalyst additive so that the production of light olefins, particularly propylene, can be increased significantly.

The thermocatalytic cracking (TCC) process has been developed with the objective to selectively produce light olefins particularly ethylene and propylene in quite equal proportions from liquid hydrocarbon feedstocks such as petroleum naphthas and gas oils. [63-65] The TCC process, which combines the (mild) thermal cracking with the effect of a moderately acidic catalyst, can provide very high yields of ethylene and propylene (and other light olefins) while operating at a temperature much lower than those used for steam cracking. Most of the catalysts used are in the hybrid configuration, i.e., they are composed of two porous components: a main component which has cracking properties, and a co-catalyst which has active sites that can affect the product selectivity of the former (cracking) sites. These two catalyst particles are bound to each other by an

inorganic binder that, in most cases, is bentonite clay. The "ideally sparse particles configuration" in the hybrid catalyst [65] ensures an easy two-way diffusion of reaction intermediates within the catalyst network; this is the so-called "pore continuum" effect, which has been observed on many occasions, such as in adsorption/desorption [66] and in different catalytic reactions such as aromatization and cracking. [67-70] Because the reaction temperature is relatively high (700-750 °C), the active support must be very thermally stable (such as the amorphous alumina aerogel being stabilized by yttria [71] or ZSM-5 zeolite being stabilized by lanthanum, which has been done in this work).

The role that the co-catalyst is expected to play is to produce some hydrogen species, in virtue of its steam-reforming activity, and to spill them over its surface to the acidic sites of the main catalyst component. It is believed that, with such a catalyst working concept, the coking can be reduced, so that the run length (the period of time separating two catalyst decoking operations when a tubular reactor is used) can be increased. The first experimental evidence of this beneficial effect was reported by Le Van Mao et al., [65] when co-catalysts that contained Pt and Pd-Sn were used. In the present work, nickel-loaded (nickel alone or doped with rhenium or ruthenium) co-catalysts are used instead, because they are more thermally and chemically resistant than the Pt or Pd co-catalysts, because the overall reaction system is subjected to very drastic conditions (high temperature, the presence of steam, etc.) and contaminants (sulfur, for example).

2.2. EXPERIMENTAL

2.2.1. Catalyst Preparation

2.2.1.1. Preparation of the "Alumina Aerogel" Support (AAS)

The yttria-stabilized alumina aerogel was prepared using a (sol-gel) procedure that was similar to that reported by Le Van Mao et al. [60] After the solid material has been activated at 750 °C for 3 h, it shows the following (approximate) chemical composition: 10 wt % Y_2O_3, with the balance being Al_2O_3.

2.2.1.2. Preparation of the Main Catalyst Components (MCC)

2.2.1.2.1. MCC-1

A solution of 4.81 g of ammonium molybdate hexahydrate (Aldrich) in 100 mL of 1.8 N H_3PO_4 was homogeneously impregnated onto 40.02 g of alumina aerogel support (AAS). After drying at 120 ℃ overnight, the resulting solid was impregnated with a solution that was composed of 1.04 g of cerium(III) nitrate (Aldrich) in 30 mL of deionized water. The solid (MCC-1) was first dried at 120 ℃ overnight and activated in air at 500 ℃ for 3 h. Its chemical composition was as follows: MoO_3, 7.8 wt %; CeO_2, 0.8 wt %; phosphorus, 3.7 wt %; and Y-Al_2O_3, balance.

2.2.1.2.2. MCC-2

A solution that was composed of 1.79 g of lanthanum nitrate hydrate (Strem Chemicals) in 50 mL of deionized water was homogeneously impregnated onto 20.00 g of ZSM-5 zeolite/25H (powder, acid form, silica/alumina molar ratio = 34, purchased from Zeochem), which had been previously dried at 120 ℃ overnight. After being left at room temperature for 1 h and dried at 120 ℃ overnight, the solid was activated in air at 500 ℃ for 3 h. The solid was then homogeneously impregnated with a solution of 2.73 g of ammonium molybdate hexahydrate (Aldrich) in 36 mL of 3 N H_3PO_4 and 15 mL of deionized water. The solid was dried at 120 ℃ overnight and activated at 500 ℃ for 3 h. Its chemical composition was as follows: MoO_3, 8.3 wt %; La_2O_3, 3.7 wt %; phosphorus,

4.2 wt %; and zeolite, balance.

2.2.1.3. Preparation of the Co-catalysts (Co-Cat)

2.2.1.3.1. Co-Cat 1(*n*)

Nickel-loaded co-catalysts were prepared as follows. A solution of X g of nickel nitrate hexahydrate (Strem) in 15 mL of deionized water was homogeneously impregnated onto 5.00 g of AAS. After drying at 120℃ overnight, the solid was activated in air at 500℃ for 3 h. The resulting solids were called Co-Cat 1(1), Co-Cat 1(2), and Co-Cat 1(3) when X was 0.42, 0.70, and 0.83, respectively. The nickel contents of these co-catalysts were 1.7, 2.8, and 3.4 wt %, respectively.

2.2.1.3.2. Co-Cat 2

A solution of 1.05 g of nickel nitrate hexahydrate (Strem) and 0.23 g of $ReCl_3$ (Alfa Ceasar) in 20 mL of deionized water was homogeneously impregnated onto 10.00 g of AAS. After drying at 120℃ overnight, the solid was activated in air at 500℃ for 3 h. The resulting solid was called Co-Cat 2, which had the following chemical composition: nickel, 2.1 wt %; rhenium, 1.5 wt %; and Y-Al_2O_3, balance.

2.2.1.3.3. Co-Cat 3

Solution A was obtained by dissolving 1.30 g of nickel nitrate hexahydrate (Strem) in 10 mL of deionized water. Solution B was prepared by dissolving 0.011 g of ruthenium acetylacetonate (Strem) in 10 mL of methanol. The mixture of A and B was homogeneously impregnated onto 10.00 g of AAS. After drying at 120℃ overnight, the solid was activated in air at 500℃ for 3 h. The resulting solid was called Co-Cat 3, which had the following chemical composition: nickel, 2.6 wt %; ruthenium, 0.03 wt %; and Al_2O_3, balance.

2.2.1.4. Preparation of the Final Hybrid Catalysts

Hybrid catalysts were obtained by extruding the main component (MCC) with the co-catalyst (Co-Cat) in the following proportions: MCC, 65.6 wt %; Co-Cat, 16.4 wt %; and binder, 18.0 wt %. Bentonite clay (Aldrich) was used as the extruding and binding medium.

The hybrid catalysts HYB 1(1), HYB 1(2), HYB 1(3), and HYB 1(4) were prepared using the MCC 1 with the Co-Cat 1(1), Co-Cat 1(2), Co-Cat 1(3), and Co-Cat 2, respectively.

HYB 2 and HYB 3 were obtained by extruding the MCC 2 with Co-Cat 2 and Co-Cat 3, respectively. Reference catalysts, identified as REF-1 and REF-2, were obtained by extruding MCC-1 and MCC-2 with pure AAS, respectively.

2.2.2. Catalyst Characterization

The characterization of the catalysts has multiple facets:

(1) The various catalyst components were analyzed by atomic absorption spectroscopy for their chemical compositions.

(2) The BET total surface area and pore size of these samples were determined by nitrogen adsorption/desorption, using a Micromeretics ASAP 2000 apparatus.

(3) The surface acidity was studied using the ammonia adsorption and temperature-programmed desorption (TPD) technique. The analytical system used was a pH meter that had been equipped with an ion-selective electrode (ISE), [72] which allowed easy assessment of the density of acid sites, as well as their distribution, in terms of strength. In particular, the density of acid sites was determined by NH_3-TPD/back titration, whereas the acid strength profile was recorded with an ISE/pH meter. [72]

(4) Fourier transform infrared (FT-IR) spectra of adsorbed pyridine were used to elucidate the nature of the acid sites. The transmission spectra were recorded with a Nicolet FT-IR spectrometer (Magna 500 model) in the region of 1400-1700 cm^{-1}, with resolution of 4 cm^{-1}. The samples, in the form of a self-supporting thin wafer, were obtained by compressing a uniform layer of powder (sample/KBr mixture ≈ 0.020 g). The thin wafer was then placed in a pyrex cell and outgassed under vacuum (10^{-2} mbar) at 300℃ for 4 h. Pyridine adsorption then was performed at 100℃ for 2 h. After evacuation at 100℃ for 1 h, the spectra of adsorbed pyridine were recorded at ambient temperature.

(5) Thermogravimetric analysis (TGA) and differential thermal analysis (DTA), using a PL Thermal Sciences Model STA-1500 DTA/TGA apparatus, were used to determine the amount of bound species and/or coke deposited onto the catalyst surface. The flow rates of argon (inert gas) and air (oxidative gas) were set at 20 mL/min. The rate of the temperature-programmed heating (TPH) was set at 10℃ /min.

Table 1 reports the main physicochemical properties of the catalysts used in this work.

2.2.3. Characterization of the Feeds (Hydrocarbon Feedstocks)

The composition of various feeds (hydrocarbon feedstocks) was determined using a Hewlett-Packard gas chromatograph (Model 5890, with flame ionization detection (FID)) that was equipped with a Heliflex AT-5 column (Alltech, 30 m, nonpolar). In particular, naphthalene, phenanthrene, and benzo(a)pyrene were used as model molecules for dinuclear, trinuclear, and polynuclear aromatic hydrocarbons (with boiling point ranges of 200-300℃, 300-400℃, and >400℃). Table 2 reports the chemical compositions of the feeds used in this work.

2.2.4. Experimental Setup and Testing Procedure

Experiments were performed using a Lindberg tubular furnace with three heating zones. The experimental setup and testing procedure were similar to those reported elsewhere. [65] Liquids namely, hydrocarbon feed and water were injected into vaporizers using two infusion pumps. Steam and vaporized hydrocarbons were thoroughly mixed, and the resulting gaseous mixture was then sent into the tubular reactor (a quartz tube with a length of 140 cm, outer diameter (OD) of 1.5 cm, and inner diameter (ID) of 1.2 cm).

Product liquid and gaseous fractions were collected separately, using a system of condensers. The gas-phase components were analyzed using a Hewlett-Packard Model 5890 FID gas chromatograph that was equipped with a 30-m GS-alumina micropacked column (J & W Scientific), whereas the liquid phase analysis was performed using the same GC system as that reported in the previous section, "Characterization of the Feeds". The amounts of hydrogen and carbon oxides evolved were determined using a gas chromatograph (Hewlett-Packard Model HP 5890, with thermal conductivity detection (TCD)) that was equipped with a molecular-sieve packed column.

The testing conditions used were as follows: temperature, 725-740 ℃; total weight hourly space velocity (WHSV) (in reference to feed and steam), 1.7-4.0 h^{-1}; catalyst weight, 5.0-7.0 g; steam/feed weight ratio, 0.5-1.0; and feeds, hydrocarbon liquids from light naphtha to vacuum gas oil.

The yield of product *i* was expressed as the number of grams of product *i* recovered by 100 g of feed injected (wt %).

It is important to note that the experimental error usually observed on calculated

product yields was ±0.2 wt %.

Table 2.1: Main Physicochemical Characteristics of the Hybrid Catalysts and their Components [a]

				Surface Acidity			
				Medium Acid Site		Strong Acid Site	
catalyst/component	density d (g/cm^3)	BET specific surface area, (m^2/g)	total (mmol/g of solid)	mmol/g of solid	NH_3 desorption peak temperature[b] (°C)	mmol/g of solid	NH_3 desorption peak temperature[b] (°C)
ZSM-5 (25H[c])	n.a.	395	0.90	0.56	245	0.34	440
AAS	n.a.	291	0.27	n.o.		n.o.	
MCC-1	n.a.	235	0.62	0.34	281	0.28	411
MCC-2	n.a.	211	0.79	0.45	260	0.34	421
Co-Cat 2	n.a.	267	0.27	n.o.		n.o.	
HYB-1(4) (fresh)	0.372	201					
HYB-1 (4) (used)[d]		157					
HYB-2 (fresh)	0.414	205					
HYB-2 (used)[d]		196					
REF-1(Fresh)	0.333	184					
REF-1 (used)[d]		181					
REF-2 (fresh)	0.407	217					
REF-2 (used)[d]		200					

[a] Legend of abbreviations: n.a. = not applicable; n.o. = not observable. [b] Temperature of the corresponding NH_3 desorption peak. [c] SiO_2/Al_2O_3 molar ratio = 34, Na2O content is <0.05 wt %. [d] Regenerated in air at 600 °C overnight after >40 h of reaction.

Table 2.2: Characteristics of the Hydrocarbon Feedstocks Tested [a]

feedstock	density, *d* (g/mL)	boiling point, bp (°C)	non-BTX C_5-200 °C	BTX aromatics	200-300 °C	300-400 °C	>400 °C
light naphtha, L-N	0.650	45-100	95.2	4.6	0.2	0.0	0.0
medium-range naphtha, m-N[b]	0.729	100-150	87.6	12.2	0.2	0.0	0.0
atmospheric gas oil, AGO-1	0.854	240-350	4.1	0.6	17.2	78.1	0.1
heavy atmospheric gas oil, AGO-2	0.86	175-400	0.1	0.0	25.6	73.7	0.6
vacuum gas oil, VGO	0.892	350-550	2.9	0.3	2.0	85.9	9.0

[a] Sources: L-N, m-N, AGO-1, and VGO were kindly supplied by Ultramar Canada; AGO-2 was kindly supplied by Nova Chemicals. [b] Also called heavy naphtha.

2.3. RESULTS AND DISCUSSION

2.3.1. Effect of the Hydrogen Spilt-Over Species on the Product Yields

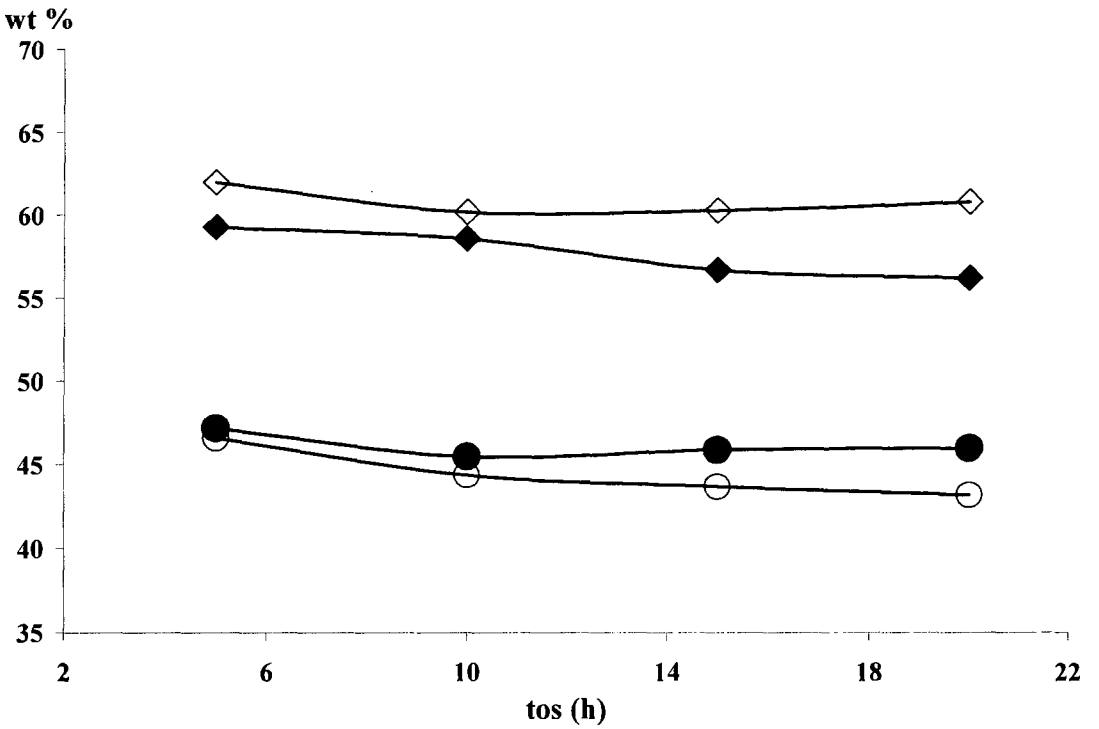

Fig.2.1: On-stream behaviour of hybrid catalyst HYB-1(1) and reference catalyst REF-1. Y_{E+P} = combined product yield of ethylene and propylene, and YUC_2-C_4 =yield of C_2-C_4 unsaturated products (empty symbols denote HYB-1 and full symbols denote REF-1) versus the time-on-stream (tos, given in hours), respectively. Reaction conditions: temperature, 740 ℃; mass of catalyst (W), 5 g; weight hourly space velocity (WHSV) (in reference to feed), 2.0 h^{-1}; feed, light naphtha (L-N); and steam/feed weight ratio, 0.9. Observed product propylene/ethylene ratio = 0.86.

As shown in Fig.2.1, the reference catalyst REF-1, which did not contain any "active" co-catalyst, experienced a slow but noticeable activity decay with the time-on-stream (the activity being represented by the combined product yield of ethylene and propylene, and also the yield of C_2-C_4 unsaturated products). However, the activity of hybrid catalyst, HYB-1(1), which contained a nickel loaded co-catalyst, reached a plateau

after 10 h of continuous reaction. This activity stabilization of the HYB-1(1) catalyst remarkably evidenced the positive role of the Ni species of the co-catalyst on the cracking sites (MoO_3) of the main catalyst component. It was suggested in our previous work [60] that transition-metal species (Pt, Pd, Ni, ...) incorporated onto the co-catalyst surface could produce very active hydrogen. These species, when spilt-over to the surface of the main catalyst component, could slow the coking phenomena on the latter surface. Taking into consideration the presence of hydrocarbons and steam at a relatively high temperature, these hydrogen species were believed to be produced by steam reforming (and subsequent water-gas shift reaction) over the Ni sites of the co-catalyst. In fact, over the hybrid catalyst HYB-1(1) (and not over the reference catalyst REF-1), the carbon oxides (CO and CO_2) were formed in significant amounts at the beginning of the reaction. However, after an induction period that usually lasted 20-30 min, the production of these carbon oxides stabilized at <0.2 wt %.

It is worth noting that such an interpretation of the experimental results was based on the following facts:

(a) Nickel-based catalysts are being used for the production of hydrogen from hydrocarbons, particularly methane, by steam reforming and subsequent reactions. [61, 73]

(b) Hydrogen spill-over species are known to have "cleaning properties", with respect to coke in several reactions. [74-77] In the dehydroaromatization of methane, even small amounts of hydrogen and steam could have some significant coke removal effect. [78]

Table 2.3: Effect of the co-catalyst on the product selectivity of the resulting hybrid catalyst (series HYB 1) [a]

hybrid catalyst	co-catalyst (Ni wt%)	product hydrogen	C_2-C_4 unsaturated (olefins)	(ethylene + propylene) (propylene/ethylene)	BTX	heavy products (200-400+°C)
REF-1	AAS	1.46	49.0	39.1	14.1	9.4
	(0.0)		(45.4)	(0.80)		
HYB-1(1)	Co-Cat 1(1)	1.52	51.2	40.7	13.4	7.4
	(1.7)		(47.1)	(0.81)		
HYB-1(2)	Co-Cat 1(2)	1.53	51.0	40.8	13.3	7.3
	(2.8)		(46.9)	(0.77)		
HYB-1(3)	Co-Cat 1(3)	1.57	53.1	41.5	11.1	6.2
	(3.4)		(48.8)	(0.79)		

[a] Reaction conditions: temperature, 725 °C; total weight hourly space velocity (WHSV) = 1.7 h^{-1}; catalyst weight, 7g; feed, AGO-2 (heavy atmospheric gas oil); steam/feed ratio (by weight), 1.0. All product yields were determined at reaction time of 10 h

Table 2.3 provides more results in support of such hypothesis. In fact, when the nickel content of the co-catalyst increased from 1.7 wt % to 3.4 wt %, the production of heavy products, which contained great amounts of polynuclear aromatics, decreased significantly, whereas the yield of light olefins (particularly, ethylene and propylene) visibly increased. All these phenomena occurred while the production of hydrogen increased only by an extremely small amount, compared to the molecular hydrogen produced by cracking (mostly thermal cracking) when the reference catalyst (with no Ni co-catalyst) was used. In fact, the presence of the nickel-loaded co-catalysts in the hybrid catalysts of Table 3 induced small but noticeable increases in the hydrogen production, when compared to that of the REF-1 catalyst (the nickel-free co-catalyst). Such an increase (Δ) in hydrogen yield was 4.1, 4.8, and 7.5 wt %, for HYB-1(1), HYB-1(2), and HYB-1(3), respectively. On one hand, with the same hybrid catalysts, observed increases in yields of light olefinic products (see Table 3) were as follows: (i) $\Delta(C_2\text{-}C_4$ olefins)) 4.5, 4.1, and 8.4 wt %, respectively; Δ(ethylene and propylene) 4.1, 4.4, and 6.1 wt %, respectively. On the other hand, as previously mentioned, the production of heavy products (200-400+℃), significantly decreased when compared to that of REF-1 catalyst (Δ) 21.3, 22.3, and 34.0 wt %, respectively). Thus, these variations of the product yields had, as a common denominator, the presence of nickel on the co-catalyst surface, which was believed to produce such new hydrogen species by hydrocarbon steam reforming. At this stage of research, the nature of these spilt-over hydrogen species (probably atomic species) was not known with absolute certainty. However, what we can say at the moment is that they were very active, because a small amount of these species was sufficient to induce significant changes in the product selectivity (see Table 2.3).

Table 2.4: Performance of the Reference Catalyst REF-2, using various feedstocks[a]

	Value			
parameter	L-N	m-N	AGO-1	VGO
steam/feed ratio, R (wt/wt)	0.5	0.6	0.8	1.0
product yield (wt %)				
hydrogen	1.70	1.54	1.49	1.48
methane	9.4	9.8	10.2	9.4
ethane	5.3	4.3	4.0	3.5
ethylene	22.1	21.3	22.2	21.7
propane	1.6	0.6	0.5	0.4
propylene	23.2	19.3	16.8	16.4
butanes	1.2	0.0	0.0	0.0
n-butenes	8.8	1.9	1.6	1.3
isobutene	6.5	8.3	7.7	7.6
1,3-butadiene	2.1	3.6	4.3	4.0
C_5-200 °C, non-BTX	10.0	8.7	7.2	6.7
benzene	4.9	6.4	5.1	4.3
ethyl benzene	1.4	1.1	1.9	0.7
toluene	1.4	7.2	3.4	2.9
xylenes	0.3	4.3	0.9	1.7
200-400 °C	0.3	1.7	12.8	17.3
>400°C	0.0	0.0	0.0	0.7
ethylene + propylene	45.3	40.6	39	38.1
propylene/ethylene	1.05	0.90	0.76	0.76
$C_2^=$-$C_4^=$	54.7	49.6	47.3	46.3
C_2-C_4 unsaturated	46.8	53.2	51.6	50.3
BTX[b]	8.0	19.0	11.3	9.6

[a] Reaction conditions: temperature, 725 °C; weight houly space velocity (WHSV; in reference to only the hydrocarbon feed), 2.0 h^{-1}; and W (catalyst), 5 g. =All thedata were collected at a reaction time of 10h. [b] BTX = benzene, toluene, xylenes (and ethylbenzene)

Table 2.5: Performance of the hybrid catalyst HYB-2 (MCC-2 and Co-Cat 2), using various Feedstocks[a]

	Value				
parameter	L-N	m-N	AGO-1	VGO	VGO[b]
steam/feed ratio, R (wt/wt)	0.5	0.6	0.8	1.0	1.0
product yield (wt %)					
hydrogen	1.73	1.62	1.5	1.57	1.62
methane	10.4	11.3	10.8	10.8	12.1
ethane	4.7	4.8	4.5	4.5	4.3
ethylene	22.7	24.0	23.3	23.3	24.0
propane	0.7	0.5	0.4	0.5	0.6
propylene	22.9	18.6	16.9	17.8	18.6
butanes	0.0	0.0	0.0	0.0	0.0
n-butenes	10.0	1.5	1.3	1.4	1.2
isobutene	3.8	7.3	6.8	7.9	6.8
1,3-butadiene	3.2	4.2	3.1	3.7	4.5
C_5-200 °C, non-BTX	11.3	8.0	6.4	6.7	7.4
benzene	6.0	6.5	5.5	3.8	3.0
ethyl benzene	0.2	0.8	0.6	0.5	0.5
toluene	1.4	5.0	3.8	2.6	2.0
xylenes	0.5	2.6	1.6	1.6	1.2
200-400 °C	0.6	2.3	13.5	13.1	11.4
>400°C	0.0	0.0	0.0	0.2	0.3
ethylene + propylene	45.6	42.5	40.0	41.1	42.6
propylene/ethylene	1.02	0.77	0.71	0.76	0.78
$C_2^=$-$C_4^=$	54.5	50.5	47.4	49.6	50.0
C_2-C_4 unsaturated	57.7	54.7	50.5	53.3	54.5
BTX	8.1	14.9	11.5	8.5	6.7

[a] Reaction conditions were the same as those given in Table 2.4. [b] Data obtained with HYB-3 using VGO.

The data in Tables 2.4 and 2.5 suggest that, at the time these product yields were determined (10 h of reaction), the changes in the product selectivity on goint from REF-2 to HYB-2 were more significant when heavy feeds such as vacuum gas oil, were used. In

fact, at a relatively short time-on-stream of 10 h, the light naphtha (L-N) did not induce very significant differences in terms of yields of light olefins between the HYB-2 and REF-2 (Tables 2.4 and 2.5), meaning that the coke deposition - being quite slow - was not significantly different for both catalyst surfaces. However, the use of VGO feed resulted in much larger differences in terms of yields of light olefins and heavy products (200-400℃ and higher) (see Tables 2.4 and 2.5). In particular, with the VGO over the HYB-2 hybrid catalyst, the heavy products determined in the reaction out-stream amounted only to 13 wt % (see Table 2.5), whereas the REF-2 sample showed a production of ca. 18 wt.% of these heavy products (Table 2.4). Meanwhile, the yields of light olefins (C_2-C_4 olefins, and also ethylene + propylene) were much higher for the HYB-2 hybrid catalyst (see Tables 2.4 and 2.5). In the case of HYB-3 catalyst, when compared to the reference REF-2, these product yields showed even much larger differences; for example, the combined yield of heavy products (boiling-point range of 200-400℃ and higher) and BTX aromatics was 18.4 wt % against 27.6 wt %, i.e. there was a reduction of ca. 33% in the production of aromatics (Tables 2.5 and 2.4).

These results indicate that the hybrid catalysts HYB-2 and HYB-3 succeeded to slow the rate of formation of (and/or to dearomatize) these polynuclear aromatics significantly. While the yield of the BTX aromatics also decreased, there was a significant increase in the production of light olefins. However, when lighter feeds such as light naphtha (L-N) were used, there was, in practice, no such large differences in terms of product yields (determined at the same time on-stream) between the reference catalyst (REF-2) and the hybrid catalyst (HYB-2) (see Tables 4 and 5), as similarly reported in Figure 1 for the HYB-1(1) and REF-1.

These results suggest the following interpretation:

(a) Polynuclear aromatics are precursors of coke that is formed through a complex sequence of reactions, [79] with, as an immediately preceding step, the formation of carboids. [80] These condensed, cross-linked polymers can also be formed from aromatic polycyclic hydrocarbons, which directly undergo condensation reactions, resulting in the final formation of carboids. [79] Therefore, the presence in the feed of these polynuclear aromatics (case of heavy feedstocks such as the VGO) accelerates the formation of coke, thus leading to a more rapid activity decay.

(b) The presence of active hydrogen species coming from the nickel-bearing co-catalyst surface is believed to partially retard such coking reactions by their de-aromatizing action on the "normal" sequence of coke formation or/and directly on the polynuclear aromatics of the feed, as depicted in Fig.2.2. For the moment, we have no direct evidence of their action on the reaction intermediates. However, the "indirect" evidence stands on two quite suggestive facts: (i) their influence on the product yields (see Table 2.3) and (ii) their effect on the carbonaceous deposition and the adsorbed species on the catalyst surface (see Table 2.6).

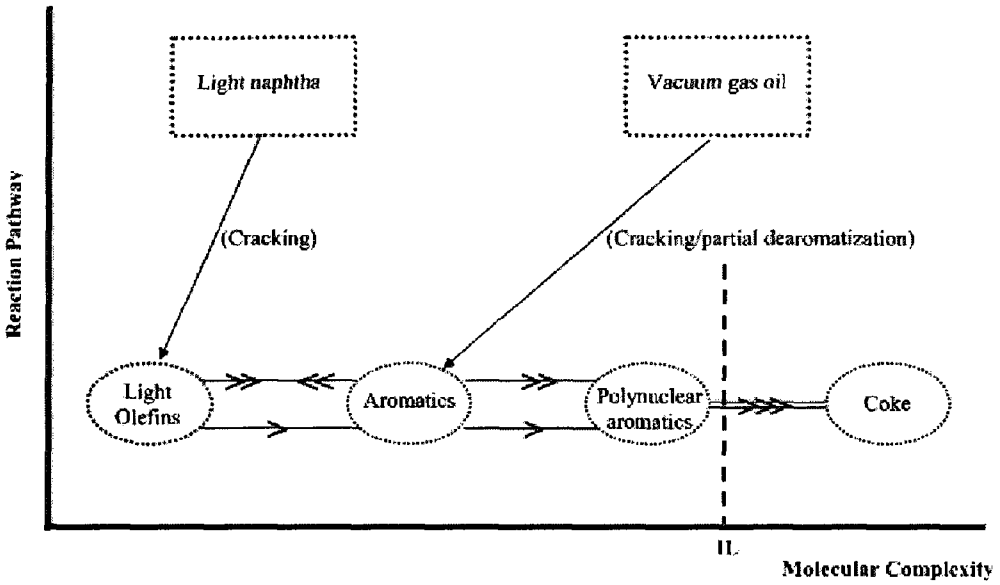

Fig.2.2: Assumed intervention level (IL) of the hydrogen spilt-over species (being produced in situ on the co-catalyst surface) on the reaction intermediates at the cracking sites

(c) The fact that, after 10 h time-on-stream (a very short period of time), the hybrid catalysts had almost little effect on lighter hydrocarbon feedstocks, whereas heavier feedstocks were significantly affected, suggests that the dearomatization of these existing polynuclear aromatics was predominant, compared to the retarding effect on their formation from smaller hydrocarbons of the feed (Fig.2.2).

Table 2.6: Tabulated results for the DTA/TGA analysis of reference (REF-2) and hybrid (HYB-2) catalysts in various environments[a]

	Value			
	REF-2		HYB-2	
parameter	in argon	in air	in argon	in air
weight loss	29.6 wt %	21.8 wt %	31.5 wt %	6.3 wt %
temperature	807 °C	552 °C	682 °C	470 °C
assumed type of reaction (DTA)	thermal decomposition	combustion	thermal decomposition	combustion

[a] The desorption of adsorbed species (water and others) is not reported herein.

2.3.2. Coke and Its "Advanced" Precursors

The previous interpretation of catalytic results was confirmed by the TGA/DTA study of the coked catalysts, i.e., with heavy feeds (in our case, VGO), hybrid catalysts, having active sites present on the co-catalyst surface, were capable of activating hydrogen and, thus, producing less coke than reference catalysts. In fact, table 6 reports the DTA/TGA results of coked reference (REF-2) and hybrid (HYB-2) catalysts. Each coked catalyst was submitted first to a temperature-programmed heating (TPH) under inert atmosphere (argon) from ambient temperature up to 900℃ and then, after a rapid cooling to ambient temperature, to another TPH from ambient temperature to 800℃, but this time, in air.

Thus, it can be observed (from Table 2.6) that (i) in an argon atmosphere, there was (predominantly) thermal decomposition of the heavy species firmly bound to the catalyst surface (and which were not desorbed in diethyl ether [81]), which led to the same weight loss for both catalysts (these bound species were believed to be "advanced" precursors of coke); and (ii) in the subsequent heating step that was performed in an oxidative atmosphere (air), there was combustion of the coke deposition: the weight loss experienced by the hybrid catalyst was less than one-third of that experienced, under the same conditions of analysis, by the reference catalyst.

Moreover, the temperatures of thermal decomposition and coke combustion observed with the hybrid catalyst were significantly lower than those recorded with the reference catalyst. This suggests that the species bound to (and the coke deposited on) the hybrid catalyst surface were much lighter than the corresponding species on the reference

catalyst surface, where there were no hydrogen spilt-over species in action.

On the other hand, the combined action of the two components in the hybrid catalyst did not result in negative effect on the yields of light olefins. Instead, significant increases in their production were observed, probably because more cracking sites on the main catalyst component were available for much longer reaction times.

2.3.3. Effect of the Cracking Component (Main Catalyst Component) on the Product Propylene/Ethylene Ratio

Table 2.7: Performance of hybrid catalyst HYB-1(4) and reference catalyst REF-1[a]

	REF-1	HYB-1(4)	
parameter	at 725 °C	at 725 °C	at 740 °C
product yield (wt %)			
hydrogen	1.61	1.62	1.69
methane	9.9	10.9	11.8
ethane	4.0	3.9	3.8
ethylene	18.8	19.6	22.8
propane	0.5	0.5	0.4
propylene	19.5	19.8	19.4
butanes	1.7	1.7	1.4
n-butenes	13.3	12.5	9.8
isobutene	7.4	6.9	5.3
1,3-butadiene	2.6	2.6	3.5
C_5-200 °C, non-BTX	15.4	12.1	11.2
benzene	4.1	6.0	6.4
ethyl benzene	0.1	0.2	0.2
toluene	0.6	1.1	1.3
xylenes	0.2	0.3	0.4
200-400 °C	0.2	0.4	0.7
>400°C	0.0	0.0	0.0
ethylene + propylene	38.3	39.4	42.2
propylene/ethylene	1.03	1.01	0.85
$C_2^=$-$C_4^=$	51.6	51.8	52.3
C_2-C_4 unsaturated	54.2	54.4	55.8
BTX	4.9	7.6	8.2

[a] Reaction conditions were the same as those of Table 2.4. Results were obtained with a L-N feed

Note that the hybrid catalyst HYB-1(4) showed yields in product light olefins that are much lower than those of HYB-2 (see Tables 2.7 and 2.5, respectively). They both contained the same co-catalyst (Co-Cat 2), but they differed from each other by the main catalyst component (i.e., MCC-1 and MCC-2) used in the preparation of the final catalyst

(HYB-1(4) and HYB-2, respectively). On the MCC-1 surface, the cracking sites were acid sites developed by the MoO_3 species [82] deposited on quasineutral yttria-stabilized alumina aerogel (AAS; see Table 2.1). Such surfaces (MCC-1 and AAS) do not show any significant Brønsted acidity (1546 cm^{-1}) besides the Lewis acid sites (1450 cm^{-1}) [83] (see Fig.2.3C and Fig.2.3A). Instead, the lanthanum stabilized ZSM-5 zeolite was used in the preparation of the MCC-2 whose surface exhibited, compared to that of the MCC-1, a larger amount of Brønsted acid sites (see Fig.2.3D), a higher acid sites density (Table 2.1), and a higher density of slightly stronger acid sites (see Table 2.1; higher density and slightly higher desorption temperature for peak S). The major contributor to this enhanced acidity was the ZSM-5 zeolite (see Fig.2.3B and Fig.2.4).

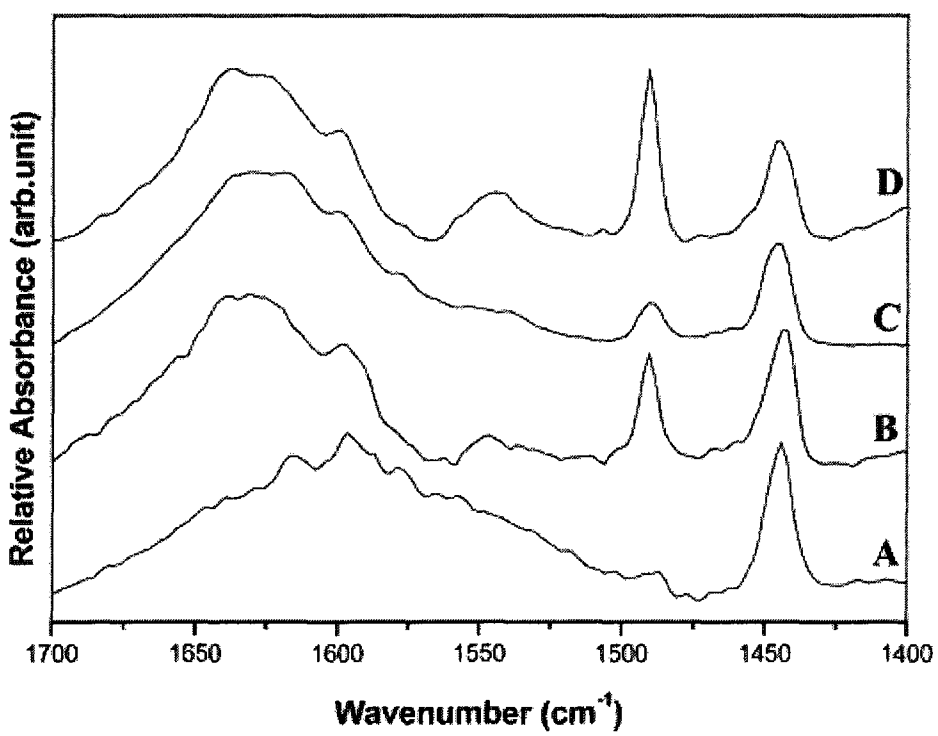

Fig.2.3: FT-IR spectra of adsorbed pyridine of the main components (MCC-1 (spectrum C) and MCC-2 (spectrum D)) and their corresponding "active" supports (AAS (spectrum A) and ZSM-5 zeolite (spectrum B))

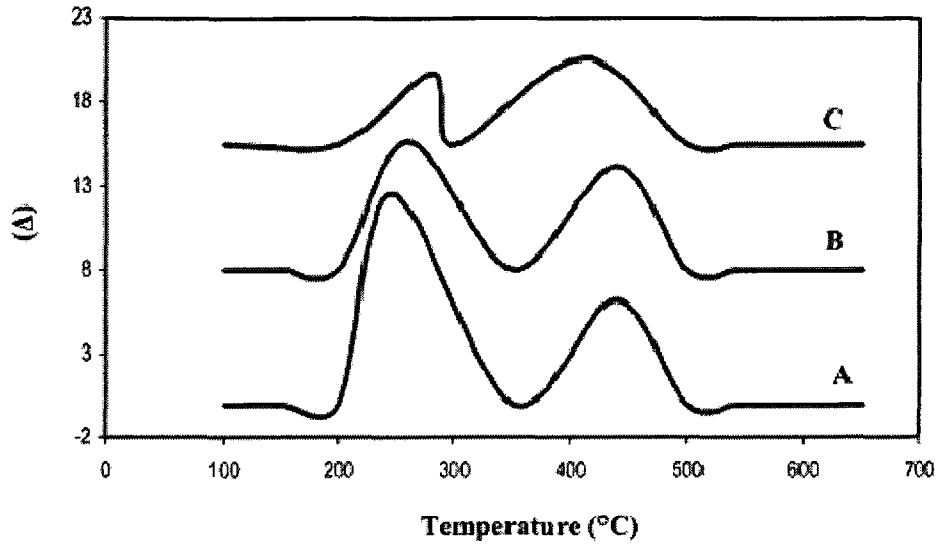

Fig.2.4: Acid strength profile obtained using the NH3-TPD/ISE method: (A) H-ZSM5, (B) MCC-2, and (C) MCC-1. (Δ)) d[NH4]/dt (given in units of mmol $g^{-1}℃^{-1}$)

Therefore, to have the same level of conversion, catalytic testing was performed on the HYB-1(4) (and other catalysts using the same AAS support) at a significantly higher temperature (i.e., 740℃ instead of 725℃; see Fig.2.1 and Table 2.7). Such higher reaction temperature led to a lower product propylene/ethylene ratio (Fig.2.1 and Table 2.7), as usually observed with thermal or steam cracking. Thus, the use of ZSM-5 zeolite containing hybrid catalysts, tested at the standard reaction temperature (725℃) and particularly with light hydrocarbon feedstocks, resulted in a higher combined yield of ethylene and propylene and a higher propylene/ethylene ratio (Table 2.5, L-N as feed). According to Corma et al., [84] in the FCC naphtha cracking, the selectivity to propylene increases when hydrogen-transfer reactions are minimized using shape-selective catalysts (such as the ZSM-5 zeolite). However, we believe that, in our case, the use of higher temperature to compensate the lower surface acidity of the nonzeolitic main component such as in the HYB-1(4) was the main cause for such significant variations of the propylene/ethylene ratio.

2.4. CONCLUSION

We have shown in this work that the hydrogen spill-over effect may play a key role in improving the catalytic activity of the hybrid catalysts of the TCC process. Because the latter process has been developed for the production of light olefins, this effect, when fully controlled, may advantageously contribute to (i) increasing the yields of light olefins, (ii) producing less heavy compounds, and (iii) lengthening the run length when a fixed bed (and tubular) reactor is used.

The concept of hybrid catalysts that contain co-catalysts being capable of producing hydrogen spill-over species is proven to have powerful dearomatizing/ring opening properties. Therefore, the use of such catalysts may reduce polynuclear aromatics in middle-distillate fuels, which are known for "producing particulates in the exhaust gases and, in addition, having poor ignition properties (i.e., low cetane number in diesel fuel and high smoke point in jet fuel)". [85] More-efficient hydrotreating catalysts would be prepared using this concept of long-distance hydrogen spillover. [75, 86]

Finally, note that recent progress in the understanding of these hydrogen spillover phenomena will result in very important applications in several sectors of catalysis, fuel-cell technology, and material science. [87-90]

2.5. AUTHOR'S NOTES AND SIGNIFICANCE OF PAPER TO THESIS

This work on the phenomena of the hydrogen spill over was the first article published in the literature on the effect of the spilt-over hydrogen species on the product yields of the hybrid catalysts used in the thermo-catalytic cracking (TCC) process for the production of light olefins. The Ni bearing co-catalyst was found to be able to produce very active hydrogen species by steam reforming. Once these species were transferred

(spilt-over) onto the surface of the main catalyst component (cracking sites), they could interact with the adsorbed reaction intermediates, resulting in a decreased rate of coke formation and the dearomatization/ring-opening of some heavy compounds of the feed. Although the amounts of these hydrogen spilt-over species were very small, their effect on the conversion of heavy feedstocks (such as vacuum gas oils) was very significant.

The following chapter shows the influence of hydrogen spilt-over species on the cracking of model molecules (n-hexane) at the level of the zeolite acid sites. It is well known that hydrogen spilt-over species play an important role in the retardment of coke formation and the improvement of the stability of catalyst. However, the nature of these hydrogen species remains unknown. Therefore, the Thermo-Catalytic Cracking performance of the hybrid catalyst on n-hexane containing some polymethylbenzenes will be investigated in order to determine the effect of coke precursors (polymethylbenzenes) on the reactivity of the zeolite component. This study also will allow us to estimate the maximum distance at which the hydrogen spilt-over species remain effective.

Chapter III

The Thermo-Catalytic Cracking of Hydrocarbons: Effect of Polymethylbenzenes Added to the *n*-Hexane Feed on the Reactivity of ZSM-5 Zeolite Containing Hybrid Catalyst

Published as:

H. T. Yan and R. Le Van Mao

Catal. Lett. **(2009)** 130:558

3.1. INTRODUCTION

The thermo-catalytic cracking process (TCC) has been recently developed to crack heavy hydrocarbon feedstocks (naphthas, gas oils) [91, 92] or heavy olefins [93] into propylene, ethylene and other light olefins. The most recent TCC catalysts have a hybrid configuration, comprising a main (acidic) component and a co-catalyst. [91-93] Modified ZSM-5 zeolite is the acidic component while the co-catalyst is obtained by dispersing a noble metal (Pt or Pd) or Ni on a hydrothermally stable support. The role of the co-catalyst is to prevent or slow down the normally rapid formation of coke due to cracking and related reactions at relatively high temperatures. Ni bearing co-catalyst is capable of producing some active hydrogen species by steam-reforming. [92] These species might be then split-over (HSO) onto the main acidic catalyst surface with, as a final result, a significant retarding effect on the formation of coke precursors, i.e. polycyclic aromatic hydrocarbons (PAH). [91, 92] It is to note that the heavy PAH are already present in the feed, alongside with BTX aromatics and some polymethylbenzenes, or can be formed during the reaction.

More than a decade ago, it was shown that the formation of various hydrocarbons from methanol proceeded via a hydrocarbon pool mechanism [94–96] rather than via an initial C–C bond formation. [95, 97] The quite complicated reaction pattern as depicted in the pool mechanism, was recently evoked to explain the delayed coking effect in the thermo-catalytic cracking (TCC) of hydrocarbons that made use of hybrid catalysts. [92] It is to note that such PAH may derive from heptamethylbenzenium ion (HMB^+), the main reaction intermediate being hypothesized in the pool mechanism. This ion is assumed to "control" not only the formation of gaseous products but also that of coke.

[98] However, in a more recent paper, Bjorgen et al. [99] showed that with ZSM-5 zeolite catalysts, the mechanism of methanol conversion to hydrocarbons was more complicated than that previously proposed.

In the present work, to the *n*-hexane (feed currently used to study the TCC reaction) is added in increasing amount, one of these two polymethylbenzenes (P-methylbenzenes): pentamethylbenzene (PMB) or 1,2,4-trimethylbenzene (TMB). The former co-fed molecule is too bulky to be sorbed by the zeolite micropores whereas the latter has a molecular diameter small enough to allow a significant sorption onto the internal surface of these micropores. In addition, the size of the TMB molecules is such that some of them can remain trapped inside these micropores.

Thus, the expected results are:

What kind of disturbance the co-fed TMB can create on the catalytic performance (product yields or selectivity)?

More importantly, what is the range of action of these hydrogen species (HSO), formed on the co-catalyst surface and spilt-over onto that of the zeolite bearing component? Can these HSO reach the internal surface of the zeolite micropores?

3.2. EXPERIMENTAL

3.2.1. Catalyst Preparation

Both hybrid and reference catalysts were prepared according the method described in the previous papers. [91, 92]

3.2.1.1. Main Catalyst Component (M-Cat)

Fifty gram of HZSM-5 (powder, acid form, silica/alumina molar ratio = 50, purchased from Zeochem, Switzerland) were added to a solution that was composed of

25.0 g of lanthanum nitrate hydrate (Strem Chemicals) in 500 mL of deionized water. The suspension, gently stirred, was heated to 80 °C for 2 h. After filtration, the obtained solid was washed on the filter with 500 mL of water, then dried at 120 °C overnight and finally activated at 500 °C for 3 h. This material was called La-HZSM-5.

A solution of 5.52 g of ammonium molybdate hexahydrate (Aldrich) in 89 mL of 2.3 N H_3PO_4 was homogeneously impregnated onto 40.02 g of La-HZSM-5. The solid was died at 120 °C overnight and finally activated at 500 °C for 3 h.

Its chemical composition was as follows: MoO_3, 8.0 wt%; La_2O_3, 2.5 wt%; phosphorous, 4.1 wt%; and zeolite, balance.

3.2.1.2. Co-Catalyst (Co-Cat)

A mixture of 2.59 g of nickel nitrate hexahydrate (Strem) in 20 mL of deionized water and 0.036 g of ruthenium acetylacetonate (Strem) in 25 mL of methanol was homogeneously impregnated onto 20.0 g of yttria-stabilized alumina aerogel, Y-AA. [92] After drying at 120 °C overnight, the solid was activated at 500 °C for 3 h. Its chemical composition was: nickel, 2.5 wt%; ruthenium, 0.05 wt%; and Y-Al_2O_3, balance.

It is to note that, because TCC catalysts have to operate at relatively high temperatures (650–750 °C), the co-catalyst and its support (Y-AA) should be hydrothermally stable at those temperatures. [100, 101]

3.2.1.3. Hybrid Catalyst (Z-HYB) and Reference Catalyst (Z-REF)

The hybrid catalyst (Z-HYB) was obtained by extruding the main component (M-Cat) with the co-catalyst (Co-Cat) in the following proportions: M-Cat, 65.6 wt%; Co-Cat, 16.4 wt%; and binder, 18.0 wt%. Bentonite clay (Aldrich) was used as the extruding and binding medium.

The reference catalyst (Z-REF) was obtained by extruding M-Cat with pure Y-AA and bentonite in the same proportions as for HYB.

Z-HYB and Z-REF were dried at 120 °C overnight and finally activated at 750 °C for 3 h.

3.2.2. Catalyst Characterization

1. The various catalyst components were analyzed by atomic absorption spectroscopy for their chemical composition.
2. The BET total surface area and pore size of these samples were determined by nitrogen adsorption/desorption, using a Micromeretics ASAP 2000 apparatus.
3. Thermogravimetric analysis (TGA) and differential thermal analysis (DTA), using a PL Thermal Sciences Model STA-1500 DTA/TGA apparatus, were used to determine the amount of bound species and/or coke deposited onto the catalyst surface. The flow rate of air was set at 35 mL/min. The rate of the temperature-programmed heating (TPH) was set at 10 °C/min.

3.2.3. Experimental Set-up and Testing Procedure

Experiments were performed using a Lindberg one zone tubular furnace. The reactor vessel consisted of a quartz tube 50 cm long, 1.5 cm in outer diameter and 1.2 cm in inner diameter. The temperatures were controlled and regulated by automatic devices that were connected to chromel-alumel thermocouples (set in the catalyst bed and in the pre-heating zone) and the heating furnace.

n-hexane (Aldrich) was used as a model feed to that pentamethylbenzene (PMB, Aldrich) or 1,2,4-trimethylbenzene (TMB, Aldrich) was added in various concentrations. The feed and water were injected into a vaporizer using two infusion pumps. In the

vaporizer, some nitrogen, used as carrier gas, was mixed with the vapours and the gaseous stream was then sent into the tubular reactor. The testing conditions used were as follows: temperature, 700 °C; total weight hourly space velocity (WHSV, feed and steam), 1.52 h^{-1}; catalyst weight, 2.1 g; steam/feed weight ratio, 0.5.

Product liquid and gaseous fractions were collected separately, using a system of condensers. The gas-phase components were analyzed using a Hewlett-Packard Model 5890 FID gas chromatograph that was equipped with a 30-m GS-alumina micropacked column (J & W Scientific), whereas the liquid phase analysis was performed using the a Hewlett-Packard gas chromatograph [Model 5890, with flame ionization detection (FID)] that was equipped with a Heliflex AT-5 column (Alltech, 30 m, nonpolar).

The total conversion (wt%) was expressed as the number of grams of all the products collected at the reactor outlet by 100 g of feed, referring thus to the mixture of n-hexane with P-methylbenzene (polymethylbenzene, in our work: PMB or TMB), therein called COMB, as follows.

Conversion (wt%) = $[(COMB_{in}–COMB_{out})/COMB_{in}]$ 100 (wt%), with $COMB_{in}$ and $COMB_{out}$ being the total weight of (*n*-hexane and polymethylbenzene) injected into the reactor and determined in the reactor outstream, respectively.

The yield of product i (Y_i) was expressed as the number of grams of product i recovered by 100 g of feed injected (wt%). It is important to note that the experimental error usually observed on total conversion and calculated product yields was ± 0.2 wt%.

3.3. RESULTS AND DISCUSSION

Table 3.1 reports the pore characteristics of the ZSM-5 zeolite (Silica/Alumina molar ratio = 36) and the yttria-stabilized alumina aerogel (Y-AA) used for the

preparation of the hybrid catalyst, Z-HYB.

Table 3.1: Pore characteristics of the ZSM-5 zeolite, the Y-AA, the Z-HYB catalyst and Z-REF

	Total BET SA	SA of micropore	SA of mesopores and larger
ZSM-5 zeolite	420	270 (64%)	150 (36%)
Y-AA	270	18 (17%)	252 (93%)
Bentonite	0.5	0	0.5
Z-REF	213	127 (60%)	86 (40%)
Z-HYB	188	116 (62%)	72 (38%)

It is to note that the surface areas corresponding to pores larger than the micropores in the catalyst extrudates (Z-REF and Z-HYB), represented important fractions of the total surface area (40 and 38%, respectively). It is also reasonable to assume that the surface area of the micropores of the hybrid catalyst came mostly from its zeolitic component whose particle showed the same proportion for large pores (36%). All this means that the external surface of the zeolite particles (which also includes that of the large micropore openings) was quite significant.

The incorporation of La^{3+} onto the ZSM-5 zeolite particles and that of (P-Mo) species had as main objectives to decrease the strength of the zeolite acid sites, particularly those located on the external surface [102] and to create new larger pores with moderately acidic surface [93], respectively. These large pores were located in the outer-skirt of these zeolite particles and the corresponding mild acid sites were destined to crack large molecules of the feed.

Catalytic data of the hybrid catalyst (HYB) and its reference (REF) reported in the following sections were average values obtained during a period of time of 5 h (after an

initial period of 5 h, needed for stabilizing the catalytic reaction). We preferred using mixtures of *n*-hexane with poly-methylbenzene in increasing and significant concentration. This is because, in the case of TMB that could be adsorbed and trapped inside the micropores of the ZSM-5 zeolite particles, the effect on the conversion of the TMB, added in small amounts (for instance, 0.3 wt%) to *n*-hexane, would take too much time (16 h and more) to be noticed.

3.3.1. Tests with Pentamethyl Benzene (PMB) Added to n-Hexane Feed

Fig.3.1 shows the variation of the conversion of the feed (*n*-hexane + PMB) versus the weight percent of PMB added to the *n*-hexane. It appears that there was almost no difference between the two curves drawn for the two catalysts (Z-HYB and Z-REF). The same behaviors were reported for the yields of light products (Fig.3.2) and the heavy products (Fig.3.1).

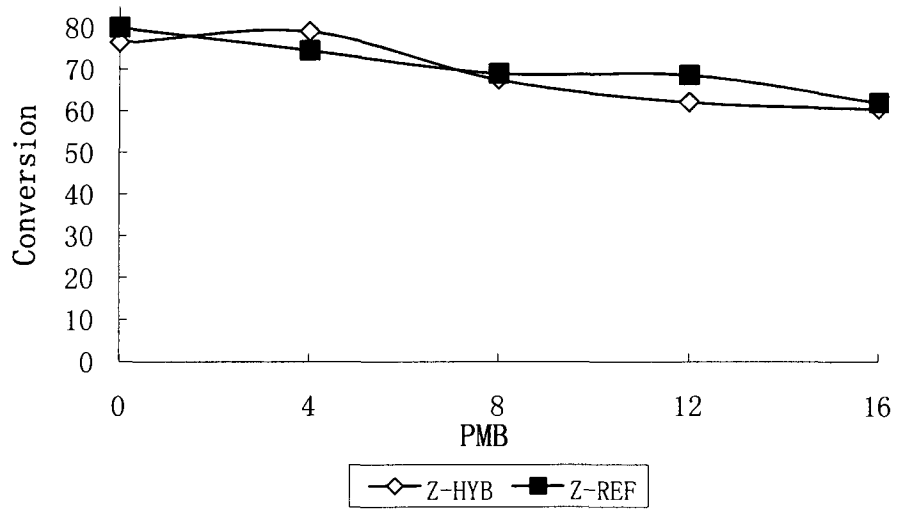

Fig.3.1: Total conversion (wt%) versus concentration (wt%) of PMB in hexane

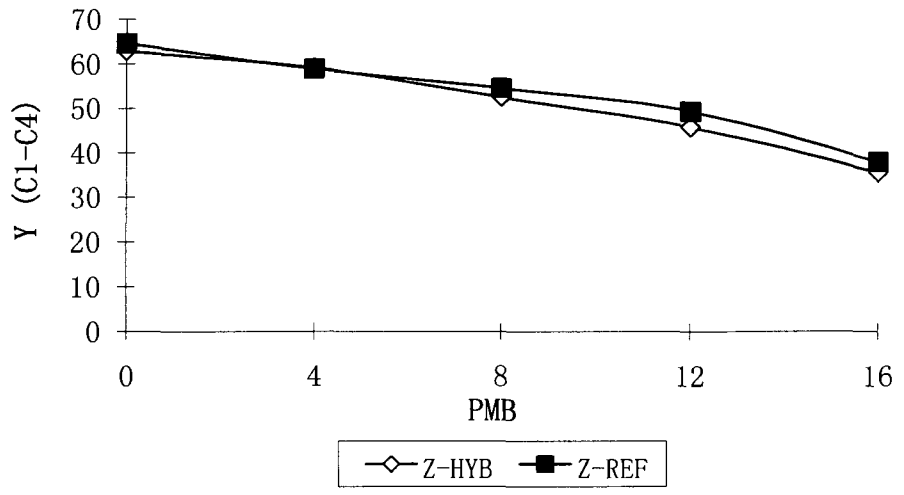

Fig.3.2: Product yield (wt%) in C_1–C_4 hydrocarbons versus concentration (wt%) of PMB in hexane

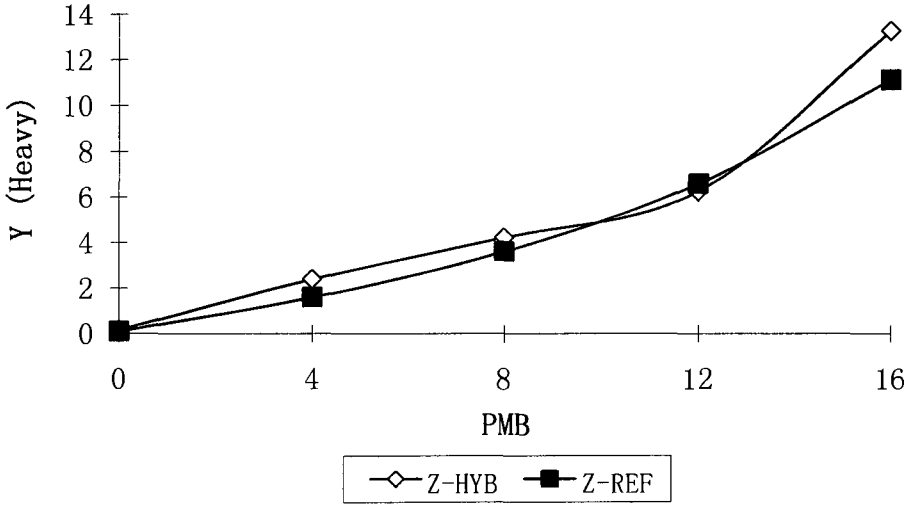

Fig.3.3: Product yield (wt%) in heavy hydrocarbons versus concentration (wt%) of PMB in hexane

It is well-known that the ten-rings micropores of the ZSM-5 zeolite have average sizes of 0.55 nm for straight channels and 0.53 nm for sinusoidal channels: thus, these pores reject all guest molecules having critical dimensions larger than 0.78 nm. [103]

PMB having a critical diameter larger than 0.78 nm (same as 1,3,5-trimethylbenzene) [104, 105] is obviously excluded from these zeolite channels, i.e. from all the surface areas of the Z-HYB and Z-REF assigned to micropores (Table 3.1). In our tests, if PMB had had some effect on the conversion and products yields, it would have expressed such effect on the surface of larger pores, i.e. the external surface of the zeolite particles which hosted the acid sites active for cracking.

Although there was no apparent difference in activity between the two catalysts (Figs. 3.1, 3.2, 3.3), the co-catalyst of the hybrid catalyst exhibited lower coke deposition (Fig. 3.4) and lighter coke nature, i.e. lower combustion temperature for coke (Fig.3.5) than the reference catalyst. This was another evidence of the influence of the hydrogen split-over species produced by the steam-reforming over the active Ni sites of the co-catalyst of the Z-HYB. Such Ni sites were not present in the Z-REF sample. [91, 92]

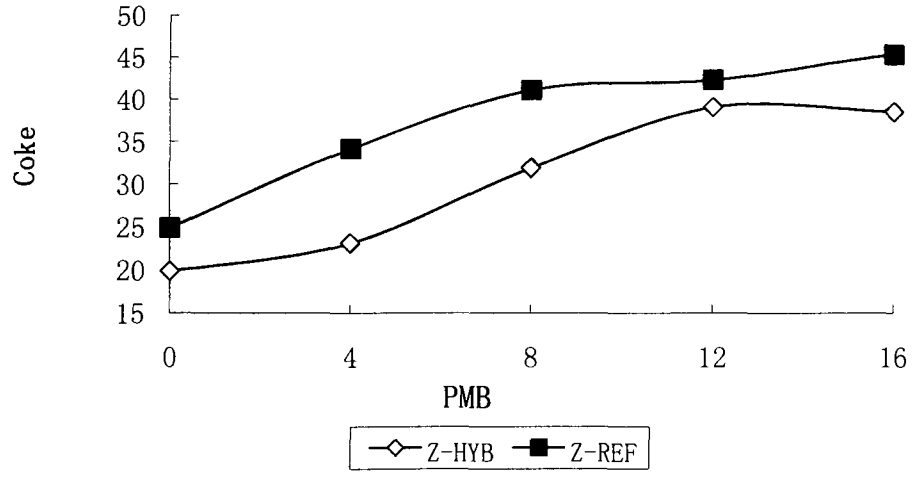

Fig.3.4: Coke deposition (wt%) versus concentration (wt%) of PMB in hexane

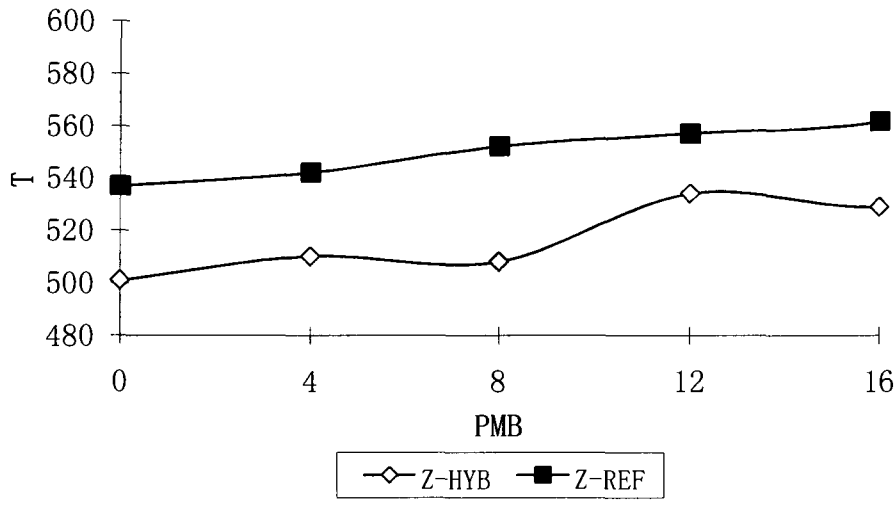

Fig.3.5: Combustion temperature of coke (T in °C) versus concentration (wt%) of PMB in hexane

3.3.2. Tests with 1,2,4-Trimethylbenzene (TMB) Added to n-Hexane Feed

Fig.3.6 reports the variation of the conversion versus the content of 1,2,4-trimethylbenzene in the feed.

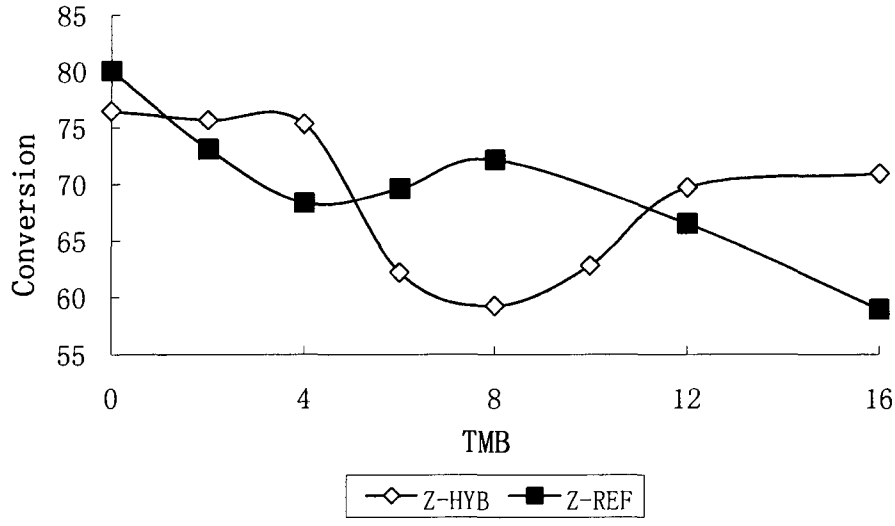

Fig.3.6: Total conversion (wt%) versus concentration (wt%) of TMB in hexane

The catalytic behaviours of both catalysts (Z-HYB and Z-REF, Fig.3.6) were

extremely different from those reported in Fig.3.1 where the n-hexane feed contained various concentrations of PMB. In addition, there was a significant difference in catalytic behaviour (conversion and product yields) between the Z-HYB and Z-REF samples (Figs. 3.6, 3.7, 3.8). To ensure that the obtained graphs were not due to experimental errors (normally lower than 0.5% for all the data), several tests for each set of experimental parameters were carefully performed and the average values were reported in the graphs.

The interpretation of these catalytic data were based on the critical dimension and kinetic diameter of the 1,2,4-trimethylbenzene (TMB), that were estimated equal to 0.8 nm [104, 105] and 0.61 nm [106], respectively.

Whereas PMB could not enter the ZSM-5 zeolite channels, the TMB having a narrower molecular size, could instead diffuse into these micropores. [100, 101] According to Choudary et al. [100], the inward diffusion of the 1,2,4-trimethylbenzene was possible in most situations while the outward diffusion of such molecule could be difficult. Therefore, a certain accumulation of TMB inside the ZSM-5 channels could occur at a significant TMB concentration in the feed.

Let us consider the graphs of the variation of the conversion versus the concentration of TMB in the feed as reported in Fig.3.6.

With the reference catalyst (Z-REF), there was a sharp decrease of the total conversion (much sharper than with the feed containing PMB, Fig. 3.1) because some TMB was rapidly adsorbed inside the ZSM-5 channels, inducing some partial pore blockage. Over 8 wt% of TMB, when the (partial) zeolite pore blockage by the adsorbed TMB became more serious, only the external surface of the zeolite was fully exposed to

the reactant (*n*-hexane and TMB), so that the activity decay was now mainly due to the cracking reaction on the external surface of the zeolite particles.

With the hybrid catalyst (Z-HYB), there was a certain resistance to activity decay induced by hydrogen spillover (HSO), up to a concentration of 4 wt% of TMB. Then the accumulation of TMB inside the ZSM-5 micropores resulted in almost the same profile of variation of the total conversion as with the Z-REF catalyst. However, such conversion minimum was shifted to higher value of TMB concentration. Over 8 wt% of TMB in hexane, there was some kind of return to the situation as previously observed with PMB at high concentrations in the *n*-hexane feed: the difference in the total conversion was mostly related to the catalytic activity on the external surface of the Z-HYB and Z-REF samples. Finally, at a concentration of TMB higher than 12 wt%, the conversion (Fig.3.6) and the yields in C_1–C_4 and heavy products (Figs.3.7, 3.8) of the Z-HYB catalyst were significantly higher and more stable than those shown by the Z-REF sample, suggesting thus some noticeable influence of the hydrogen split-over species.

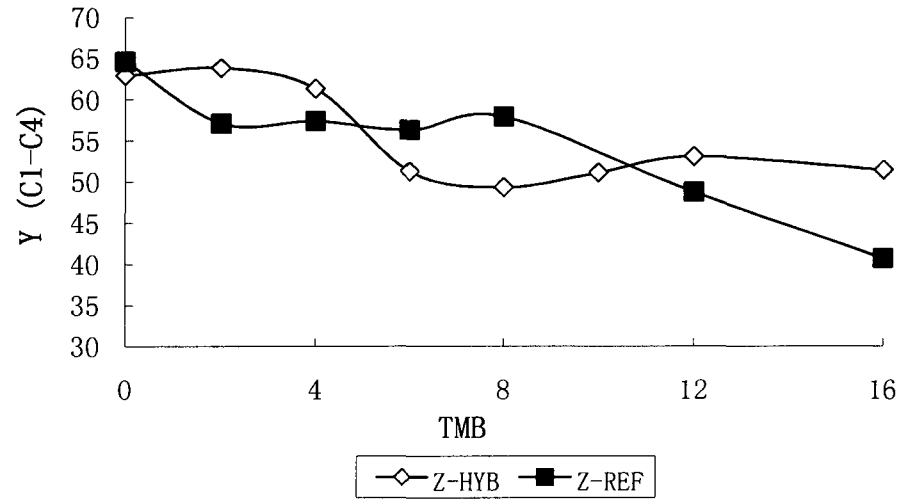

Fig.3.7: C_1–C_4 product yield (wt%) versus concentration (wt%) of TMB in hexane

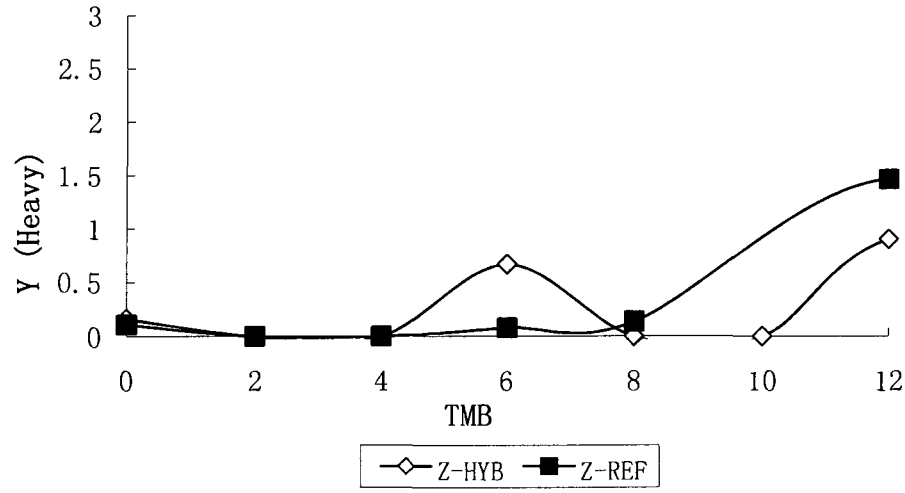

Fig.3.8: Heavy product yield (wt%) versus concentration (wt%) of TMB in hexane

Remarkably, all the variations of the conversion (and product yields: Figs.3.6, 3.7, 3.8) were closely reproduced in Figs.3.9 and 3.10 that compare the amounts of the deposition of coke and its nature (combustion temperature), respectively.

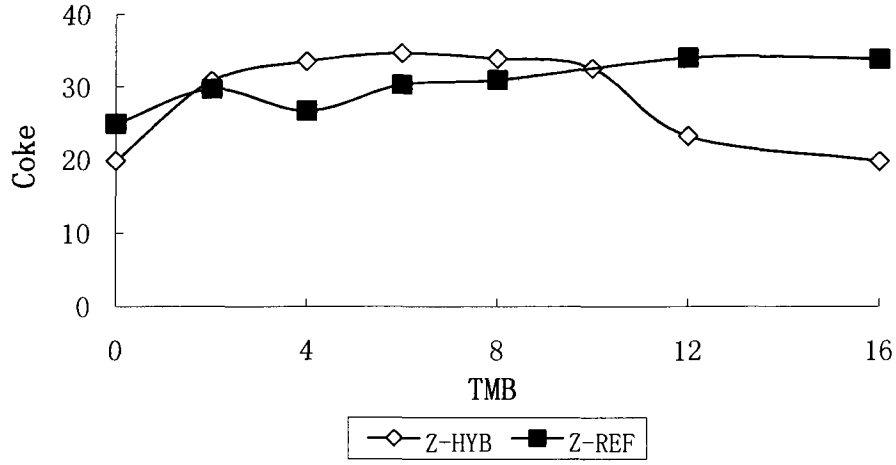

Fig.3.9: Amount of coke deposited (wt%) versus concentration (wt%) of TMB in hexane

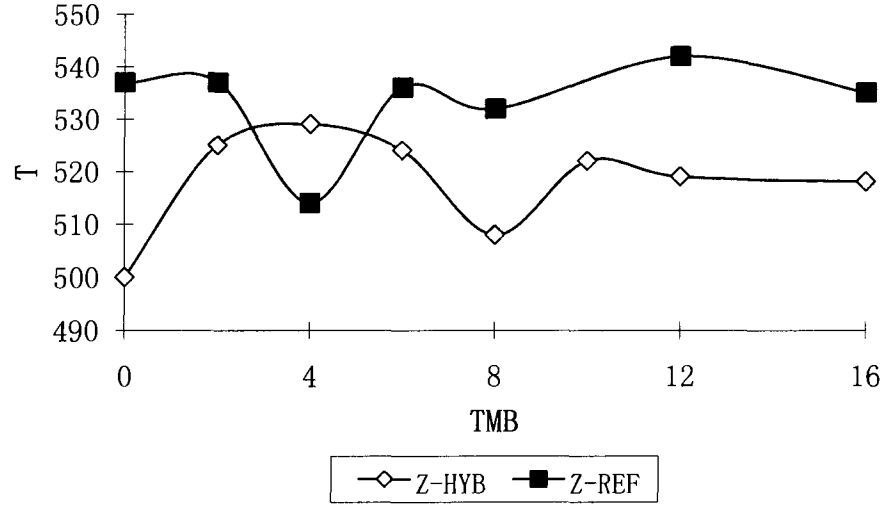

Fig.3.10: Combustion temperature of coke (T in °C) versus concentration (wt%) of TMB in hexane

3.4. CONCLUSIONS

The use of two different polymethylbenzenes, the pentamethylbenzene (PMB) and the 1,2,4-trimethylbenzene (TMB) co-fed with n-hexane, has allowed us to draw the following conclusions:

1. Data of total conversion and yields of C_1–C_4 cracking products show that the hybrid catalyst (Z-HYB) having steam-reforming Ni sites located on the co-catalyst surface, performs significantly better than the reference catalyst (Z-REF). This is another experimental evidence of the action of the hydrogen split-over (HSO) species. [91, 92] In addition, compared to the reference catalyst (Z-REF), the lower amount and the lighter nature of the coke deposited onto the hybrid catalyst, assure to the Z-HYB a longer catalyst "on-stream" stability and an easier catalyst regeneration (by coke combustion), respectively. These properties are particularly useful in the TCC conversion of heavy liquid hydrocarbons. [91, 92]
2. With respect to the Z-REF, the improvement of the catalytic activity of the Z-HYB in the presence of the (*n*-hexane/TMB) feed, mostly at high concentration of TMB (higher than 12 wt%), is more important than when the (*n*-hexane/PMB) feed is used. This is in agreement with the hydrocarbon pool mechanism in which "the reaction mainly proceeds via penta-and hexamethylbenzene" as coke precursors. [102] Adsorbed TMB being less methylated than PMB is relatively far from turning into coke and thus, may lead to a larger difference in reactivity between the Z-HYB and Z-REF catalysts. This recalls the most recent and extremely interesting paper of Bjorgen et al. [94] who showed that over ZSM-5 zeolite catalysts there might be two reaction cycles, one through a "modified hydrocarbon pool mechanism" (for lower methylbenzenes) and the other one, going through alkene methylation and interconversions.
3. The unusual behavior of the Z-HYB catalyst when converting the *n*-hexane/TMB feed is due to the accessibility of the TMB into the zeolite micropores of the main

component and its difficulty to move out of such pore system. This also shows the limitation in the motion of the hydrogen split-over species that can be transferred from the co-catalyst surface to the external surface of the ZSM-5 zeolite particles, but not inside the small pores of such zeolite.

These results may have important applications in the TCC process and others, where HSO action is required to continuously clean the acidic active surface (cracking) of the catalyst. If the acidic component is a mesoporous material [103] instead of a microporous zeolite, can the HSO effect be more efficient?

3.5. AUTHOR'S NOTES AND SIGNIFICANCE OF PAPER TO THESIS

This work on the effect of hydrogen spilt-over species was the first article in the literature showing the effect of polymethylbenzenes (added to the *n*-hexane feed) on the reactivity of the ZSM-5 zeolite containing hybrid catalysts. The results of this study indicated that the hydrogen spilt-over species could be transferred from the co-catalyst surface to the external surface of the main catalyst (ZSM-5 zeolite) particle; however, they could not penetrate the small pores of that particle. Thus, the hydrogen spilt-over species could affect the reaction intermediates only when the latter were formed on the external surface of the zeolite particle.

The following chapter is a continuous effort toward the understanding of the coke of the zeolite component within the hybrid catalyst. In the next chapter, we will be exploring the influence of the pore characteristics and the acidity properties of the ZSM-5 zeolite-based component on the overall performance of the hybrid catalysts.

Chapter IV

Hybrid Catalysts Used in the Thermo-Catalytic Cracking Process (TCC): Influence of the Pore Characteristics and the Acidity Properties of the ZSM-5 Zeolite-Based Component on the Overall Performance

To be submitted to: Applied Catalysis: A

H. T. Yan and R. Le Van Mao

4.1. INTRODUCTION

Ethylene and propylene are the most important intermediates used in the production of main plastics and synthetic fibres. [109] The current technology of production of these olefins is steam-cracking, using various hydrocarbon feedstocks (light paraffins, naphthas or gas oils). Setting aside this special period of economic recession, market demands for ethylene and propylene have experienced significant and constant increases, with a higher growth rate for propylene. [110] However, because the product selectivity of the steam-cracking for propylene is quite low, the supply of this light olefin can be compensated through the use of other production processes, such as propane dehydrogenation, olefin metathesis, and, primarily, fluid catalytic cracking (FCC). The latter technology, whose main objective is to produce gasoline, must incorporate some ZSM-5 type zeolite as a catalyst additive so that the production of light olefins, particularly propylene, can be increased significantly.

The thermo-catalytic cracking (TCC) process has been developed with the objective to selectively produce light olefins from liquid hydrocarbon feedstocks such as naphthas and gas oils [111-114], and more recently, heavy olefins. [115] The TCC process, which combines the (mild) thermal cracking with the acid-promoted cracking of a zeolite-based catalyst, can provide very high yields of light olefins (with the possibility of varying the propylene-to-ethylene ratio) while operating at a temperature much lower than those used in the steam-cracking process. Most of the catalysts used in the TCC process are in the hybrid configuration, i.e., they are comprised of two porous components with relatively high surface area: a main zeolite-based component, which has cracking properties, and a co-catalyst, which has active sites that can affect the product

selectivity of the former (acidic) sites. These two catalyst particles are firmly bound to each other by an inorganic binder that, in most cases, is bentonite clay. The "ideally sparse particles configuration" in the hybrid catalyst [113] ensures an easy two-way diffusion (of reaction intermediates) within the catalyst network; this is the so-called "pore continuum" effect, which has been observed on many occasions, such as in adsorption / desorption [116], and in different catalytic reactions such as aromatisation and cracking. [117-120] Because the reaction temperature is relatively high (620-750 °C), the co-catalyst support must be very thermally and hydrothermally stable (such as the amorphous alumina aerogel, being stabilized by yttria [121,122]). On the other hand, the ZSM-5 zeolite is further stabilized by lanthanum. [114]

The role that the co-catalyst is expected to play, is to produce some hydrogen species, in virtue of its steam-reforming activity, and to spill them over (its surface) to the acidic sites of the main catalyst component. These hydrogen spilt-over (HSO) species can exert some "cleaning action" on the coke precursors so that coking can be significantly reduced and the run length (the period of time separating two catalyst decoking operations - when the fixed-bed technology is used) can be improved. In our most recent paper [123], it was shown that these HSO could easily reach the external surface of the zeolite particle (surface area of the external part of the particle and the acid sites located at the micropore mouths) but cannot go too deep inside the micropore network.

In previous works, the chemical/physical properties of the active surfaces (of both zeolite and co-catalyst) have been thoroughly studied. [113,114,116,120-122,124,125] In the present paper, we want to investigate in more detail the influence of the pore characteristics and the acid properties of the ZSM-5 zeolite on the overall

performance of the hybrid catalyst. Some tests of surface contamination by 1,3,5-trimethylbenzene were also carried out, just to exacerbate the fouling phenomena.

4.2. EXPERIMENTAL

4.2.1 Catalyst preparation

Both hybrid and reference catalysts were prepared according the method described in the previous papers. [113,114]

4.2.1.1 Main catalyst component (M-Cat)

50 g of HZSM-5 (powder, acid form, silicon/aluminum molar ratio = 25, 50, 100, 400, 1000, respectively, purchased from Zeochem, Switzerland) were added to a solution that was prepared by dissolving 25.0 g of lanthanum nitrate hydrate (Strem Chemicals) in 500 mL of deionized water. The suspension, gently stirred, was heated to 80℃ for 2 h. After filtration, the obtained solid was washed on the filter with 500 mL of water, then dried at 120℃ overnight and finally activated at 500℃ for 3 h. This material was called La-HZSM-5.

Then, a solution of 5.52 g of ammonium molybdate hexahydrate (Aldrich) in 89 mL of 3N H_3PO_4 was homogeneously impregnated onto 40.02g of La-HZSM-5. The solid was dried at 120℃ overnight and finally activated at 500℃ for 3 h.

Its chemical composition was as follows: MoO_3, 8.0 wt %; La_2O_3, 2.5 wt %; phosphorous, 4.1 wt %; and zeolite, balance.

4.2.1.2 Co-catalyst (Co-Cat)

A mixture of 2.59 g of nickel nitrate hexahydrate (Strem) in 20 mL of deionized water and 0.036g of ruthenium acetylacetonate (Strem) in 25 mL of methanol, was homogeneously impregnated onto 20.0 g of yttria-stabilized alumina aerogel, Y-AA.

After drying at 120 ℃ overnight, the solid was activated at 500 ℃ for 3 h. Its chemical composition was: nickel, 2.5 wt %; ruthenium, 0.05 wt %; and Y- AA, balance.

It is to note that, because TCC catalysts have to operate at relatively high temperatures (620 ℃ – 750 ℃), the co-catalyst and its support (Y-AA) should be hydrothermally stable at those temperatures, as already mentioned. [121,122]

4.2.1.3 Hybrid catalyst (Z-HYB) and reference catalyst (Z-REF)

The hybrid catalyst (Z-HYB) was obtained by extruding the main component (M-Cat) with the co-catalyst (Co-Cat) in the following proportions: M-Cat, 65.6 wt %; Co-Cat, 16.4 wt %; and binder, 18.0 wt %. Bentonite clay (Aldrich) was used as the extruding and binding medium.

The reference catalyst (Z-REF) was obtained by extruding M-Cat with pure Y-AA and bentonite in the same proportions as for HYB.

Z-HYB and Z-REF were dried at 120 ℃ overnight and finally activated at 750 ℃ for 3 h.

4.2.2 Catalyst Characterization

4.2.2.1 Chemical composition

The chemical composition of various catalyst components were determined by atomic absorption spectroscopy.

4.2.2.2 Physical prpperties

The BET total surface area and pore size of these samples were determined by nitrogen adsorption/desorption at 77K, using a Micromeretics ASAP 2000 apparatus. Samples were out-gassed in vacuum for 4h at 220 ℃ before N_2 physisorption. Specific surface areas were calculated according to the Brunauer-Emmett-Teller (BET) method.

4.2.2.3 Acid sites properties

(a) Density of acid sites:

The NH_3-TPD of various samples was recorded using a fixed-bed reactor equipped with a programmable temperature controller. The total surface acidity was measured by a back-titration method as described elsewhere. [126]

(b) Nature of acidic sites and strength profile:

Fourier transform infrared spectra of adsorbed pyridine were recorded in order to evaluate the nature of acidic sites (i.e. Bronsted and Lewis sites). The transmission spectra were recorded using a Nicolet FTIR spectrometer (Magna 500 model) in the region of 1400-1800 cm^{-1}, with resolution of 4 cm^{-1}. The detailed measurements have been previously described. [120, 124]

The identification and the assignment of the bands formed upon pyridine adsorption is well documented in the literature. [127-129]

Particularly, the distribution of the acid sites of the zeolites in terms of strength was previously studied by NH_3-TPD method using a pH-meter equipped with an ion-selective electrode. [126]

4.2.2.4 Study of coke deposition

Thermogravimetric analysis (TGA) and differential thermal analysis (DTA), using a PL Thermal Sciences Model STA-1500 DTA/TGA apparatus, were used to determine the amount of bound species and/or coke deposited onto the catalyst surface. The flow rate of air was set at 30 mL/min. The rate of the temperature-programmed heating (TPH) was set at 10℃/min.

4.2.3 Experimental Set-up and Testing Procedure

Experiments were performed using a Lindberg one-zone tubular furnace. The reactor vessel consisted of a quartz tube 50 cm long, 1.5 cm in outer diameter and 1.2 cm in inner diameter. The temperatures were controlled and regulated by automatic devices that were connected to chromel-alumel thermocouples (set in the catalyst bed and in the pre-heating zone) and the heating furnace.

n-hexane (Aldrich) was used as a model for liquid hydrocarbon feed. In some tests of surface contamination, 1,3,5-trimethylbenzene (135TMB, Aldrich) was added in various concentrations. The feed and water were injected into a vaporizer using two infusion pumps. In the vaporizer, nitrogen used as carrier gas, was mixed with the vaporized feed/steam, and the gaseous stream was then sent into the tubular reactor. The testing conditions used were as follows: temperature, 700 ℃; total weight hourly space velocity (WHSV, feed and steam), $1.52h^{-1}$; catalyst weight, 2.1g; steam/feed weight ratio, 0.5.

Liquid and gaseous products were collected separately, using a system of condensers. The gas-phase components were analyzed using a Hewlett-Packard Model 5890 FID gas chromatograph that was equipped with a 30-m GS-alumina micro-packed column (J & W Scientific), whereas the analysis of the liquid phase was performed using a Hewlett-Packard gas chromatograph (Model 5890, with flame ionization detection (FID)) that was equipped with a Heliflex AT-5 column (Alltech, 30m, nonpolar).

The total conversion (wt %) was expressed as the number of grams of all the products collected at the reactor outlet, by 100g of feed, referring to n-hexane or eventually to the mixture of *n*-hexane and 1,3,5-TMB, therein called FEED, as follows.

Conversion (wt %) = $[(FEED_{in} - FEED_{out})/FEED_{in}]$ 100 (wt %), with FEED in and FEED out being the total weight of (*n*-hexane and eventually, 1,3.5-TMB) injected into the reactor and the unconverted feed determined in the reactor out-stream, respectively.

The selectivity of product i (Y_i) was expressed as the number of grams of product i recovered, by 100 g of total products collected (wt %). It is important to note that the experimental error usually observed on total conversion and calculated product selectivity was ± 0.2 wt %.

4.3. RESULTS AND DISCUSSION

4.3.1 Main physico-chemical properties of the hybrid catalyst components

In our previous paper [109], the main chemical properties of the two components of the hybrid catalyst, the acidic ZSM-5 zeolite and the Ni bearing support (Y-alumina aerogel or Y-AA), were reported. In the present paper, the pore characteristics and the surface acidity properties were carefully investigated because they were believed to have a great influence on the overall catalytic performance.

4.3.1.1 Determination of the extent of the external surface area of the ZSM-5 zeolite particles:

Table 4.1 reports the results of the BET analysis of the various hybrid catalysts and their corresponding references. Herein, the BET surface area corresponding to the micropores was assigned to the internal surface of the zeolite particle whereas that of larger pores was attributed to its external surface. Thus, the external surface included the surface area that was external to the zeolite particle, and the surface area corresponding to that of the (large - sized) mouths of the micropores.

Except for the very SiO_2 rich 1000H sample, all these other ZSM-5 samples or corresponding catalysts showed an external surface area higher than 1/3 of the total surface area (Table 4.1): on such "open" surface, the catalytic reaction was not submitted to the same constraints (shape-selectivity) as on the micropores-related internal surface. It is to note that the SAR values (external to internal surface area ratio) of the hybrid catalysts and their corresponding references showed the same variation trend (with with increasing zeolite SiO_2/Al_2O_3 ratio) as that of the parent zeolites, the co-catalyst or co-catalyst support being incorporated in the same percentage.

Table 4.1: BET Surface Areas of Various Catalyst Components or Catalysts Used in This Work (SAR = external/internal surface area ratio)

	SiO_2/Al_2O_3	Total (m^2/g)	Internal (m^2/g)	External (m^2/g)	External (%)	SAR
Zeolite (powder)						
25H	22	420	270	150	36	0.56
50H	37	403	262	141	35	0.54
100H	98	497	229	268	54	1.17
400H	443	361	231	130	36	0.56
1000H	765	408	235	173	24	0.74
Co-catalyst support						
Y-AA (powder)	0	270	18	252	93	14
Catalysts (extrudates)						
25 HYB		187	116	71	38	0.61
25 Ref		213	127	86	40	0.68
50 HYB		200	124	76	38	0.61
50 REF		205	129	76	37	0.59
100 HYB		196	87	109	56	1.25
100 REF		214	91	123	57	1.35
400 HYB		185	121	61	33	0.5
400 REF		183	89	94	52	1.06
1000 HYB		173	89	84	49	0.94
1000 REF		216	144	72	33	0.5

4.3.1.2 Surface acidity characteristics

Table 4.2 reports the data of surface acidity of the same samples. The two characteristics shown are the density of acid sites and the distribution of these sites according to their strengths. We also made the assumption that these acid sites were homogeneously distributed on all over the surface of the zeolite particle, so that the external/internal surface area ratio (SAR) previously calculated in Table 4.1 is also the

distribution ratio of the acid sites on the external surface to those of the internal surface of the zeolite particle. In terms of acid strength, as expected, a zeolite material with higher Si/Al atom ratio provides stronger acid sites that corresponded to higher desorption temperatures for pre-adsorbed NH_3. It is to note that the ISE method used for the investigation on the distribution of the acid site strength, was not sensitive enough to detect the very low concentration of the desorbed NH_3 (case of 1000H and related materials). However, it is not illogical to say that, by considering the trend in the strength distribution in Table 4.2, most of the acid sites of the 1000H zeolite were strong: this statement was later confirmed by the qualitative investigation of the acid sites using the FT-IR technique applied to pre-adsorbed pyridine (Fig.4.1 to Fig.4.3, in the following section).

Table 4.2: Surface Acidity Properties of Parent ZSM-5 Zeolites and Corresponding Catalysts (The density of acid sites was obtained by back-titration method and the distribution of acid site strength (zeolites) was determined by ISE method.)

	Density of Acid Sites		**Acid Site Strength (distribution)**	
	10^{-3} mol/g	10^{17} sites/m^2	Weak + Medium (%)	Strong (%)
Zeolites (powder)				
25H	1.55	22.3	54	46
50H	0.64	9.6	31	69
100H	0.49	6.0	33	67
400H	0.13	2.4	21	79
1000H	0.12	1.8	n.a.	n.a.
Co-Catalyst support				
Y-AA	0	0		
Catalysts (extrudates)				
25 HYB	0.49	15.7		
25 REF	0.67	19.3		
50 HYB	0.38	11.4		
50 REF	0.44	13.2		
100 HYB	0.29	9.0		
100 REF	0.34	9.6		
400 HYB	0.19	6.0		
400 REF	0.17	5.4		
1000 HYB	0.20	6.3		
1000 REF	0.21	6.6		

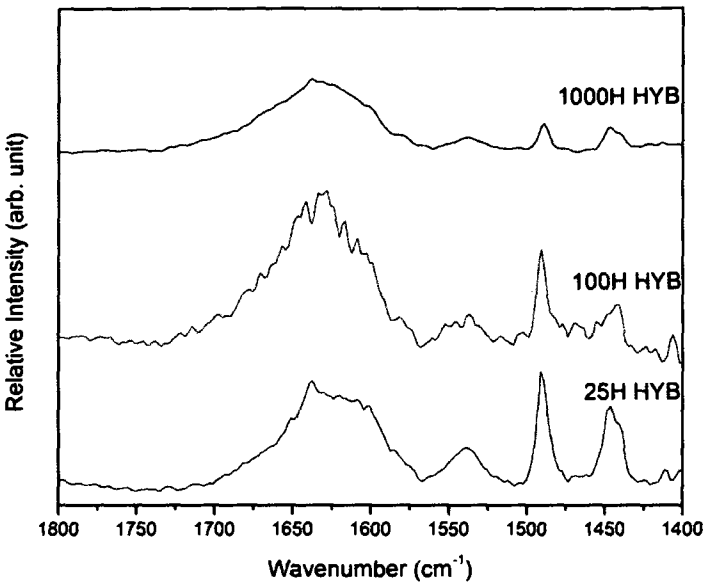

Fig.4.1: FT-IR spectra of pyridine adsorbed onto various hybrid catalysts (recorded at 100 °C)

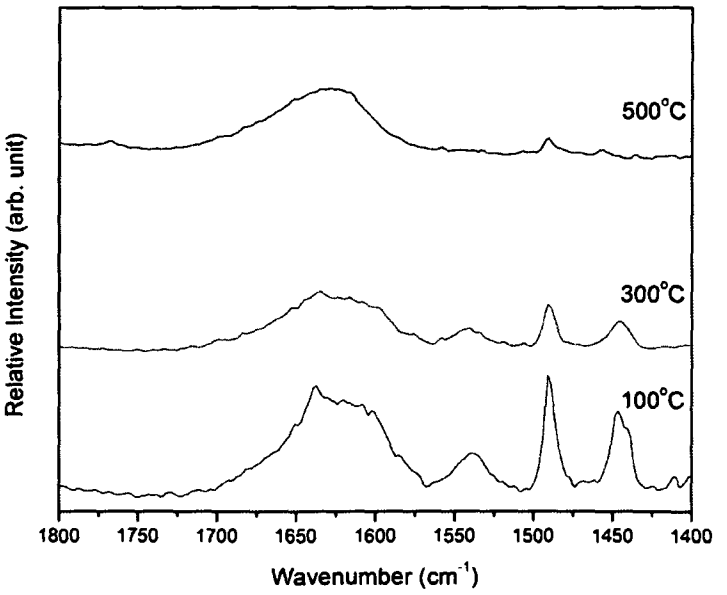

Fig.4.2: FT-IR spectra of pyridine adsorbed onto the (25H HYB) hybrid catalyst (recorded at various temperatures)

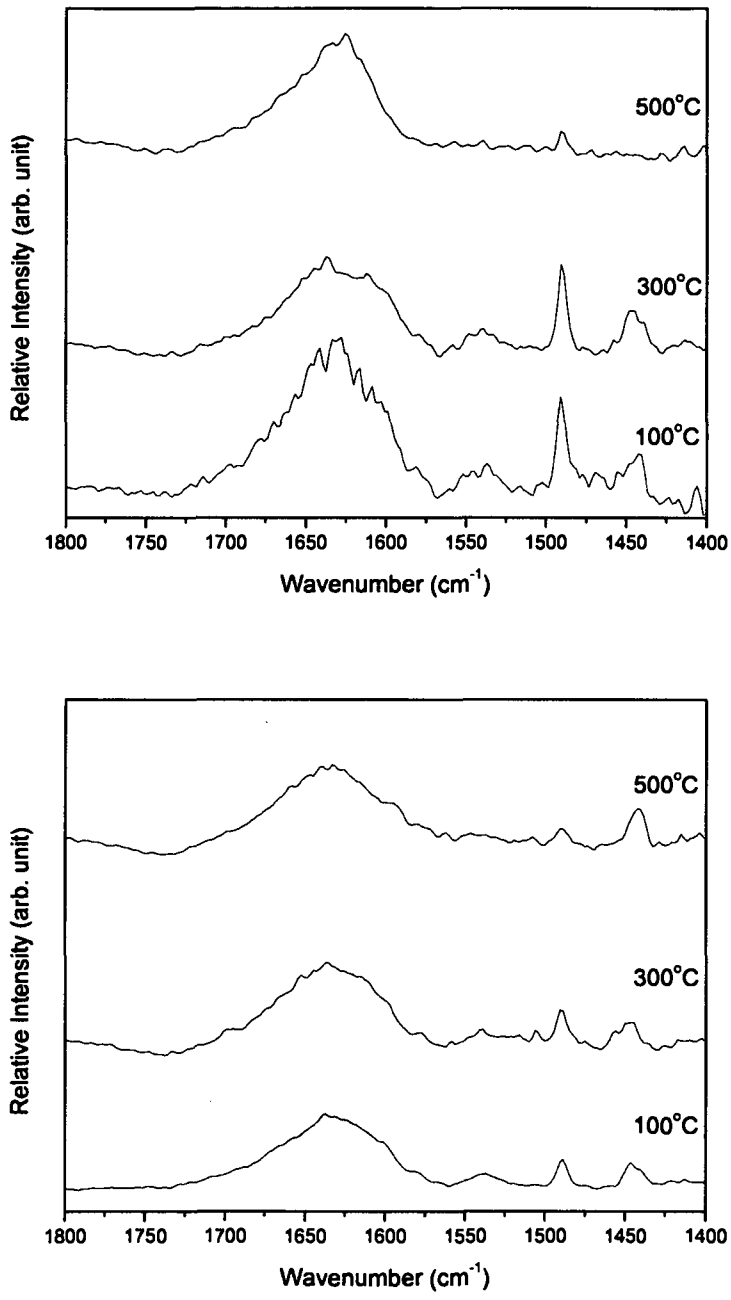

Fig.4.3: FT-IR spectra of pyridine adsorbed onto the (100H HYB (up) and 1000H HYB (bottom)) hybrid catalyst (recorded at various temperatures)

The acidity study using FT-IR technique applied to pyridine adsorption showed that:

1) The FT-IR band at ca. 1540 cm^{-1} that is usually assigned to pyridine molecules adsorbed on Brönsted acid sites, as well as the band at ca. 1485 cm^{-1} that is usually assigned to pyridine molecules adsorbed on both Brönsted and Lewis acid sites, decreased with higher zeolite SiO_2/Al_2O_3 mol ratios (Fig.4.1). Such observation is perfectly coincident with the results of Table 4.2 that showed the same trend for the total density of acid sites.

2) The desorption of the pre-adsorbed pyridine by increasing the temperature of the FT-IR cell, both FT-IR bands recorded on the 25 HYB catalyst prepared from the 25H ZSM-5 zeolite, significantly decreased, suggesting that the acid sites of that catalyst were quite weak, or at least not very strong (Fig.4.2).

3) The FT-IR band assigned to the Lewis acid sites (ca. 1450 cm^{-1}) of the 1000 HYB catalyst appeared to withstand much better high desorption temperatures (Fig.4.3): this suggests that the 1000H zeolite possessed much stronger Lewis acid sites.

4.3.2. Catalytic performance of various hybrid catalysts, related to the Si/Al atom ratio of their zeolite components

Table 4.3 reports the catalytic performance of the hybrid catalysts and their references measured in the testing conditions as mentioned in the experimental section.

There are some (minor) differences between the hybrid catalysts and their corresponding references in terms of catalytic behaviour (total conversion, product selectivity into light olefins and other reaction products). However, the differences became very significant when the coke deposition was considered (Table 4.3):

a) Total coke deposition (wt %) was much larger for the reference samples, indicating the strong "cleaning" effect of the hydrogen spilt-over species.

b) Coke deposition per mmol of acid sites (g/mmol, Table 4.3) became much larger for the reference samples at higher Si/Al atom ratio, indicating that when the acid sites were stronger (Table 4.2) the effect of the hydrogen spilt-over species was more significant.

Table 4.3: Catalytic performances of hybrid catalysts and their corresponding references

Catalyst	Conversion	Product Selectivity (wt %)			Coke Deposition		
	(wt %)	($C_2^=$-$C_4^=$)	($C_3^=/C_2^=$)	(others)	(wt %)	(T, °C)	(g/mmol)
25 HYB	78.50	76.00	1.32	24.00	15.70	552	0.32
25 REF	80.00	66.10	1.49	33.90	24.90	537	0.37
50 HYB	85.00	72.80	1.08	27.20	16.30	548	0.43
50 REF	88.60	70.90	1.11	29.10	21.70	567	0.49
100 HYB	74.80	74.10	1.00	25.90	16.50	572	0.57
100 REF	77.80	74.80	1.09	25.20	22.30	582	0.66
400 HYB	64.00	77.70	0.90	22.30	12.30	559	0.65
400 REF	63.80	76.00	0.91	24.00	23.00	584	1.35
1000HYB	63.20	78.80	0.90	21.30	13.40	567	0.67
1000REF	64.70	76.90	0.88	23.10	25.50	563	1.21

At higher Si/Al atom ratios (of the ZSM-5 zeolite of the main cracking component), the acid density decreased (Table 4.2) and thus, the total conversion decreased as well as the product propylene-to-ethylene ratio ($C_3^=/C_2^=$). However, in order to investigate in more detail the effect of the Si/Al atom ratio of the zeolite component on the catalytic performance of the hybrid catalyst, mostly on the product propylene/ethylene ratio, we managed to obtain, in a separate series of catalytic tests, almost the same conversion for all the couples of "hybrid/reference" catalysts. It can be seen in Table 4.4 that the lower the zeolite SiO_2/Al_2O_3 mol ratio, the higher the propylene/ethylene ratio.

First, it is to note that the acid sites of the ZSM-5 zeolite provided the β-scission cracking action leading to most of product propylene for all the thermo-catalytic cracking reaction. Thus, the higher the acid sites density, the higher the propylene/ethylene ratio. The strength of these acid sites did not show any large influence on this product light olefin ratio.

Table 4.4: Propylene-to-ethylene ratio as a function of the Si/Al ratio of the zeolite component

Catalyst	SiO_2/Al_2O_3(zeolite component)	Conversion (%)	$(C_3^=/C_2^=)$
25 HYB	22	65.00	1.52
50 HYB	37	63.50	1.37
100 HYB	98	64.00	1.21
400 HYB	443	63.70	0.90
1000 HYB	765	63.20	0.90

4.3.3. Multi-facet experimental evidence of the beneficial effect of the co-catalyst

In agreement with previous results [123,124], the coke deposited onto the hybrid catalyst surface was less than that laid onto the surface of the corresponding reference catalyst (Table 4.3). This clearly indicates the beneficial "cleaning" effect of the

hydrogen species, being generated by the Ni co-catalyst sites and then "spilt-over" onto the surface of the zeolite particles.

In the present study, another experimental evidence was given by the following series of tests. In these experiments, the same hybrid configuration, 50 HYB, was used. However, the weight of the Ni supported co-catalyst was varied from 0 g to 1.5 g, the balance being the co-catalyst support, Y-AA. It is to note that the bare Y-AA surface did not show any generation of hydrogen species in the presence of n-hexane and steam. The coke deposited was burnt in the DTA-TGA system and the results (weight loss and combustion temperature, T_c) are reported in Table 4.5.

Table 4.5: Co-catalyst content versus the coke deposition

Wt of co-catalyst (g)	Wt of Y-AA (g)	Wt loss (%)	T_c (^{0}C)
1.5 (same as 50 HYB)	0.0	16.3	548
1.0	0.5	16.6	558
0.5	1.0	20.1	556
1.5 (same as 50 REF)	1.5	21.7	567

Therefore, this means that a higher amount of co-catalyst used in the hybrid composition resulted in a larger production of hydrogen spilt-over species and thus, a more efficient cleaning action.

4.3.4 Acceleration of the coke deposition by the "contamination" method

In accordance with the originally hypothesized reaction mechanism known as "hydrocarbon pool mechanism" [130] and its recently modified version [131], polymethylbenzenes play a key role in the conversion of methanol into higher hydrocarbons. In our previous work [123], it was shown that 1,2,4-trimethyl benzene (1,2,4-TMB) when added to the (*n*-hexane) feed in quite modest content could

significantly modify the catalytic results. Our interpretation was, because 1,2,4-TMB had a molecular cross-section narrow enough so that it could be adsorbed into the ZSM-5 zeolite micropores, this contaminant would block certain accesses to these micropores. On the external surface of the zeolite particle, 1,2,4-TMB acted as adsorption competitor to n-hexane, causing some significant activity decay. However, "contamination" by a bulkier pentamethyl benzene (PMB) did not result in "abnormal" catalytic behaviour, except for monotonic decreases of total conversion and product selectivity due to competitive adsorption of PMB with reacting *n*-hexane.

In the present work, the contaminant used was 1,3,5-trimethylbenzene (1,3,5-TMB). This molecule behaved like the PMB, i.e. it could affect only the adsorption (and thus the reaction) of *n*-hexane on the external surface because with its large molecular cross-section dimension, it was totally excluded from the internal surface (micropores) of the zeolite particles. The obtained catalytic results (Fig.4.4, Fig.4.5) and coke deposition (Fig.4.6) were similar to those of PMB (added to *n*-hexane, [123]), i.e. quite smooth activity decrease, up to 8 wt % of 1,3,5 -TMB and then, more pronounced activity decay at higher contaminant concentration.

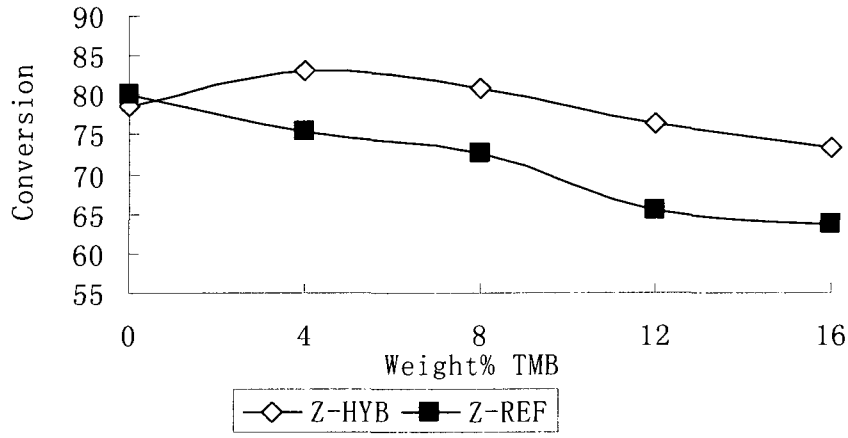

Fig.4.4: Effect of the 1,3,5-TMB "contamination" on the total conversion of the (25H) hybrid and that of the (25H) reference catalysts

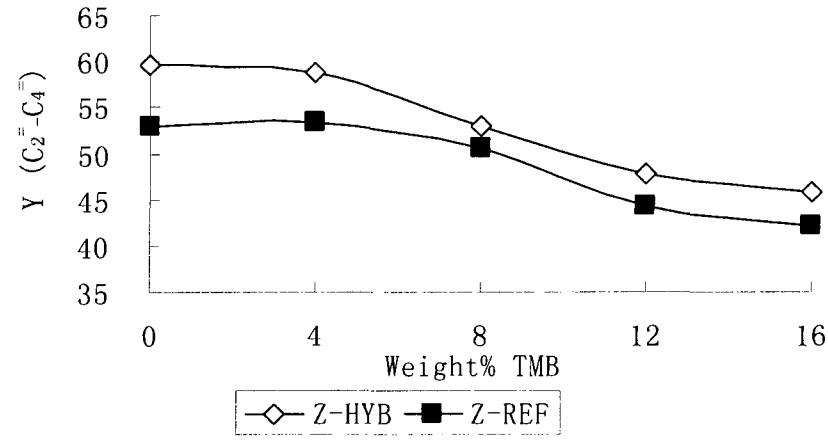

Fig.4.5: Effect of the 1,3,5-TMB contamination on the selectivity in C_2–C_4 olefins of the (25H) hybrid and that of the (25H) reference catalysts

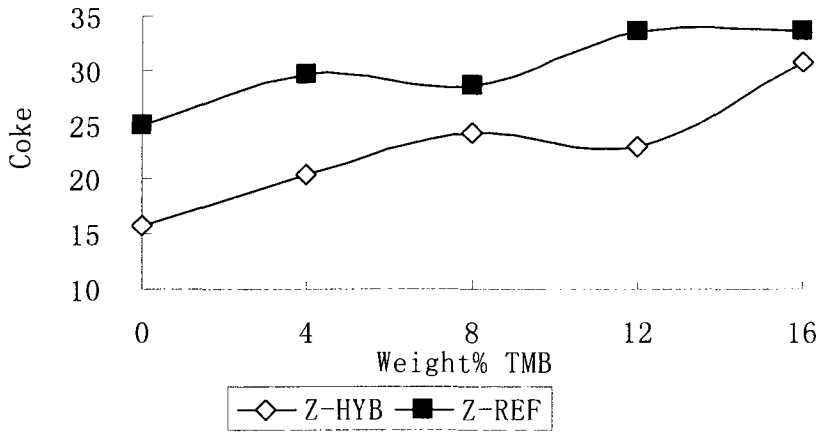

Fig.4.6: Coke deposition onto the (25H) hybrid and reference catalysts in the presence of 1,3,5-TMB contaminant

In one special series of tests, a massive contamination by 1,2,4-TMB (16 wt % in hexane) was performed in runs using catalysts containing ZSM-5 zeolites of various SiO_2/Al_2O_3 mol ratios (Fig.4.7 to Fig.4.10). 1,2,4-TMB was known to affect both the external surface and the internal surface, i.e. the micropores of the ZSM-5 zeolite. [123] The conversion and the selectivity in light olefins, as reported in Fig.4.7 and Fig.4.8, showed significantly higher levels of catalytic activity for the hybrid catalysts 25H and 50H; however, this was not the case for the other catalysts. In fact, although the difference in the coke formation was almost the same for all the couples "hybrid and reference catalysts" (Fig.4.9), catalysts prepared with silica-richer ZSM-5 zeolites (higher SiO_2/Al_2O_3 mol ratio: 100H, 400H, and 1000H) produced coke with heavier nature (whose combustion required higher temperatures, Fig.4.10). This suggests that strong acid sites found in these zeolites induced the formation of heavier coke that was much harder to be removed. In those cases, the hydrogen spilt-over species, produced by the

co-catalyst, were not capable to efficiently clean the cracking surface as in the case of catalysts having milder surface acidity (25H and 50H).

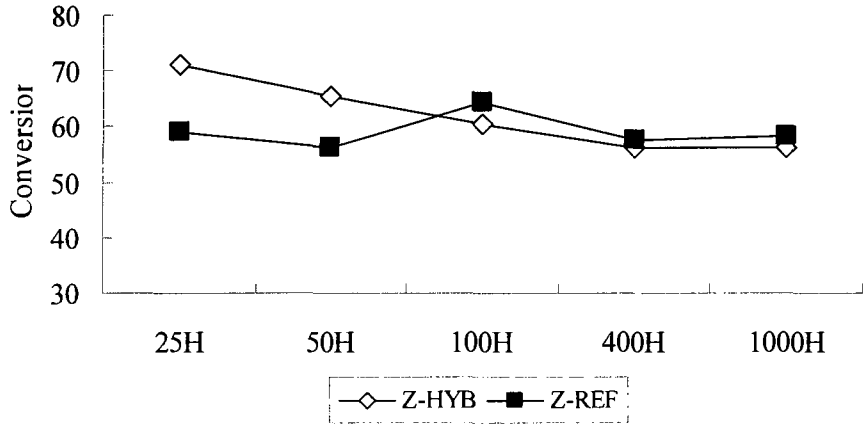

Fig.4.7: Effect of the massive contamination by 1,2,4-TMB on the total conversion

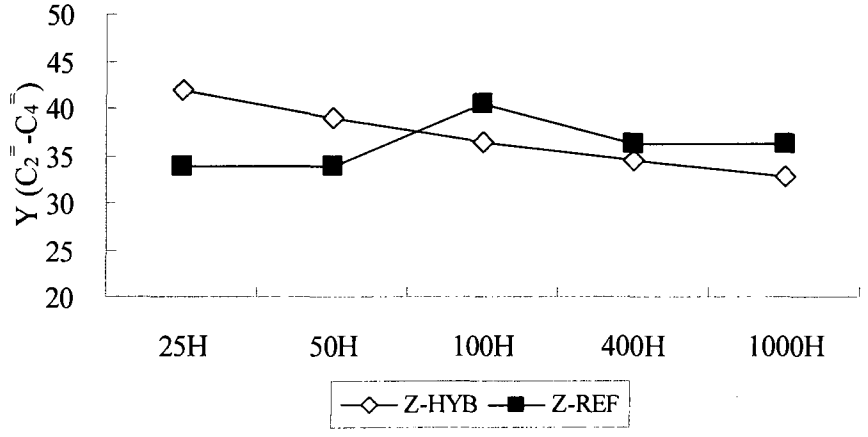

Fig.4.8: Effect of the massive contamination by 1,2,4-TMB on the selectivity in C_2-C_4 olefins

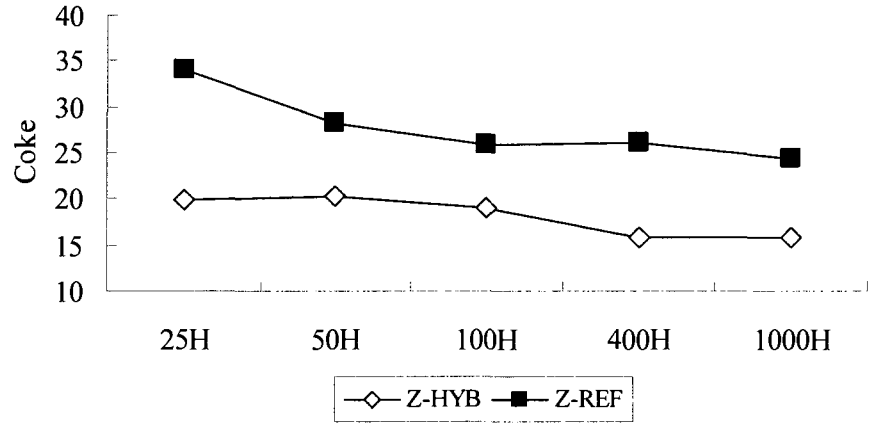

Fig.4.9: Effect of the massive contamination by 1,2,4-TMB on the coke deposition

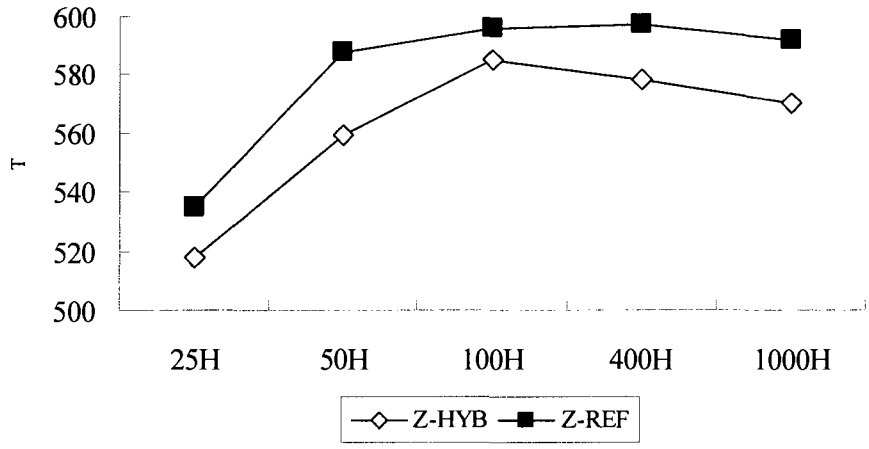

Fig.4.10: Effect of the massive contamination by 1,2,4-TMB on the nature of the coke deposited

4.4. CONCLUSION

First of all, in all the experiments carried out in this work, the beneficial effect of the Ni bearing co-catalyst was clearly observed: coke deposition onto the hybrid catalyst was always significantly lower than that of the corresponding reference catalysts. This "cleaning action", as mentioned in the introduction, would allow the hybrid catalyst to

slow down the "fouling" phenomena and thus, lengthen the on-stream duration between the two decoking operations.

The present data, related to the intrinsic properties of the zeolite component, are useful for the development of the hybrid catalysts being used in the Thermo-Catalytic Cracking process (TCC, fixed-bed technology) because of the following implications:

1) Higher yields in light olefins, mostly ethylene and propylene, and higher product propylene-to-ethylene ratio can be obtained.

2) Higher catalyst on-stream stability can be achieved.

In fact, these data show that, to obtain high yields in light olefins, the ZSM-5 zeolite must have a relatively low SiO_2/Al_2O_3 mol ratio, so that the density of acid sites is high (resulting thus in high total conversion) with an acidity strength relatively mild (favouring thus a high propylene/ethylene ratio). On the other hand, such milder acid sites also lead to a lower amount of deposited coke, the latter exhibiting actually a lighter chemical nature. This will ease the cleaning action of the hydrogen spilt-over species, resulting finally in a greater (and desired) on-stream stability of the hybrid catalyst.

On the other hand, today's trend is to blend to the heavy petroleum feedstocks used in the process, some bio-compounds that can be available in the future, such as alcohols or glycerol. However, these co-reactants should not show too strong adsorption properties onto the cracking surface, in order not to promote a strong competitive adsorption with the feed molecules, or a disastrous self-trapping in the narrow zeolite micropores. This means that the larger the external surface of the zeolite particles, the better the catalytic performance. Therefore, as the ZSM-5 zeolite is concerned, submicron-sized particles have to be preferably used. [132]

The information resulting from this work will also be helpful for the development of the TCC catalysts for the fluidized-bed technology.

4.5. AUTHOR'S NOTES AND SIGNIFICANCE OF PAPER TO THESIS

The results reported in this chapter clearly evidenced the "cleaning action" of the hydrogen spilt-over species. In fact, the coke deposition onto the hybrid catalyst was always significantly lower than that of the corresponding reference catalysts. Data of the present work also showed that the ZSM-5 zeolite component should have a relative low SiO_2/Al_2O_3 ratio (i.e. a high density of acid sites) so that high yields in light olefins could be obtained. The acidity strength of these acid sites should be relative mild, in order to favour a high propylene/ethylene product ratio. In addition, these milder acid sites led to a lower coke deposition. In summary, the "cleaning action" of the hydrogen spilt-over species resulted in several advantages for the TCC process: 1) easy catalyst regeneration, 2) lower emissions of greenhouse gases (CO_2) and 3) lower energy consumption.

Chapter V

GENERAL CONCLUSIONS and FUTURE WORK

5.1. GENERAL CONCLUSIONS

The results obtained in this thesis successfully demonstrated the positive role of the hydrogen spill-over species in improving the catalytic activity and stability of the hybrid catalysts used in the Thermo-Catalytic Cracking (TCC) process. These hydrogen species, which were produced by Ni bearing co-catalysts through steam-reforming, were found to be able to perform certain "cleaning action", allowing the hybrid catalyst to slow down the "fouling" rate and thus, improve its on-stream stability.

Most of the catalysts used in the TCC process were in the hybrid configuration. They consisted of two porous components: a main component having cracking properties and a co-catalyst having active sites that can affect the product selectivity of the former (cracking) sites. [114] The results obtained from the on-stream tests showed that nickel-based catalysts could produce hydrogen species from hydrocarbons, particularly methane, by steam reforming and subsequent reactions (water-gas shift). These hydrogen species were believed to partially retard coking reactions by their de-aromatizing action: impact the "normal" sequence to coke involves aromatics generated by olefinic species (cracking reactions), which subsequently converted fast into coke precursors and finally coke. These hydrogen species might directly react with polynuclear aromatics already present in the feedstock. However, after a very short period of time-on-stream of 10 hours, Ni containing hybrid catalysts had very little effect on lighter hydrocarbon feedstocks suggesting that dearomatization of existing polynuclear aromatics was predominant. [114] In addition, the temperatures of thermal decomposition and coke combustion observed from the DTA/TGA study indicated that the coke deposited on the hybrid

catalysts were not only in much smaller amounts but had also a much lighter nature, in comparison with the coke laid down on the reference catalysts. A lower coking rate represents several advantages for the entire process: a) higher on-stream stability; b) easier catalyst regeneration (lower energy consumption) and c) lower emission of greenhouse gases (CO_2). Moreover, the concept of hybrid catalysts that can induce hydrogen spill-over effect is proven to have powerful dearomatizing/ring opening properties. The use of this type of catalysts may reduce polynuclear aromatics in middle-distillate fuels, which are known for "producing particulates in the exhaust gases and, in addition, having poor ignition properties."

Tests for on-stream stability were also carried out with model molecules. According to the "hydrogen pool mechanism", pentamethylbenzene (PMB) and 1,2,4-trimethylbenzene (1,2,4-TMB) were chosen as coke precursors and added into the *n*-hexane feed in the cracking reaction. PMB having a critical diameter larger than the average size of the micropores of the ZSM-5 zeolite, could only expressed some contamination effect on the external surface of the zeolite particles. Although there was no apparent difference in activity between the hybrid catalyst and the reference catalyst because the exposure time was too short, the former one did exhibit a lower coke deposition and a lighter coke nature, i.e. lower combustion temperature of coke. This was another experimental evidence of the influence of the hydrogen spilt-over species. On the other hand, 1,2,4-TMB, which has smaller critical diameter, can easily diffuse into the ZSM-5 zeolite channels and induce a certain pore blockage due to a significant amount of 1,2,4-TMB firmly adsorbed on the micropore surface. The results, from the cracking of *n*-hexane containing a relatively large amount of 1,2,4-TMB, showed that the hybrid

catalyst was more active and more stable than the reference catalyst, again suggesting a noticeable influence of the hydrogen split-over species on the catalyst activity. Therefore, the unusual behaviour of the hybrid catalyst when converting the mixed *n*-hexane/1,2,4-TMB feed could be attributed to the limitation of the motion of the hydrogen split-over species that could be transferred from the co-catalysts furface to the external surface of the ZSM-5 zeolite particles but not to the inside of the zeolite micropores. [123]

Furthermore, the influence of the pore characteristics and the acidity properties of the ZSM-5 zeolite-based component on the overall catalytic performance was investigated. It was found that the cracking component (ZSM-5 zeolite) of the hybrid catalyst used in the Thermo-Catalytic Cracking (TCC) process required a relatively low SiO_2/Al_2O_3 mole ratio because its high density of acid sites would lead to a high total conversion and its mild acid strength would favour a high propylene/ethylene ratio. Milder acid sites would also result in a lower amount of coke deposition. In addition, the lighter nature of coke would ease the catalyst regeneration in the industrial process. Therefore, this present data, related to the intrinsic properties of the zeolite component, is useful for the development of the hybrid catalysts being used in the Thermo-Catalytic Cracking process.

5.2. FUTURE WORK

The results obtained in this thesis are very interesting from a fundamental and applied viewpoint. However, the nature of the hydrogen spilt-over species remains not known with an absolute certainty. [114] The study of the nature of the hydrogen split-over species is not an easy task because this would need investigation techniques and equipment which are able to reach the molecular level of the reaction that has to be

carried out in real working conditions. Because the reaction must be performed in-situ, i.e. inside the analytical apparatus, the incorporation of a small reactor into such equipment that would allow one to identify the hydrogen species (such as solid state NMR or FT-IR) is very hard due mainly to the harsh reaction conditions of the cracking process, i.e. high temperatures. However, certain reactions may allow us to obtain more acceptable insights about the nature of the hydrogen split-over species. For example, hydrogenation of benzene into cyclohexane may be used to compare the hydrogenating efficiency of molecular hydrogen and atomic hydrogen. Conventional hydrogenation of benzene takes place in the presence of an oxide catalyst (such as Cr_2O_3 or V_2O_5) at a relatively high temperature (400-500 ℃) under quite high pressure of hydrogen. However, with a Ni containing hybrid catalyst which has the ability to produce active hydrogen species (presumably atomic) through steam reforming, the hydrogenation of benzene may take place in the presence of a much limited amount of steam and co-fed hydrocarbon (methane or *n*-hexane, for instance). The expected results help us demonstrate that atomic hydrogen species are responsible for the hydrogenation reaction. Therefore, hydrogenation of benzene in the presence of limited amounts of steam and light alkane over a Ni containing hybrid catalyst can provide precious indications about the nature and even the catalytic action of these hydrogen spilt-over species.

Chapter VI

REFERENCES

[1] Wade, L. G.; in: Organic Chemistry; Pearson Prentice Hall, 6th Edition; (**2006**) pp.279

[2] Moss, G. P.; Smith, P.A.S.; *Pure and Applied Chemistry* (**1995**) 67:1307

[3] Matar, S.; Hatch, L. F.; in: Chemistry of Petrochemical Processes; 2nd edition, (Gulf Professional Publishing); (**2001**) pp.1-48

[4] Eramo, M.; *Oil & Gas Journal* 103 (**2005**) 45:52

[5] Aitani, A. M.; Oil,Gas (Hamburg) Germany (**2004**) 30:36

[6] Al-Yassir, N.; Ph.D. thesis; Concordia University; Canada; (**2006**) pp.1-33

[7] Chang, T.; *Oil & Gas Journal* 99 (**2001**) 17:58

[8] Plotkin, J. S.; *Catal. Today.* (**2005**) 106:10

[9] Severn, J. R.; Chadwich, J. C.; Duchateau, R.; Friederichs, N.; *Chem. Rev.* (**2005**) 105:4073

[10] Matar, S.; Hatch, L. F.; in: Chemistry of Petrochemical Processes; 2nd edition, (Gulf Professional Publishing); (**2001**) pp.188-261

[11] Chauvel, A.; and Lefebvre, G.; in: Petrochemical Processes; Vol.1, (Editions Technip, Paries); (**1989**) pp.118-194 and 169-227

[12] Hunt, D. A.; in: Handbook of Petroleum Refining Processes; 2nd edition, ed. Meyers, R. A., (McGraw Hill, Boston); (**1997**)

[13] http://www.chem.tamu.edu/class/majors/chem470/Steam_Cracking.html

[14] Speight, J. G.; in: The Chemistry and Technology of Petroleum; 4th Edition, (CRC Press); (**2006**) pp.521-545

[15] Leprince, P.; in: Conversion Processes; (Editions Technip, Paris); (**1998**) pp.169-223

[16] Decroocq, D.; in: Catalytic Cracking of Heavy Petroleum Reactions; (Editions Technip, Paris,); (**1984**) pp.73-114

[17] Aitani, A.; Yoshikawa, T.; Ino, T.; *Catal. Today.* (**2000**) 60:111

[18] Buchanan, J. S.; *Cataly. Today.* (**2000**) 55:207

[19] Corma, A.; Martinez, A.; in: M. Guisnet, J-P Gilson (Eds) Zeolites for Cleaner Technogies; Vol.3, (Imperial College Press); (**2002**) pp.29-55

[20] Raseev, S.; in: Thermal and Catalytic Processes in Petroleum Refining; (Marcel Dekker, Inc. New York); (**2003**) pp.275-421

[21] kotrel, S.; Knozinger, H.; Gates, B. C.; *Micropor. Mesopor. Mater.* (**2000**) 35:11

[22] Hagen, J.; in: Industrial Catalysis, A Practical Approach; 1st edition, (Wiley-VCH Verlag Gmbh, Weinheim, Germany); (**1999**) pp.83-98

[23] Gats, B. C.; in: Catlytic Chemistry; (John Wiley & Sons, Inc., New York); (**1992**) pp.268-275

[24] Tung, S. E.; McIninch, E.; *J. Catal.* (**1968**) 10:166

[25] Nace, D. M.; *Ind. Eng. Chem. Prod. Res. Dev.* (**1969**) 8:31

[26] Borodzinski, A.; Corma, A.; Wojciechowski, B. W.; *Canad. J. Chem. Eng.* (**1980**) 58:219

[27] Greensfelder, B. S.; Voge, H. H.; Good, G. M.; *Ind. Eng. Chem.* (**1957**) 49:742

[28] Janardhan, P. B.; Rajeswari, R.; *Ind. Eng. Chem. Prod. Res. Dev.* (**1977**) 16:1

[29] Planelles, J.; Sanchez-Martin, F.; Tomas, F.; Corma, A.; *J. Mol. Catal.* (**1985**) 32:365

[30] Abbot, J.; Head, I. D.; *J. Catal.* (**1990**) 125:187

[31] Poustma, M. L.; in: Zeolite Chemistry and Catalysis ED. J. A. Rabo; (ACS Monograph, Washington DC); (**1976**) pp.117-505

[32] Raseev, S.; in: Thermal and Catalytic Processes in Petroleum Refining; (Marcel Dekker, Inc. New York); (**2003**) pp.275-421

[33] Greensfelder, B. S.; Voge, H. H.; Good, G. M.; *Ind. Eng. Chem.* (**1949**) 41:2573

[34] Haag, W. O.; Dessau, R. M.; *Proc. 8th Int. Congr. Catal.* (Berlin, Vol 2) (**1984**) pp.305

[35] Scherzer, J.; *Catal. Rev. Sci. Eng.* (**1989**) 31:215

[36] Zhao, X.; Harding, R. H.; *Ind. Eng. Chem. Res.* (**1999**) 38:3854

[37] Corma, A.; Melo, F. V.; Sauvanaud, L.; Ortega, F.; *Catal. Today.* (**2005**) 107-108:699-706

[38] Yoshimura, Y.; Kijima, N.; Hayakawa, T.; Murata, K.; Suzuki, K.; Mizukami, F.; Matano, K.; Konichi, T.; Oikawa, T.; Saito, M.; Shiojima, T.; Shiozswa, K.; Wakui, K.; Sawada, G.; Sato, K.; Matsuo, S.; Yamaoka, N.; *Catalysis Surverys from Japan* Vol.4 (**2000**) 2:157

[39] http://www.ec.gc.ca/pdb/ghg/inventory_report/2006/som-sum_eng.pdf

[40] Le Van Mao, R.; Melançon, S.; Gauthier-Campbell, C.; Kletniek, P.; *Catal. Lett.* (**2001**) 73:181

[41] Melançon, S.; Le Van Mao, R.; Kletniek, P.; Ohayon, D,; Intem, S.; Saberi, M. A.; McCann, D.; *Catal.Lett.* (**2002**) 80:103

[42] Le Van Mao, R.; Vu, N. T.; Al-Yassir, N.; François, N.; Monnier, J.; *Top.Catal.* (**2006**) 37:107

[43] Le Van Mao, R.; Vu, N. T.; Al-Yassir, N.; Yan, H. T.; *Ind. Eng. Chem. Res.* (**2008**) 47:2963

[44] Le Van Mao, R.; Muntasar, A.; Yan, H. T.; Zhao, Q.; *Catal. Lett.* (**2009**) 130:86

[45] Yan, H. T.; Le Van Mao, R.; *Catal. Lett.* (**2009**) Published online: 07 April 2009

[46] Al-Yassir, N.; Le Van Mao, R.; *Can. J. Chem.* (**2008**) 86:146

[47] Le Van Mao, R.; *Micropor. Mesopor. Mat.* (**1999**) 28:9

[48] Le Van Mao, R.; Al-Yassir, N.; Nguyen, D. T. T.; *Micropor. Mesopor. Mat.* (**2005**) 85:176

[49] Al-Yassir, N.; Le Van Mao, R.; Heng, F.; *Catal. Lett.* (**2005**) 100:1

[50] Roland, U.; Braunshweig, T.; Roessner, F.; *J. Mol. Catal. A* (**1997**) 127:61

[51] Conner, W. C.; Pajonk, G. M.; Teichner, S.; *J. Adv. Catal.* (**1986**) 34:1

[52] Zhang, A.; Nakamura, I.; Aimoto, K.; Fujimot, K.; *Ind. Eng. Chem. Res.* (**1995**) 34:1074

[53] Hattori, H.; Shishido, T.; *Catalysis Surverys form Japan* (**1997**) 1:205

[54] Udea, R.; Tomishige, K.; Fujimoto, K.; *Catal. Lett.* (**1999**) 57:145

[55] Al-Yassir, N.; Ph.D. Proposal; Concorda University; Montreal; (**2007**)

[56] Anderson, J. R.; Pratt, K. C.; In: Introduction to Characterization and Testing of Catalysts; (Academic Press, INC. London) **(1985)** pp.2-5

[57] Brunauer, S.; Emmett, P. E.; Teller, E.; *J.Am.chem. Soc.* **(1938)** 60:309

[58] Lin, L.; M.Sc. Thesis, Concordia University, Montreal, Canada **(2005)** pp.45-48

[59] Le Van Mao, R.; Al-Yassir, N.; Lu, L.; vu, N. T.; Fortier, A.; *Catal. Lett.* **(2006)** 112:13

[60] Lynch, J.; in: Analyse physico-chimique des catalyseurs industriels (ED. Technip, Paris) **(2001)** pp.270

[61] Chauvel, A.; Lefebvre, G.; In: *Petrochemical Processes*; (Editions Technip: Paris) **(1989)** Vols. 1 and 2

[62] Corma, A.; Melo, F. V.; Sauvanaud, L.; Ortega, F.; *Catal. Today* **(2005)** 107:699

[63] Le Van Mao, R.; Melancüon, S.; Gauthier-Campbell, C.; Kletniek, P.; Catal. Lett. **(2001)**73:181

[64] Melancüon, S.; Le Van Mao, R.; Kletniek, P.; Ohayon, D.; Intem, S.; Saberi, M. A.; McCann, D.; *Catal. Lett.* **(2002)**, 80:103

[65] Le Van Mao, R.; Vu, N. T.; Al-Yassir, N.; Francüois, N.; Monnier, J.; *Top. Catal.* **(2006)** 37:107

[66] Le Van Mao, R.; Al-Yassir, N.; Nguyen, D. T. T.; *Microporous Mesoporous Mater.* **(2005)** 85:176

[67] Le Van Mao, R.; *Microporous Mesoporous Mater.* **(1999)** 28:9

[68] Le Van Mao, R.; U.S. Pat. 4,732,881, **(1988)**

[69] Le Van Mao, R.; Dufresne, L.; Yao, J.; *Appl. Catal.* **(1990)** 65: 43

[70] Al-Yassir, N.; Le Van Mao, R.; Heng, F.; *Catal. Lett.* **(2005)** 100:1

[71] Al-Yassir, N.; Le Van Mao, R.; *Appl. Catal. A* **(2007)** 317:275

[72] Le Van Mao, R.; Al-Yassir, N.; Lu, L.; Vu, N. T.; Fortier, A.; *Catal. Lett.* **(2006)** 112:13

[73] Leprince, P.; In: *ConVersion Processes*; (Editions Technip: Paris) **(2001)** pp.455.

[74] Pajonk, G. M.; In: *Proceedings of the Second International Conference on Spillover*, Leipzig, German Democratic Republic, **(June 12-16, 1989)**; Steinberg, K.-H., Ed.; pp.1.

[75] Conner, W. C., Jr.; Falconner, J. L.; *Chem. Rev.* **(1995)** 95:759

[76] Delmon, B.; In: *New Aspects of Spillover Effect in Catalysis*; Inui, T., Fujimoto, K., Uchijima, T., Masai, M., Eds.; Proceedings of the Third International Conference on Spillover, Kyoto, Japan, **(August 17-20, 1993)**; (Elsevier: Amsterdam) **(1993)** pp.1.

[77] Parera, J. M.; Traffano, E. M.; Musso, J. C.; Pieck, C. L.; *Stud. Surf. Sci. Catal.* **(1983)** 17:101

[78] Ma, H.; Kojima, S.; Kikuchi, R.; Ichikawa, M.; *Catal. Lett.* **(2005)** 104: 63.

[79] Raseev, S.; In: *Thermal and Catalytic Processes in Petroleum Refining*; (Marcel Dekker: New York) **(2003)** pp.48.

[80] Du, H.; Fairbridge, C.; Yang, H.; Ring, Z.; *Appl. Catal. A* **(2005)** 294:1

[81] Le Van Mao, R.; Dufresne, L. A.; Yao, J.; Yu, Y.; *Appl. Catal. A* **(1997)** 164:81

[82] Kung, H. H.; In: *Transition Metal Oxides: Surface Chemistry and Catalysis*; Delmon, B., Yates, J. T., Eds.; (Elsevier: Amsterdam) **(1989)** Vol.45 pp.83.

[83] Lynch, J.; In: *Analyse Physico-chimique des Catalyseurs Industriels*; (Editions Technip: Paris) **(2001)** pp.273.

[84] Corma, A.; Melo, F. V.; Sauvanaud, L.; Ortega, F.; *Catal. Today* **(2005)** 107-108:699

[85] Baeza, P.; Villarroel, M.; Avila, P.; Lopez Agudo, A.; Delmon, B.; Gil-Llambias, F.; *J. Appl. Catal. A* **(2006)** 304:109

[86] Dufresne, L. A.; Le Van Mao, R.; Catal. Lett. **(1994)** 25:371

[87] Yang, H.; Chen, H.; Chen, J.; Omotoso, O.; Ring, Z.; *J. Catal.* **(2006)** 243:36

[88] Li, X.; Yang, J.; Liu, Z.-W.; Asami, K.; Fujimoto, K.; *J. Jpn. Pet. Inst.* **(2006)** 49:86

[89] Li, Y.; Yang, R. T.; *J. Am. Chem. Soc.* **(2006)** 128:8136

[90] Panayotov, D. A.; Yates, J. T., Jr.; *J. Phys. Chem. C* **(2007)** 111:2959

[91] Le Van Mao, R.; Vu, N.T.; Al-Yassir, N.; Yan, H.T.; *Ind. Eng. Chem. Res.* **(2008)** 47:2963

[92] Le Van Mao, R.; Vu, N.T.; Al-Yassir, N.; François, N.; Monnier, J.; *Top. Catal.*

(2006) 37:107

[93] Le Van Mao, R.; Muntasar, A.; Yan, H.T.; Zhao, Q.; *Catal Lett* **(2009)** (in press)

[94] Dahl, I.M.; Kolboe, S.; *J. Catal.* **(1994)** 149:458

[95] Haw, J.F.; Marcus, D.M.; **(2003)** In: Ayerbach SM, Carrado KA, Dutta PK (eds) *Handbook of zeolite science and technology*. (Marcel Dekker Inc, New York) pp. 833

[96] Haw, J.F.; *Phys. Chem.* **(2002)** 4:5431

[97] Chang, C.D.; *Catal. Rev.* **(1983)** 25:1

[98] Bjorgen, M.; Olsbye, U.; Kolboe, S.; *J. Catal.* **(2003)** 215(1):30

[99] Bjorgen, M.; Svelle, S.; Joensen, F.; Nerlov, J.; Kolboe, S.; Bonino, F.; Palumbo, L.; Bordiga, S.; Olsbye, U.; *J. Catal.* **(2007)** 249:195

[100] Al-Yassir, N.; Le Van Mao, R.; *Can. J. Chem.* **(2008)** 86:146

[101] Al-Yassir, N.; **(2007)** *Multifunctional Catalysts used in the Thermo-Catalytic Cracking of Hydrocarbon feedstocks for the production of Light Olefins*, Ph.D. thesis, Concordia University (Montreal,Canada), December, 2007

[102] Sugi, Y.; Kubota, Y.; Komura, K.; Sugiyama, N.; Hayashi, M.; Kim, J.H.; **(2005)** In: Cejka J, Zikova N, Nachtigall P (eds) *Studies in surface science and catalysis*, vol 158. (Elsevier, Amsterdam) pp.1279

[103] Barrer, R.M.; *J. Incl. Phenomena.* **(1983)** 1:105

[104] Richardson, J.T.; **(1989)** *Principles of catalyst development*. Springer, New York, p 79

[105] Choudary, V. R.; Akolekar, D.B.; *J. Catal.* **(1989)** 117:542

[106] Han, X.; Yan, Z.; Zhang, W.; Bao, X.; *Current. Org. Chem.* **(2001)** 5:1017

[107] Arstad, B.; Kolboe, S.; *J. Am. Chem. Soc.* **(2001)** 123:8137

[108] Hoang, V.T.; Huang, Q.; Eic, M.; Do, T.O.; Kaliaguine, S.; *Langmuir* **(2005)** 21:5094

[109] Chauvel, A.; Lefebvre, G.; **(1989)** *Petrochemical Processes, Editions Technip, Paris,* Vol.1 and 2.

[110] Corma, A.; Melo, F.V.; Sauvanaud, L.; Ortega, F.; *Catal. Today.* **(2005)** 107:699

[111] Le Van Mao, R.; Melançon, S.; Gauthier-Campbell, C.; Kletniek, P.; *Catal. Lett.* **(2001)** 73:181

[112] Melançon, S.; Le Van Mao, R.; Kletniek, P.; Ohayon, D.; Interim, S.; Saberi, M.A.; McCann, D.; *Catal. Lett.* **(2002)** 80:103

[113] Le Van Mao, R.; Al-Yassir, N.; François, N.; Monnier, J.; *Top. Catal.* **(2006)** 37:107

[114] Le Van Mao, R.; Vu, N.T.; Al-Yassir, N.; and Yan, H.T.; *Ind. Eng. Chem. Res.* **(2008)** 47:2963

[115] Le Van Mao, R.; Muntasar, A.; Yan, h.T.; Zhao, Q.; *Catal. Lett.* **(2009)** 130:86

[116] Le Van Mao, R.; Al-Yassir, N.; Nguyen, D.T.T.; *Microporous Mesoprous Mater.* **(2005)** 85:176

[117] Le Van Mao, R.; *Microporous Mesoporous Mater.* **(1999)** 28:9

[118] Le Van Mao, R.; U.S. Pat. 4,732,881 **(1988).**

[119] Le Van Mao, R.; Dufresne, L.; Yao, J.; *Appl. Catal.* **(1990)** 65:143

[120] Al-Yassir, N.; Le Van Mao, R.; Heng, R.; *Catal. Lett.* **(2005)** 100:1

[121] Al-Yassir, N.; Le Van Mao, R.; *Appl. Catal. A* **(2007)** 317:275

[122] Al-Yassir, N.; Le Van Mao, R.; *Can. J. Chem.* **(2008)** 86:146

[123] Yan, H.T.; Le Van Mao, R.; *Catal. Lett.* **(2009)** 130:558

[124] Al-Yassir, N.; Le Van Mao, R.; *Appl. Catal.* **(2006)** 305:130

[125] Al-Yassir, N.; Le Van Mao, R.; *Appl. Catal.* **(2007)** 332:273

[126] Le Van Mao, R.; Al-Yassir, N.; Lu, L.; Vu, N.T.; Fortier, A.; *Catal. Lett.* **(2006)** 112:13

[127] Wielers, A.F.H.; Vaarkamp, M.; Post, M.F.M.; *J. Catal.* **(1991)** 127:51

[128] Lukyanov, D.B.; *J. Catal.* **(1994)** 147:494

[129] de la Puente, G.; Souza-Aguiar, E.F.; Zotin, F.M.Z.; Camorim, V.L.D.; Sedran, U.; *Appl. Catal. A.*, **(2000)** 197:41

[130] Arstad, B.; Kolboe, S.; *J. Am. Chem. Soc.* **(2001)** 123:8137

[131] Bjorgen, M.; Svelle, S.; Joensen, F.; Nerlov, J.; Kolboe, S.; Bonino, F.; Palumbo, L.; Bordiga, S.; Olsbye, U.; *J. Catal.* **(2007)** 249:195

[132] Auerbach, A. M.; Carrado K. A.; Dutta, P. K.; Handbook of Zeolite Science and Technology, Marcel Dekker, New York, **(2003)**